

Supporting information for

Modulation of [8]CPP properties by bridging two phenylene units

Denis Ari,^a Elodie Dureau,^a Olivier Jeannin,^a Joëlle Rault-Berthelot,^a Cyril Poriel^a and Cassandre Quinton*^a

^a Univ Rennes, CNRS, ISCR-UMR CNRS 6226, F-35000 Rennes, France- email: cassandre.quinton@univ-rennes.fr

1	General information	3
1.1	Synthesis.....	3
1.2	Spectroscopy	3
1.3	Electrochemistry.....	4
1.4	Molecular modelling	4
1.5	Crystallographic informations.....	5
2	Synthetic procedures	6
2.1	((4'-bromo-[1,1'-biphenyl]-4-yl)oxy)trimethylsilane (A).....	6
2.2	4'-bromo-1-hydroxy-[1,1'-biphenyl]-4(1H)-one (B)	6
2.3	4'-bromo-1-((triethylsilyl)oxy)-[1,1'-biphenyl]-4(1H)-one (C)	7
2.4	C-shaped intermediate (1)	7
2.5	General procedure for nanohoops synthesis [8]CPP-N-Bu and [8]CPP-C=O	8
2.6	Synthesis of [8]CPP-N-Bu	8
2.7	Synthesis of [8]CPP-C=O	9
3	Photophysical properties	11
3.1	Molar extinction coefficient measurements	11
3.2	Quantum yield measurements	13
3.3	Lippert-Mataga-Ooshika solvatochromism measurements	21
3.4	Fluorescence lifetime measurements.....	24
3.5	Spectroscopic properties of thin films	25
4	Electrochemical studies	26
5.1	Summary of the energies of the frontier orbitals for the nanohoops and the corresponding (un)bridged biphenylene.....	26
5.2	Study of [8]CPP-N-Bu	27
5.3.	Study of [8]CPP-C=O	29
5.4	Study of [8]CPP.....	30
5.5	Study of the (un)bridged biphenylene units	30
5	Molecular modelling	32
5.1	TD-DFT calculations and atomic coordinates.....	32
5.2	Strain energies calculations	45
6	NMR study	47
7	Copy of NMR spectra.....	50
8	Copy of infrared spectra	62
9	X-ray diffraction.....	64
10	References	94

1 General information

1.1 Synthesis

All manipulations of oxygen and moisture-sensitive materials were conducted with a standard Schlenk technique. All glassware was kept in an oven at 80°C. Argon atmosphere was generated by three repetitive cycles of vacuum/Argon using a Schlenk ramp. Commercially available reagents and solvents were used without further purification other than those detailed below. THF was obtained through a PURE SOLV™ solvent purification system. Light petroleum refers to the fraction with bp 40-60°C. Analytical thin layer chromatography was carried out using aluminum backed plates coated with Merck Kieselgel 60 GF254 and visualized under UV light (at 254 and 360 nm). Flash chromatography was carried out using Teledyne Isco CombiFlash® Rf 400 (UV detection 200-360 nm) or Teledyne Isco CombiFlash Nextgen 300+ (UV detection 200-360 nm) over standard silica cartridges (Redisep® Isco or Puriflash® columns Interchim).¹H and ¹³C NMR spectra were recorded using a Bruker AV III 300 MHz spectrometer fitted with a BBFO probe (¹H frequency, corresponding ¹³C frequency: 75 MHz) and a Bruker AV III 400 MHz spectrometer fitted with a BBFO probe (¹H frequency, corresponding ¹³C frequency: 100 MHz); chemical shifts were recorded in ppm and J values in Hz. The residual signals for the NMR solvents used are 5.32 ppm (proton) and 53.84 ppm (carbon) for CD₂Cl₂, 7.26 ppm (proton) and 77.16 ppm (carbon) for CDCl₃.^[1] The following abbreviations have been used for the NMR assignment: s for singlet, d for doublet, t for triplet, q for quadruplet and m for multiplet. Infrared spectra were recorded directly on powder using a Bruker VERTEX 70 machine. NMR spectra were recorded at a variable temperature from 303K to 253K on a Bruker AV III HD 500 MHz spectrometer fitted with a BBFO probe. The zg30 Bruker pulse program was used for 1D ¹H NMR, with a TD of 65k, a relaxation delay 1s and 16 scans. The spectrum width was set to 20 ppm, offset was 8 ppm. Fourier transform of the acquired FID was performed with 0.3Hz apodization. 1D NOESY selective experiments were acquired using the selnogpzs.2 pulse program. The mixing time was 0.7 s, Time Domain was 65k, 16 scans were carried out with a 2 s recovery delay and an acquisition time of 3.27s. Fourier transform of the acquired FID was performed with 0.1Hz apodization. High resolution mass spectra were recorded at the Centre Régional de Mesures Physiques de l'Ouest (CRMPO-Rennes) on a Thermo Fischer Q-Exactive instrument or a Bruker MaXis 4G or a Bruker Ultraflex III.

1.2 Spectroscopy

Cyclohexane (spectroscopic grade, Acros), ethyl acetate (spectroscopic grade, Thermo Fischer Scientific), dichloromethane (spectroscopic grade, Thermo Fischer Scientific), tetrahydrofuran (spectroscopic grade, Acros), acetonitrile (spectroscopic grade, Acros), and quinine sulfate dihydrate (99+, ACROS organics) were used without further purification.

were used without further purification.

UV - visible spectra were recorded using an UV - Visible spectrophotometer JASCO - V630BIO. Molar extinction coefficients (ϵ) were calculated from the gradients extracted from the plots of absorbance vs concentration with five solutions of different concentrations for each sample and at least two mother solutions were prepared.

$$A = \epsilon \times l \times C$$

Above, l refers to the path length and C to the sample concentration.

Emission spectra were recorded with a HORIBA Scientific Fluoromax-4 equipped with a Xenon lamp. Quantum yields in solution (ϕ_{sol}) were calculated relative to quinine sulfate ($\phi_{ref} = 0.546$ in H₂SO₄ 1 N). ϕ_{sol} was determined according to the following equation,

$$\phi_{sol} = \phi_{ref} \times \frac{Grad_s}{Grad_r} \times \left(\frac{\eta_s}{\eta_r} \right)^2$$

where subscripts s and r refer respectively to the sample and reference, Grad is the gradient from the plot of integrated fluorescence intensity vs absorbance, η is the refracting index of the solvent ($\eta_s = 1.426$ for cyclohexane). Five solutions of different concentration (A < 0.1) of the sample and five solutions of the reference were prepared. The integrated area of the fluorescence peak was plotted against the

absorbance at the excitation wavelength for both sample and reference. The gradients of these plots were then injected in the equation to calculate the reported quantum yield value for the sample.

Fluorescent decay measurements were carried out on the HORIBA Scientific Fluoromax-4 equipped with its TCSPC pulsed source interface.

Lipper-Mataga-Ooshika formalism was used to estimate the excited state dipole moment according to previous works.^[2-3]

$$\Delta\nu = \frac{2(\Delta\mu)^2}{r^3hc} \Delta f + C \text{ with } \Delta f = \left(\frac{\varepsilon-1}{2\varepsilon+1} - \frac{n^2-1}{n^2+1} \right)$$

With $\Delta\nu$ (cm^{-1}) being the Stokes shift, $\Delta\mu$ (D) the dipole moment difference between S_0 and S_1 states, r (cm) the radius of the solvation sphere obtained from the crystallographic structures, the Planck constant ($6.62607 \cdot 10^{-34} \text{ m}^2 \cdot \text{kg} \cdot \text{s}^{-1}$), c the celerity ($2.99792 \times 10^8 \text{ m} \cdot \text{s}^{-1}$), Δf the orientation polarizability of the solvent calculated from its dielectric constant ε ($\text{F} \cdot \text{m}^{-1}$) and its refractive index n , and C a constant.

Experimentally, $\Delta\nu$ were calculated from the maximal wavelength emission spectra measured in five different solvents (cyclohexane, dichloromethane, tetrahydrofuran, ethanol and methanol). Δf were calculated from ε and n for the five different solvents. Then, Δf as a function of $\Delta\nu$ was plotted and the slope is calculated using a linear regression. Finally, $\Delta\mu$ is calculated as follow:

$$\Delta\mu = \sqrt{\frac{r^3hc \cdot \text{slope}}{2}}$$

Excited state dipole moment μ^* is then calculated from the ground state dipole moment μ estimated by DFT calculations (B3LYP/6-31g(d)) and $\Delta\mu$.

Absolute quantum yields of the films were recorded using a deported HORIBA Scientific Quanta-Phi integrating sphere linked to the Fluoromax-4. Spin-coated films were prepared from a 1 mg/mL in THF solution using a Labspins Tournette from Süss Microtec.

1.3 Electrochemistry

Electrochemical experiments were performed under argon atmosphere using a Pt disk electrode (diameter 1 mm). The counter electrode was a vitreous carbon rod. The reference electrode was either a silver wire in a 0.1 M AgNO_3 solution in CH_3CN for the studies of the nanohoops in oxidation and in reduction both performed in Bu_4NPF_6 0.2 M in CH_2Cl_2 or a Silver wire coated by a thin film of AgI (silver(I)iodide) in a 0.1 M Bu_4NI solution in DMF for the studies in reduction of the bridged or unbridged biphenylenes. Ferrocene was added to the electrolyte solution at the end of a series of experiments. The ferrocene/ferrocenium (Fc/Fc^+) couple served as internal standard. The three electrodes cell was connected to a potentiostat/galvanostat (Autolab/PGSTAT101) monitored with the Nova 2.1 Software. Activated Al_2O_3 was added in the electrolytic solution to remove excess moisture. For further comparison between the electrochemical and optical properties, all potentials are referred to the SCE electrode that was calibrated at - 0.405 V vs. Fc/Fc^+ system. The electrochemical gap was calculated from: $\Delta E^{\text{el}} = |\text{HOMO-LUMO}|$ (in eV).

1.4 Molecular modelling

Full geometry optimization of the ground state and vibrational frequency calculation were performed with Density Functional Theory (DFT)^[4-5] using the hybrid Becke-3 parameter exchange functional^[6-8] and the Lee-Yang-Parr non-local correlation functional^[9] (B3LYP) implemented in the Gaussian 16 program suite,^[10] using the 6-31G(d) basis set and the default convergence criterion implemented in the program. Geometry optimization was performed starting from the X-ray diffraction crystal structure geometry. All stationary points were characterized as minima by analytical frequency calculations. Optical transition diagrams were obtained through TD-DFT calculations performed using the M06-2x functionals and the 6-311+G(d,p) basis set from the geometry of S_0 .

This work was granted access to the HPC resources of CEA-TGCC under the allocation 2022-[AD010805032R1](#) awarded by GENCI. Figures were generated with GaussView 6.0 and GaussSum 3.0.

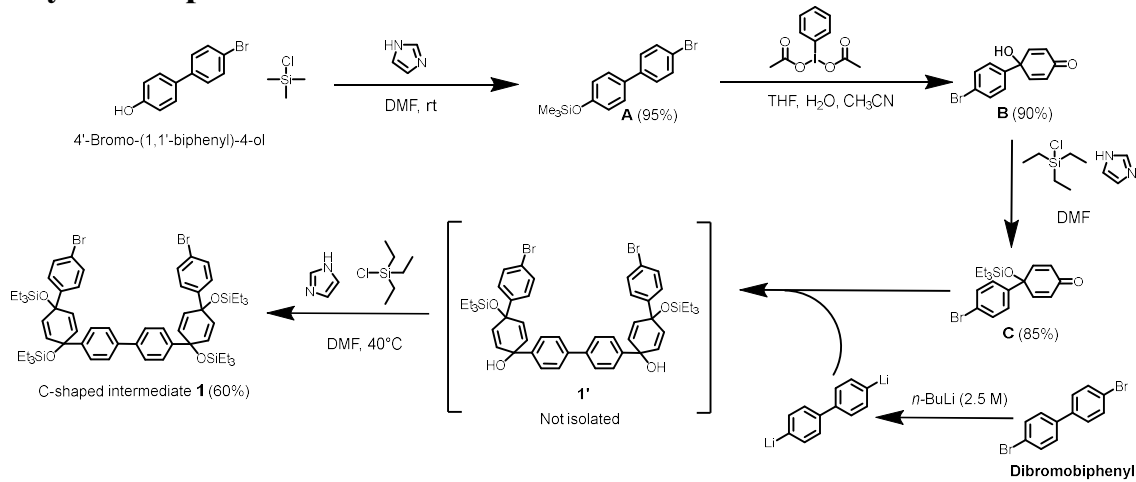
The strain energies calculations were determined by using DFT calculation at the B3LYP/6-31G(d) level of theory. Based on previous studies,^[11-12] homodesmotic reactions were considered using different fragments according to the studied nanohoop.

1.5 Crystallographic informations

Software's used to process the crystallographic data are described below.

Data collection: Bruker *APEX3* (Bruker, 2015); cell refinement: *APEX3* (Bruker, 2015); data reduction: *SAINT* (Bruker, 2014); program(s) used to solve structure: *SHELXT 2014/5* (Sheldrick, 2014); program(s) used to refine structure: *SHELXL2019/2* (Sheldrick, 2019); molecular graphics: *ORTEP* for Windows (Farrugia, 2012); software used to prepare material for publication: *WinGX* publication routines (Farrugia, 2012).

2 Synthetic procedures

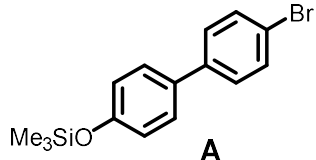


Scheme S 1 Synthesis of the C-shaped intermediate **1**.

The precursors **2a** and **2b** were synthesized according to procedures found in the literature.^[13-14]

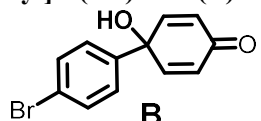
The compounds **4'-bromo-(1,1'-biphenyl)-4-ol** and the **dibromobiphenyl** are commercially available compounds, they were ordered from Fluorochem supplier.

2.1 ((4'-bromo-[1,1'-biphenyl]-4-yl)oxy)trimethylsilane (**A**)



4'-Bromo-(1,1'-biphenyl)-4-ol (15.0 g, 60.2 mmol, 1.0 equiv), imidazole (6.6 g, 96.3 mmol, 1.6 equiv) were dissolved in dry degassed dichloromethane (380 mL) under an argon atmosphere and the mixture was cooled down to 0°C. Chlorotrimethylsilane (9.9 mL, 78.3 mmol, 1.3 equiv) was then added slowly. The mixture was allowed to warm at room temperature and stirred overnight. Under stirring, 1 M aqueous sodium bicarbonate (50 mL) was added and the layers were separated. The organic layer was carefully washed with a saturated solution of NaHCO₃ (2 times) and water (1 time). The organic layer was dried over magnesium sulphate, filtered, and concentrated under reduced pressure. The residue was purified by flash chromatography on silica gel [column conditions: silica cartridge (40 g); solid deposit on Celite®; λdetection: (254 nm, 280 nm); gradient CH₂Cl₂/light petroleum from 5% to 10 % in 60 min at 40 mL/min], giving **A** as a colorless powder (18.4 g, 95%). ¹H NMR (400 MHz, CDCl₃) δ 7.59 – 7.53 (d, 2H), 7.50 – 7.39 (m, 4H), 6.97 – 6.92 (d, 2H), 0.33 (s, 9H) in agreement with literature.^[15]

2.2 4'-bromo-1-hydroxy-[1,1'-biphenyl]-4(1H)-one (**B**)



Compound **A** (17.0 g, 52.9 mmol, 1.0 equiv) was dissolved in a mixture of THF (270 mL), distilled water (120 mL) and MeCN (70 mL) before adding slowly (diacetoxyiodo)benzene (25.6 g, 79.4 mmol, 1.5 equiv). The reaction mixture was allowed to stir overnight at room temperature before concentrating under reduced pressure to afford a crude orange solid. This solid was washed with a solution of

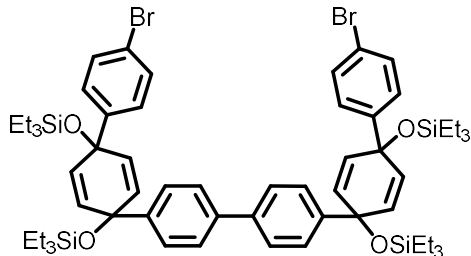
dibutylether (200 mL) and dried at 60°C under reduced pressure during several hours to give **B** as a yellow powder (12.6 g, 90%). ¹H NMR (300 MHz, CDCl₃) δ 7.59 – 7.47 (m, 2H), 7.43 – 7.32 (m, 2H), 6.93 – 6.82 (m, 2H), 6.31 – 6.19 (m, 2H) in agreement with literature.^[15]

2.3 4'-bromo-1-((triethylsilyl)oxy)-[1,1'-biphenyl]-4(1H)-one (C)



Compound **B** (10.0 g, 37.7 mmol, 1.0 equiv) and imidazole (5.1 g, 75.4 mmol, 2.0 equiv) were dissolved in dry DMF (180 ml) under argon atmosphere at room temperature. Then, Et₃SiCl (9.5 mL, 56.6 mmol, 1.5 equiv) was added dropwise to the solution. After the addition of Et₃SiCl, the mixture was heated up to 40 °C and stirred overnight. The reaction was allowed to cool to room temperature and quenched with a saturated aqueous NaHCO₃ solution and extracted with DCM. The organic layer was washed with a saturated solution of NaHCO₃ (1 time) and water (2 times). The combined organic extracts were dried over magnesium sulphate, filtered, and concentrated under reduced pressure. The residue was purified by flash chromatography on silica gel [column conditions: silica cartridge (40 g); solid deposit on Celite®; λdetection: (254 nm, 280 nm); gradient CH₂Cl₂/light petroleum from 10% at 40 mL/min], giving **C** as a yellow oil (12.1 g, 86%). ¹H NMR (400 MHz, CDCl₃) δ 7.53 – 7.45 (m, 2H), 7.38 – 7.30 (m, 2H), 6.85 – 6.77 (m, 2H), 6.29 – 6.21 (m, 2H), 0.99 (t, *J* = 7.9 Hz, 9H), 0.68 (q, *J* = 7.8 Hz, 6H) in agreement with literature.^[16]

2.4 C-shaped intermediate (1)



C-shaped intermediate (1)

In a first flask, the dibromobiphenyl (2.1 g, 6.6 mmol, 1.0 equiv) was dissolved in dry THF (55 mL) under argon atmosphere and the solution was cooled down to -78°C. *n*-BuLi (2.4 eq) was then added dropwise and the resulting mixture was stirred for 40 min.

In a second flask, **C** (5.0 g, 13.2 mmol, 2.0 equiv) was dissolved in dry THF (30 mL) under argon atmosphere, stirred 10 minutes at room temperature and 10 minutes at -78°C.

The solution of **C** was quickly injected in the first flask and the resulting mixture was allowed to stirred two hours at -78°C then quenched with water and warmed-up at room temperature. The organic layer was extracted with DCM and washed with water (3 times). The combined organic extracts were dried over magnesium sulphate, filtered, and concentrated under reduced pressure. The presence of the diol intermediate was confirmed by NMR. The obtained intermediate **1'** (6.0 g, 6.6 mmol, 1.0 equiv) and imidazole (2.7 g, 39.4 mmol, 6.0 equiv) were dissolved in dry DMF (108 mL) under argon atmosphere. Then, Et₃SiCl (3.3 mL, 19.7 mmol, 3.0 equiv) was added dropwise to the solution. After the addition of Et₃SiCl, the mixture was heated up to 40 °C and stirred overnight. The reaction was allowed to cool to room temperature and quenched with a saturated aqueous NaHCO₃ solution and extracted with DCM. The organic layer was washed with a saturated solution of NaHCO₃ (1 time) and water (2 times). The organic layer was dried over magnesium sulphate, filtered, and concentrated under reduced pressure.

The product was purified by precipitation, including the dissolution in the minimal amount of DCM (10 mL) followed by the addition of ethanol (30 mL). If the product does not precipitate in this condition, DCM was slowly evaporated under reduced pressure until precipitation. The resulting powder was filtered and washed with ethanol. This process was repeated two times giving **1** as a white powder (4.5 g, 60%). ¹H NMR (400 MHz, CDCl₃) δ 7.54 (d, *J* = 8.3 Hz, 4H), 7.44 – 7.36 (m, 8H), 7.25 (d, *J* = 8.6 Hz, 4H), 6.07 (d, *J* = 9.9 Hz, 4H), 5.98 (d, *J* = 10.1 Hz, 4H), 0.97 (t, *J* = 7.9 Hz, 36H), 0.64 (qd, *J* = 8.0, 2.6 Hz, 24H). ¹³C NMR (75 MHz, CDCl₃) δ ¹³C NMR (75 MHz, CDCl₃) δ 145.37, 145.05, 139.78, 131.98, 131.35, 131.27, 127.87, 126.93, 126.41, 121.34, 71.41 (d, *J* = 2.9 Hz), 7.18, 6.64, 6.60.in agreement with literature.^[17]

2.5 General procedure for nanohoops synthesis [8]CPP-N-Bu and [8]CPP-C=O

1st step:

C-shaped intermediate **1** (1.0 equiv, 1.7 mmol/L), bisborylated bridged biphenylene **2a** or **2b** (1.05 equiv), and SPhos Pd G3 (0.15 equiv) were dissolved under argon atmosphere in degassed dioxane and the resulting mixture was heated to 80°C. After 5 min of stirring at 80°C, a 2 M K₃PO₄ aqueous solution (100 equiv), previously degassed with argon during 1 hour, was added and the mixture was allowed to stir overnight. Dioxane was removed under reduced pressure and the crude reaction mixture was dissolved in CH₂Cl₂. A pad on celite was carried out to remove palladium residues and the organic layer was washed with H₂O (3 times), dried over magnesium sulphate, and solvent removed under reduced pressure. No further purifications were performed.

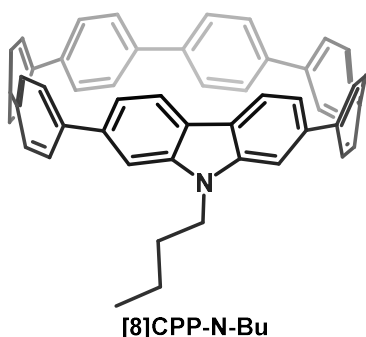
2nd step:

The crude macrocycle (1.0 equiv, 0.219 mol/L) was dissolved in THF at room temperature and TBAF 1 M (6.6 equiv) was added. The reaction was stirred for 2 h and quenched with H₂O inducing the precipitation of the product. THF was removed under reduced pressure and the resulting mixture was filtered to afford the deprotected macrocycle as a yellow powder that was rinsed with water and DCM. No further purifications were performed.

3rd step:

A solution of H₂SnCl₄ was prepared by dissolving SnCl₂ (4.4 equiv, 0.0965 mol/L) in THF before adding HCl 35% (8.8 equiv) and letting stirred for 30 min. The mixture was then cannulated in a solution of the deprotected macrocycle in THF (1.0 equiv, 8.8 mmol/L) under argon and the reaction was stirred overnight at room temperature. A pad on celite was carried out to remove thin residues before evaporating the THF under reduced pressure. The organic layer was extracted with DCM and washed with water (3 times). The combined organic extracts were dried over magnesium sulfate, filtered, and concentrated under reduced pressure. The residue was purified by flash chromatography on silica gel.

2.6 Synthesis of [8]CPP-N-Bu



The title compound was synthesized using the general procedure for nanohoops synthesis.

1st step:

1 (500 mg, 0.44 mmol, 1.0 equiv), **2a** (219 mg, 0.46 mmol, 1.05 equiv) and SPhos Pd G3 (51 mg, 0.065 mmol, 0.15 eq) were dissolved in 260 mL of degassed dioxane. The K₃PO₄ 2M aqueous solution was prepared by dissolving 17 g in 40 mL of deionized water.

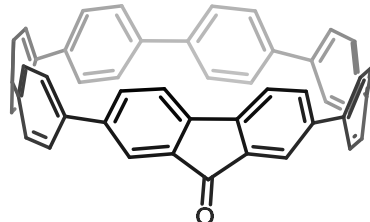
2nd step:

The crude was dissolved in 2 mL of THF and TBAF 1M was added (2.89 mL, 2.89 mmol, 6.6 equiv).

3rd step:

SnCl₂ (435 mg, 1.93 mmol, 4.4 equiv) was dissolved in 20 mL of degassed THF followed by the addition of HCl 35% (0.32 ml, 3.86 mmol, 8.8 equiv). This mixture was cannulated in a solution of the deprotected macrocycle in 50 mL of degassed THF. The residue was purified by flash chromatography on silica gel [column conditions: silica cartridge (40 g); solid deposit on Celite®; λdetection: (254 nm, 280 nm); gradient CH₂Cl₂/light petroleum from 5% to 40 % in 60 min at 40 mL/min], giving the title compound as a yellow powder (26 mg, 10% over 3 steps). ¹H NMR (400 MHz, CD₂Cl₂) δ 7.87 (dd, *J* = 8.4, 0.5 Hz, 2H), 7.65 – 7.58 (d, 8H), 7.56 – 7.51 (d, 8H), 7.50 (s, 8H), 7.45 (dd, *J* = 8.4, 1.6 Hz, 2H), 6.91 (d, *J* = 1.6 Hz, 2H), 3.86 (t, *J* = 7.1 Hz, 2H), 1.80 – 1.67 (m, 2H), 1.37 (dq, *J* = 14.4, 7.3 Hz, 2H), 0.94 (t, *J* = 7.4 Hz, 3H). ¹³C NMR (75 MHz, CDCl₃) δ 144.20 (2C), 141.21 (2C), 139.10 (2C), 138.09 (2C), 137.95 (2C), 137.69 (2C), 137.52 (2C), 137.12 (2C), 127.82 (4CH), 127.75 (4CH), 127.70 (8CH), 127.47 (8CH), 122.46 (2C), 122.41 (2CH), 116.78 (2CH), 114.63 (2CH), 42.25 (1CH₂), 31.47 (1CH₂), 20.61 (1CH₂), 13.94 (1CH₃). IR (cm⁻¹): ν=2930, 1590, 1476, 1310, 1250. HRMS (MALDI, DCTB, m/z) calculated for C₄₉H₃₀O [M+H]⁺: 677.308 found: 677.309.

2.7 Synthesis of [8]CPP-C=O



[8]CPP-C=O

The title compound was synthesized using the general procedure for nanohoops synthesis.

1st step:

C-shaped intermediate **1** (500 mg, 0.44 mmol, 1.0 equiv), **2b** (199 mg, 0.46 mmol, 1.05 equiv) and SPhos Pd G3 (51 mg, 0.065 mmol, 0.15 eq) were dissolved in 260 mL of degassed dioxane. The K₃PO₄ 2M aqueous solution was prepared by dissolving 17 g in 40 mL of deionized water.

2nd step:

The crude was dissolved in 8 mL of THF and TBAF 1M was added (5.2 mL, 5.2 mmol, 6.6 equiv).

3rd step:

SnCl₂ (435 mg, 1.93 mmol, 4.4 equiv) was dissolved in 35 mL of degassed THF followed by the addition of HCl 35% (0.32 ml, 3.86 mmol, 8.8 equiv). This mixture was cannulated in a solution of the deprotected macrocycle in 90 mL of degassed THF. The residue was purified by flash chromatography on silica gel [column conditions: silica cartridge (40 g); solid deposit on Celite®; λdetection: (254 nm,

280 nm); gradient CH₂Cl₂/light petroleum from 5% to 40 % in 60 min at 40 mL/min], followed by a sterical exclusion chromatography giving the title compound as an orange powder (18 mg, 8% over 3 steps). ¹H NMR (400 MHz, CD₂Cl₂) δ 7.78 (dd, *J* = 8.1, 1.9 Hz, 2H), 7.61 – 7.59 (d, *J* = 8.6 Hz, 8H), 7.55 – 7.53 (d, *J* = 9.4 Hz, 8H), 7.53 (s, 8H), 7.40 (m, 2H), 7.23 (dd, *J* = 1.9, 0.5 Hz, 2H). ¹³C NMR (101 MHz, CD₂Cl₂) δ 194.14 (1C=O), 142.75 (2C), 141.43 (2C), 138.27 (2C), 138.09 (2C), 137.89 (2C), 137.77 (2C), 137.73 (2C), 137.10 (2C), 136.94 (2C), 130.22 (2CH), 128.41 (2CH), 127.65 (4CH), 127.59 (4CH), 127.54 (8CH), 127.48 (8CH) 123.10 (2CH). IR (cm⁻¹): ν=2918, 1718, 1583, 1488, 1459, 1264, 1179. HRMS (MALDI, DCTB, m/z) calculated for C₄₉H₃₀O [M+H]⁺: 634.229 found: 634.228.

3 Photophysical properties

3.1 Molar extinction coefficient measurements

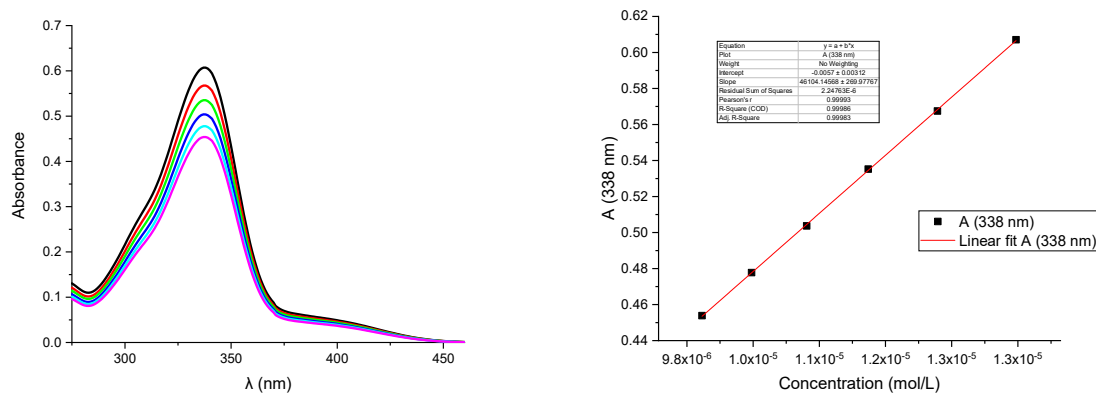


Figure S 1 Absorption spectra of [8]CPP-N-Bu in cyclohexane (left) and linear fit of the absorbance at 338 nm as a function of the concentration (right).

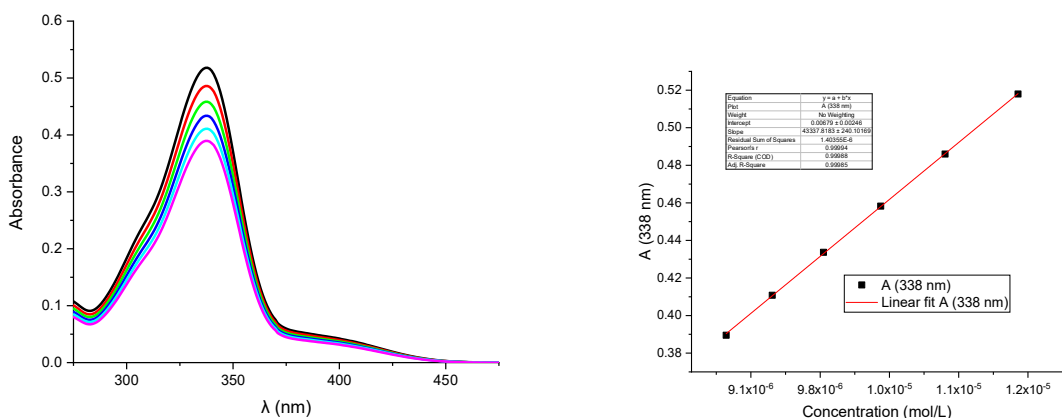


Figure S 2 Absorption spectra of [8]CPP-N-Bu in cyclohexane (left) and linear fit of the absorbance at 338 nm as a function of the concentration (right).

Table S 1 Results of molar extinction coefficient of [8]CPP-N-Bu.

Molar extinction coefficient of [8]CPP-N-Bu	Slope
Experiment n°1	46104
Experiment n°2	43338
Average	44721

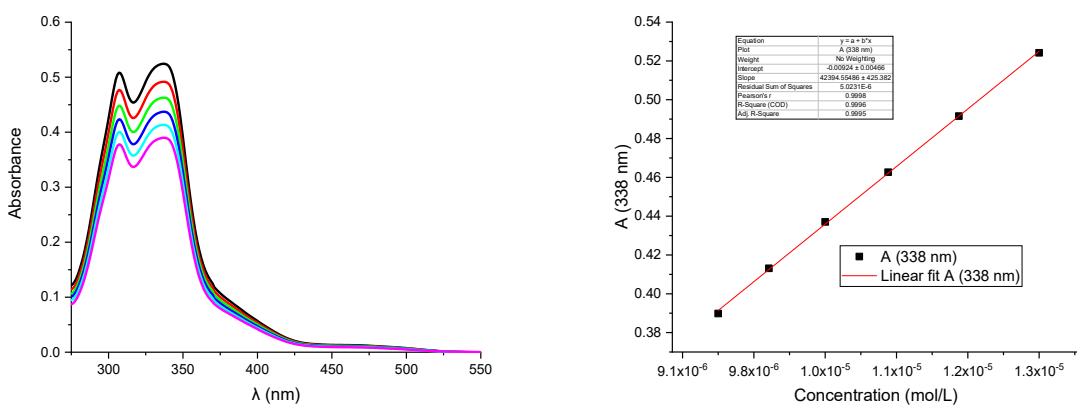


Figure S 3 Absorption spectra of [8]CPP-C=O in cyclohexane (left) and linear fit of the absorbance at 338 nm as a function of the concentration (right)

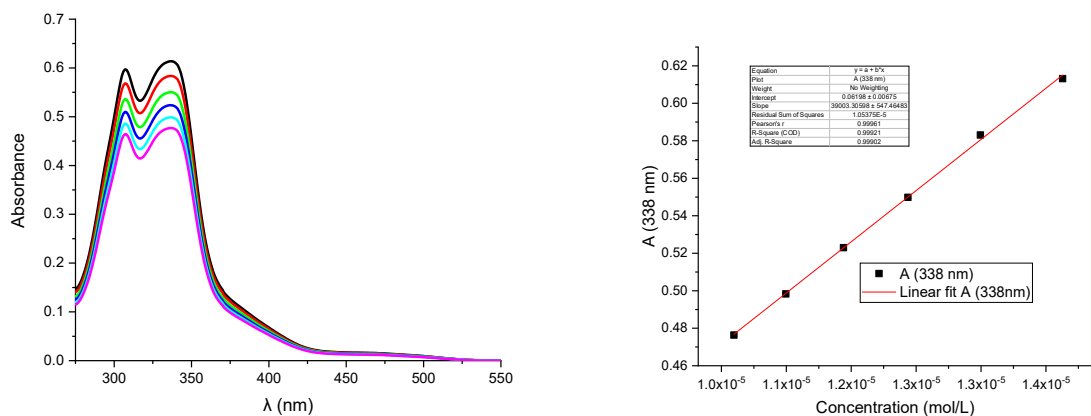


Figure S 4 Absorption spectra of [8]CPP-C=O in cyclohexane (left) and linear fit of the absorbance at 338 nm as a function of the concentration (right)

Table S 2 Results of molar extinction coefficient of [8]CPP-C=O.

Molar extinction coefficient measurements of [8]CPP-C=O	Slope
Experiment n°1	42395
Experiment n°2	39003
Average	40699

3.2 Quantum yield measurements

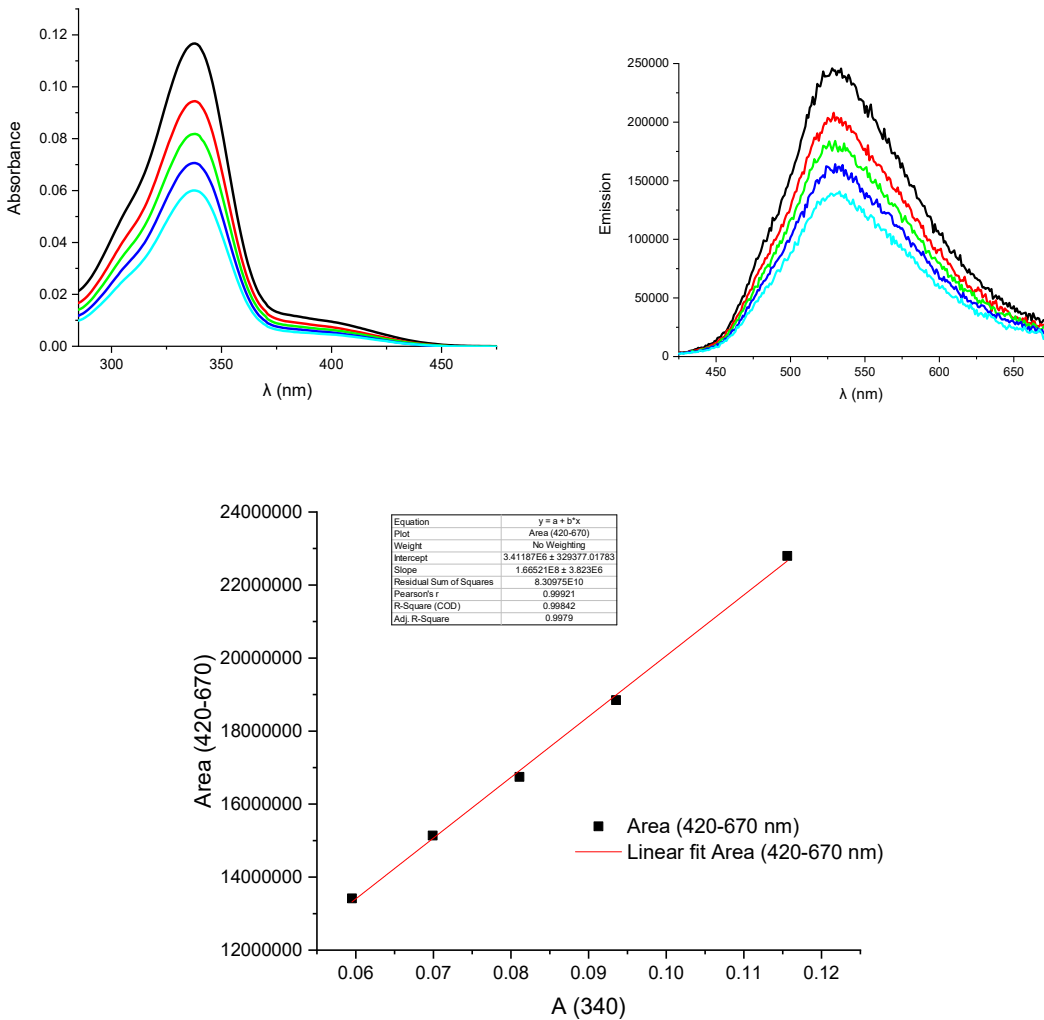


Figure S 5 Absorption (up-left) and emission (up-right) spectra of **[8]CPP-N-Bu** in cyclohexane and linear fit of the integration of the fluorescence between 420 and 670 nm as a function of the absorbance at 340 nm (bottom)

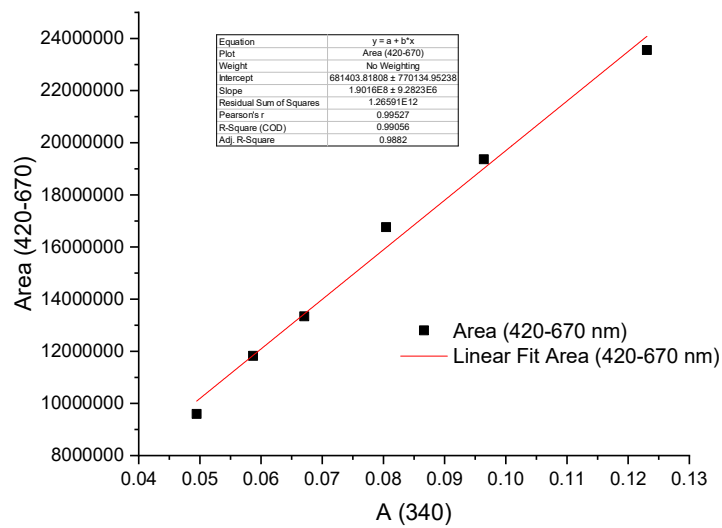
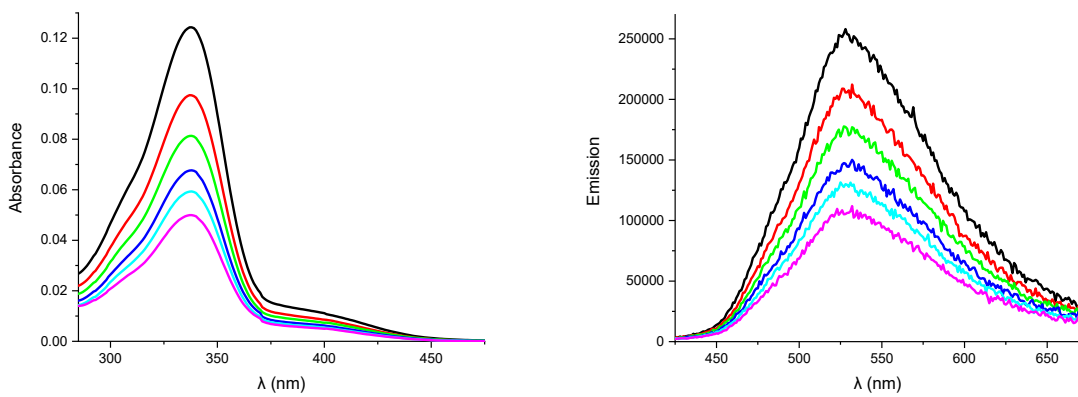


Figure S 6 Absorption (up-left) and emission (up-right) spectra of **[8]CPP-N-Bu** in cyclohexane and linear fit of the integration of the fluorescence between 420 and 670 nm as a function of the absorbance at 340 nm (bottom).

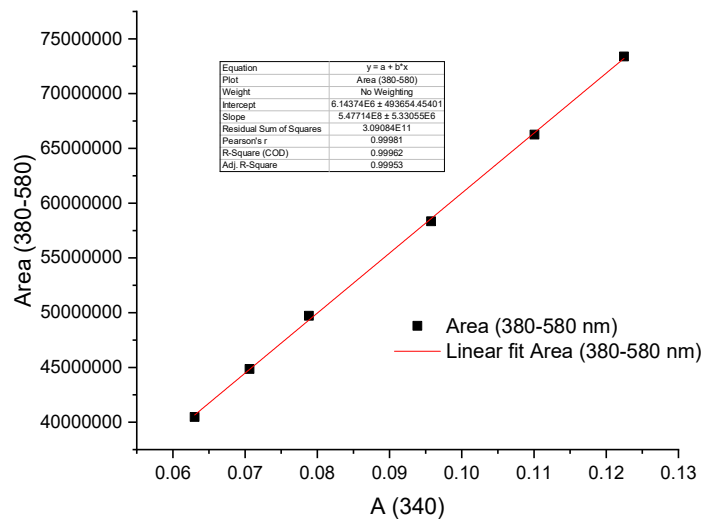
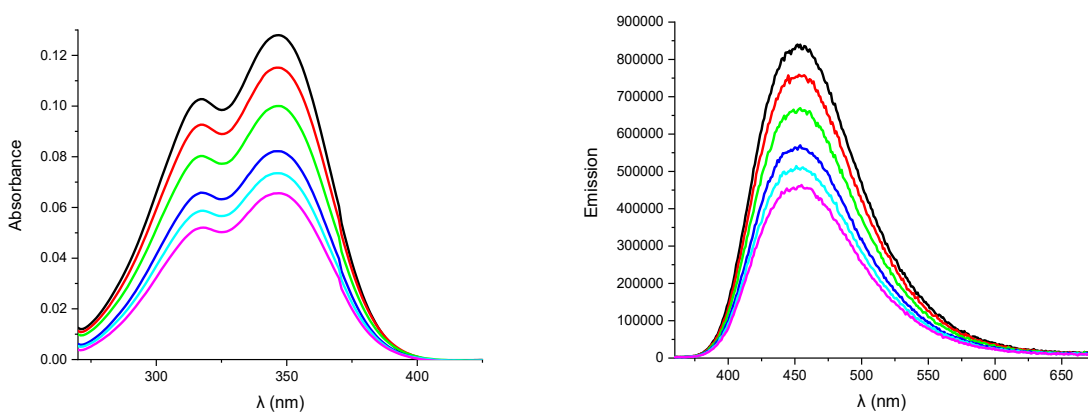


Figure S 7 Absorption and emission spectra of **quinine sulfate** in 1.0 N sulfuric acid (left) and linear fit of the integration of the fluorescence between 380 and 580 nm as a function of the absorbance at 340 nm (bottom).

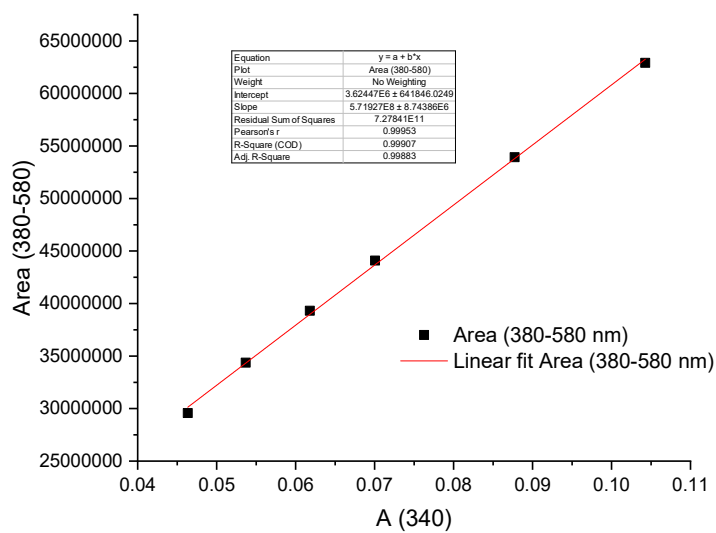
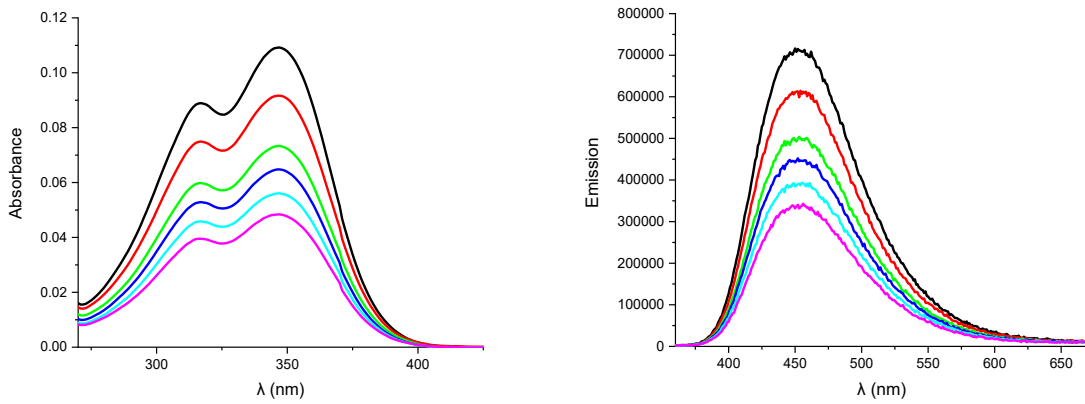


Figure S 8 Absorption and emission spectra of **quinine sulfate** in 1.0 N sulfuric acid (left) and linear fit of the integration of the fluorescence between 380 and 580 nm as a function of the absorbance at 340 nm (bottom).

	Quinine sulfate in 0.1 N sulfuric acid	[8]CPP-N-Bu in cyclohexane
Slope n°1	5.48×10^8	1.67×10^8
Slope n°2	5.72×10^8	1.90×10^8
Refractive index of the solvent	1.333	1.426
QY 1	0.546	0.190
QY 2	0.546	0.208

Average quantum yield = 20%

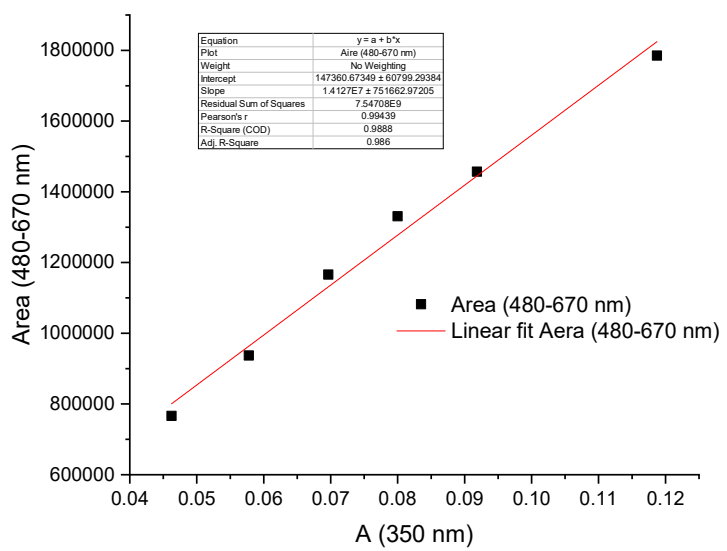
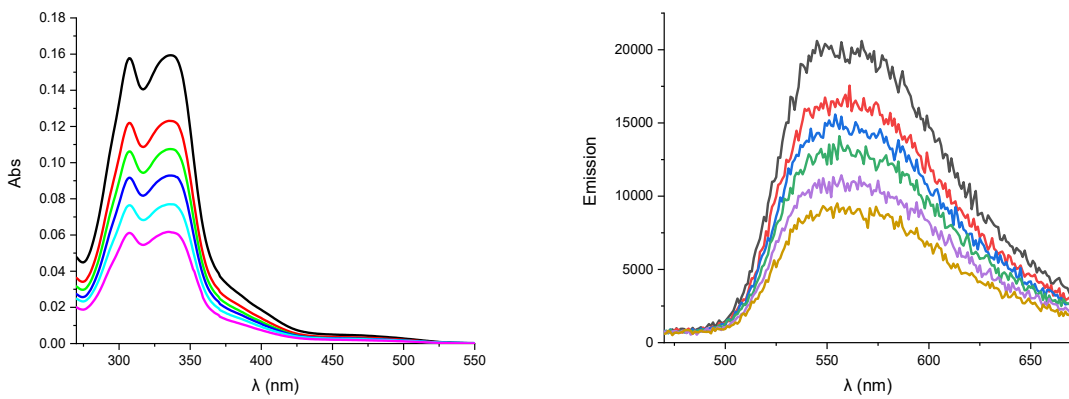


Figure S 9 Absorption (up-left) and emission (up-right) spectra of **[8]CPP-C=O** in cyclohexane and linear fit of the integration of the fluorescence between 480 and 670 nm as a function of the absorbance at 350 nm (bottom).

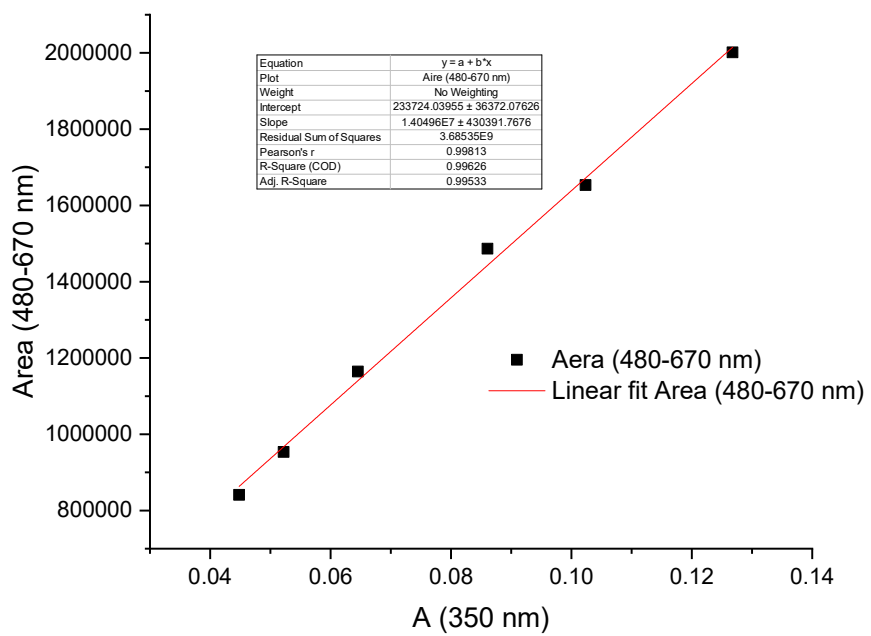
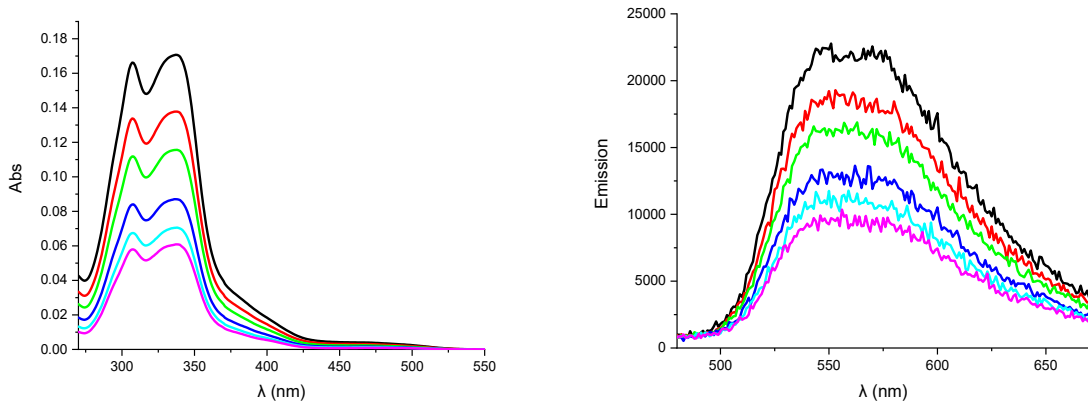


Figure S 10 Absorption (up-left) and emission (up-right) spectra of [8]CPP-C=O in cyclohexane and linear fit of the integration of the fluorescence between 480 and 670 nm as a function of the absorbance at 350 nm (bottom).

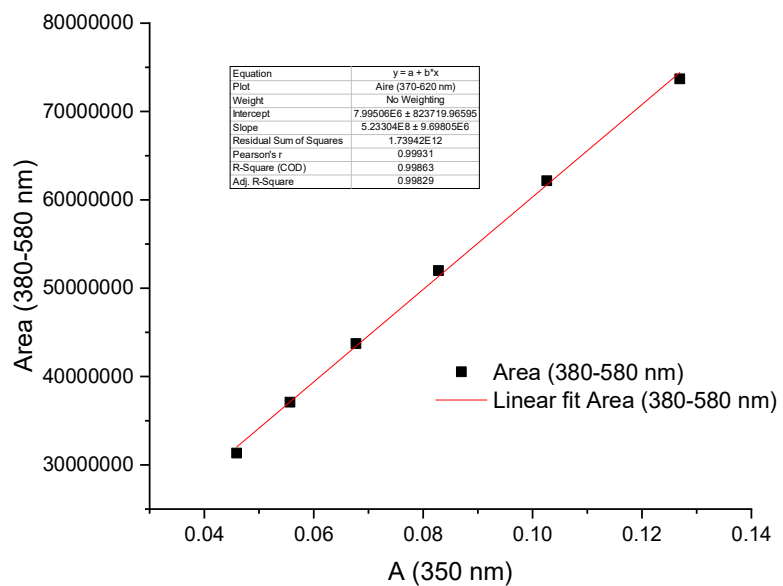
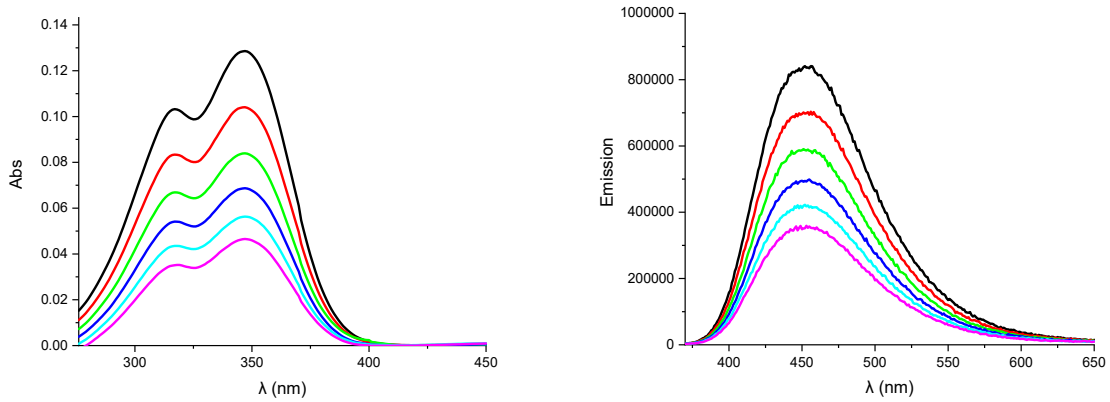


Figure S 11 Absorption and emission spectra of quinine sulfate in 1.0 N sulfuric acid (left) and linear fit of the integration of the fluorescence between 380 and 580 nm as a function of the absorbance at 350 nm (bottom).

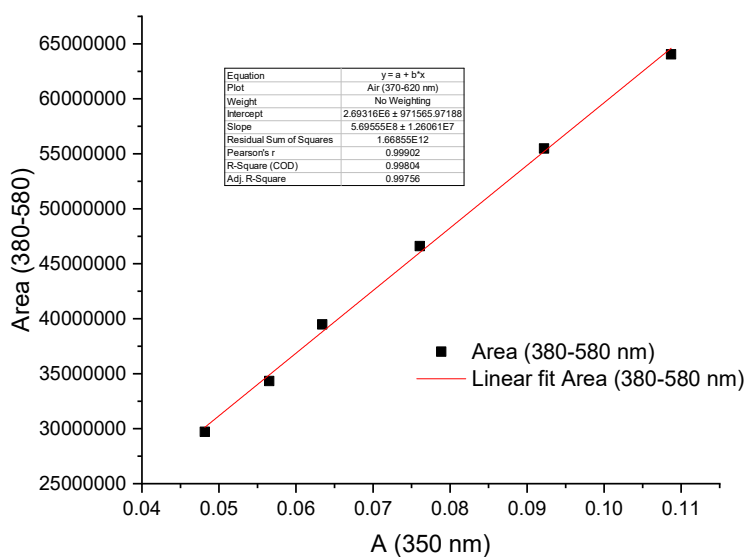
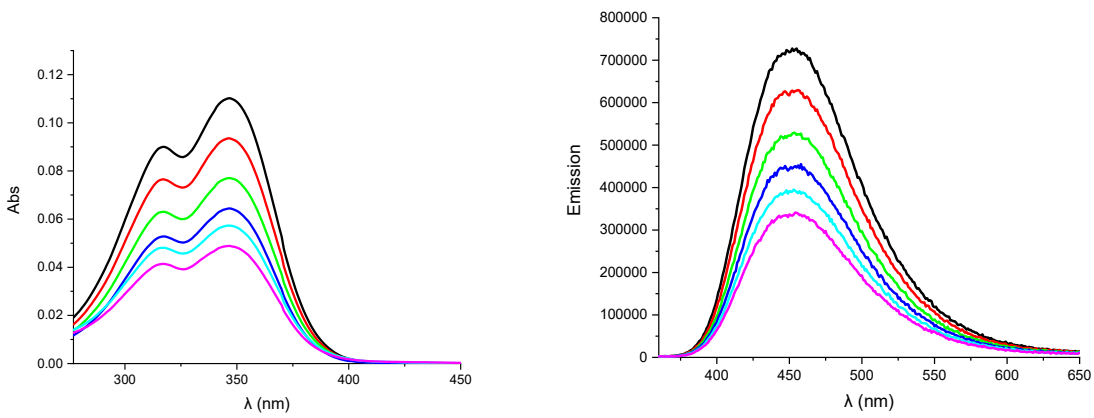


Figure S 12 Absorption and emission spectra of quinine sulfate in 1.0 N sulfuric acid (left) and linear fit of the integration of the fluorescence between 380 and 580 nm as a function of the absorbance at 350 nm (bottom).

	Quinine sulfate in 0.1 N sulfuric acid	[8]CPP-C=O in cyclohexane
Slope n°1	5.23×10^8	1.41×10^8
Slope n°2	5.70×10^8	1.40×10^8
Refractive index of the solvent	1.333	1.426
QY 1	0.546	0.017
QY 2	0.546	0.015

Average quantum yield = 2%

3.3 Lippert-Mataga-Ooshika solvatochromism measurements

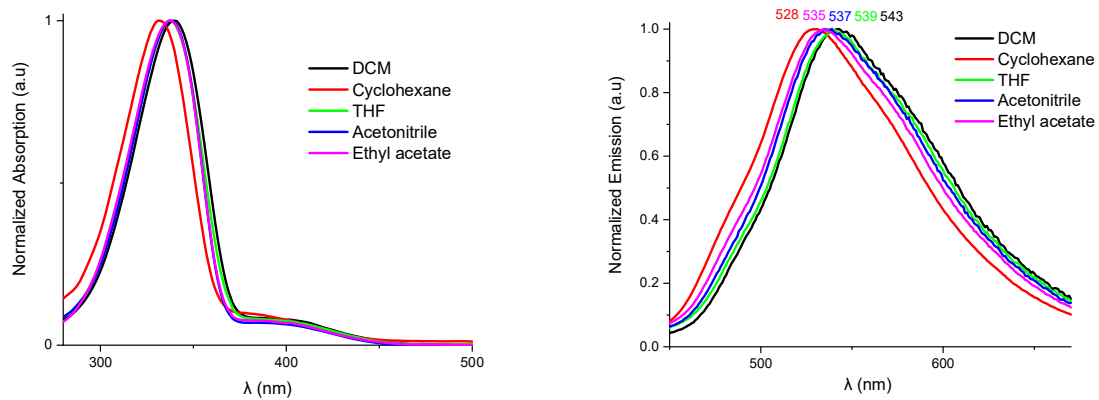


Figure S 13 Absorption spectra (left) and emission spectra (right) of [8]CPP in various solvents.

Table S 3 Absorption and emission maximal wavelength of [8]CPP in various solvents.

Solvent	λ_{abs} (nm)	λ_{em} (nm)
DCM	340	543
Cyclohexane	332	529
THF	337	539
Acetonitrile	337	537
Chloroform	340	542
Ethyl acetate	337	535

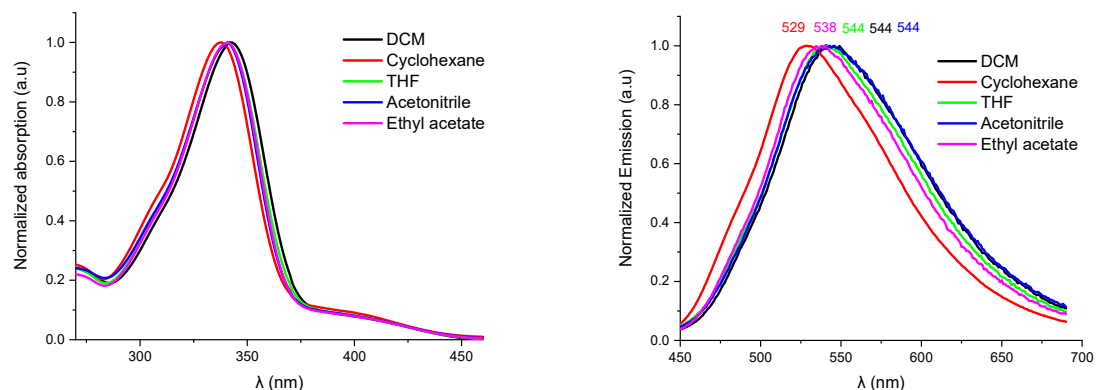


Figure S 14 Absorption spectra (left) and emission spectra (right) of **[8]CPP-N-Bu** in various solvents.

Table S 4 Absorption and emission maximal wavelength of **[8]CPP-N-Bu** in various solvents.

Solvent	λ_{abs} (nm)	λ_{em} (nm)
DCM	343	544
Cyclohexane	338	529
THF	341	544
Acetonitrile	341	544
Ethyl acetate	341	538

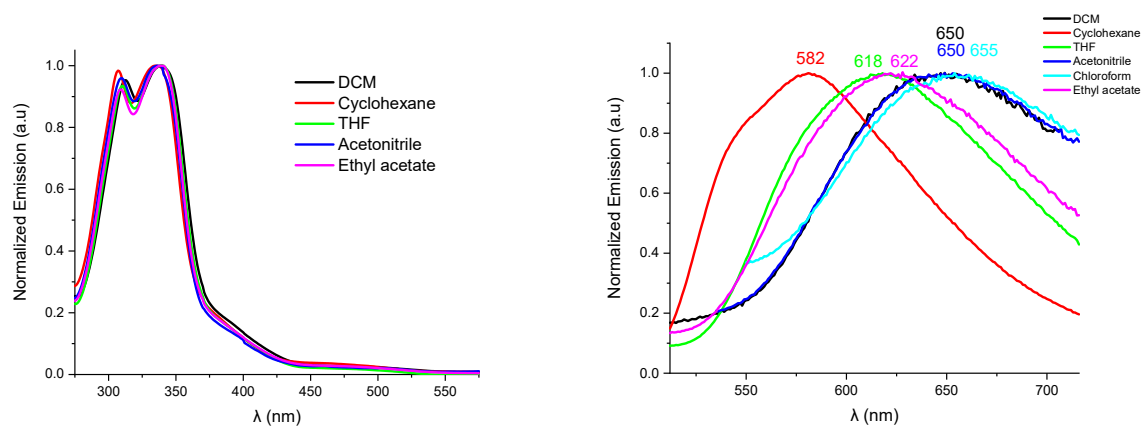


Figure S 15 Absorption spectra (left) and emission spectra (right) of **[8]CPP-C=O** in various solvents.

Table S 5 Lippert-Mataga formalism calculation of **[8]CPP-C=O** in various solvents.

Solvent	λ_{abs} (nm)	λ_{em} (nm)	ν_{abs} (cm ⁻¹)	ν_{em} (cm ⁻¹)	$\Delta\nu$ (cm ⁻¹)	ϵ	n	Δf
DCM	338	650	29585.8	15384.62	14201.18	8.93	1.4241	0.217137
Cyclohexane	336	582	29761.9	17182.13	12579.77	2.02	1.4262	-0.00165
THF	338	618	29585.8	16181.23	13404.57	7.58	1.4072	0.209572
Acetonitrile	336	650	29761.9	15384.62	14377.29	37.5	1.3441	0.305416
Chloroform	338	655	29585.8	15267.18	14318.62	4.81	1.4458	0.148295
Ethyl acetate	338	622	29585.8	16077.17	13508.63	6.02	1.3724	0.199635

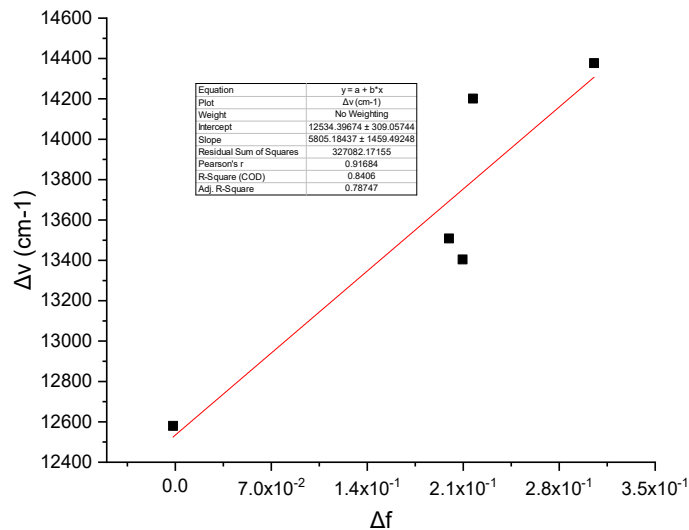


Figure S 16 Lippert-Mataga formalism linear fit for **[8]CPP-C=O**.

Table S 6 Summary of the radius of the solvation sphere (r), dipole moment at the ground (μ) and excited (μ^*) states and the difference ($\Delta\mu$) for [8]CPP-C=O.

Compound	r (Å)	$\Delta\mu$ (D)	μ (D)	μ^* (D)
[8]CPP-C=O	5.822	10.7	3.3	14.0

3.4 Fluorescence lifetime measurements

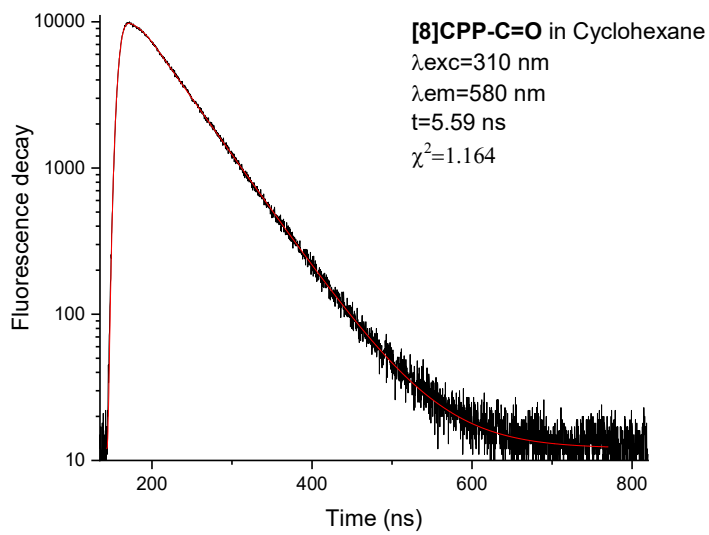
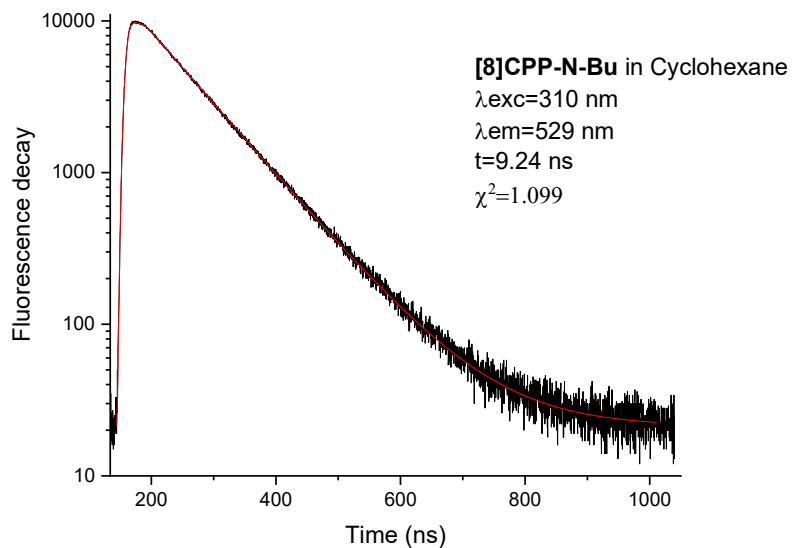


Figure S 17 Fluorescence lifetime measurements of [8]CPP-N-Bu (top) and [8]CPP-C=O (bottom).

3.5 Spectroscopic properties of thin films

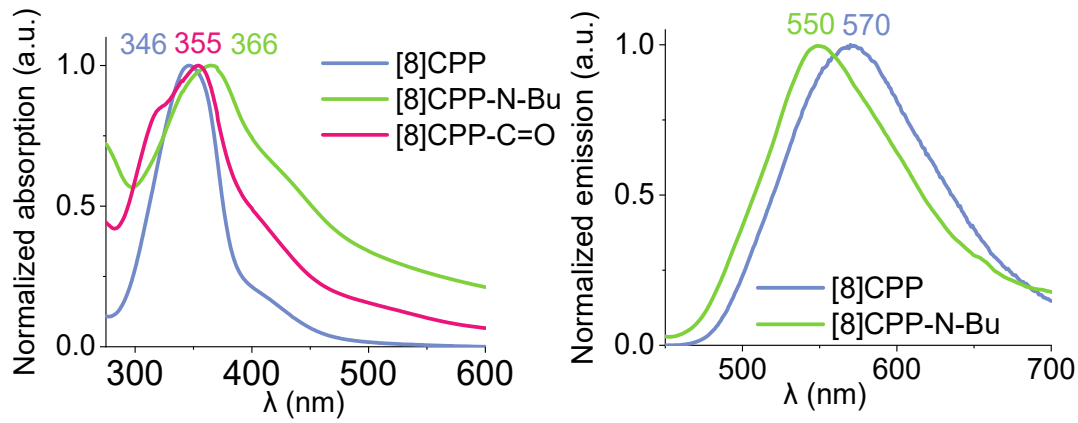


Figure S 18. Absorption (left) and emission (right) spectra of **[8]CPP**, **[8]CPP-N-Bu** and **[8]CPP-C=O** (non-emissive) in thin film ($\lambda_{\text{exc}} = 340$ nm).

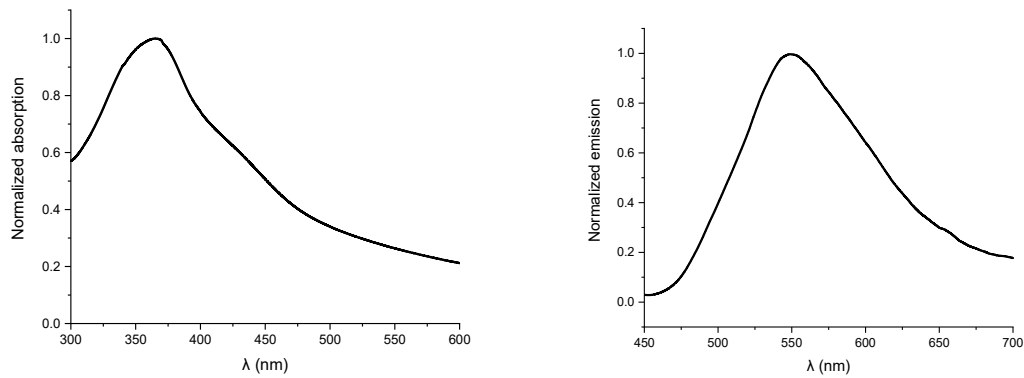


Figure S 19 Absorption (left) and emission spectra (right) of **[8]CPP-N-Bu** in thin film.

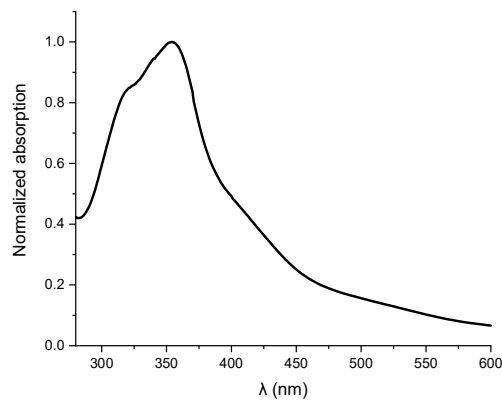


Figure S 20 Absorption spectra of **[8]CPP-C=O** in thin film.

	[8]CPP-N-Bu	[8]CPP-C=O
QY (film)	11%	0%

4 Electrochemical studies

The onset potentials E^{onset} , anodic potentials E^a , cathodic potential E^c and inflection point potentials $E^{(i)}$ have been determined according to the following reference.^[18]. Following the work of Jenekhe,^[19] we estimated the energy levels of the lowest unoccupied molecular orbital (LUMO) and or highest occupied molecular orbital (HOMO) from the redox data. The LUMO level was calculated from: LUMO (eV) = $-[E^{\text{onset}}_{\text{red}} (\text{vs SCE}) + 4.4]$. Similarly the HOMO level was calculated from: HOMO (eV) = $-[E^{\text{onset}}_{\text{ox}} (\text{vs SCE}) + 4.4]$, based on a SCE energy level of 4.4 eV relative to the vacuum. The half-wave potentials $E^{(1/2)}$ for reversible processes have been determined as $E^{(1/2)} = 0.5 \times (E^a + E^c)$. The data are summarized in the following table S7.

Table S 7. Summary of the electrochemical data (in V vs SCE)

	Potential	[8]CPP-N-Bu	[8]CPP-C=O	[8]CPP
Oxidation	$E^{\text{onset}}_{\text{ox}}$	0.89	1.02	0.88
	E^a_{ox}	1.00	1.14	1.07
	E^c_{ox}	0.92	1.04	n.d.
	$E^{(i)}_{\text{ox}}$	0.95	1.08	0.94
	$E^{(1/2)}_{\text{ox}}$	0.96	1.09	n.d.
Reduction	$E^{\text{onset}}_{\text{red}}$	-1.91	-1.22	-1.80
	E^a_{red}	n.d.	-1.25	n.d.
	E^c_{red}	2.02	-1.36	-1.93
	$E^{(i)}_{\text{red}}$	-1.96	-1.31	-1.87
	$E^{(1/2)}_{\text{red}}$	n.d.	-1.31	n.d.

n.d.: not determined

5.1. Summary of the energies of the frontier orbitals for the nanohoops and the corresponding (un)bridged biphenylene

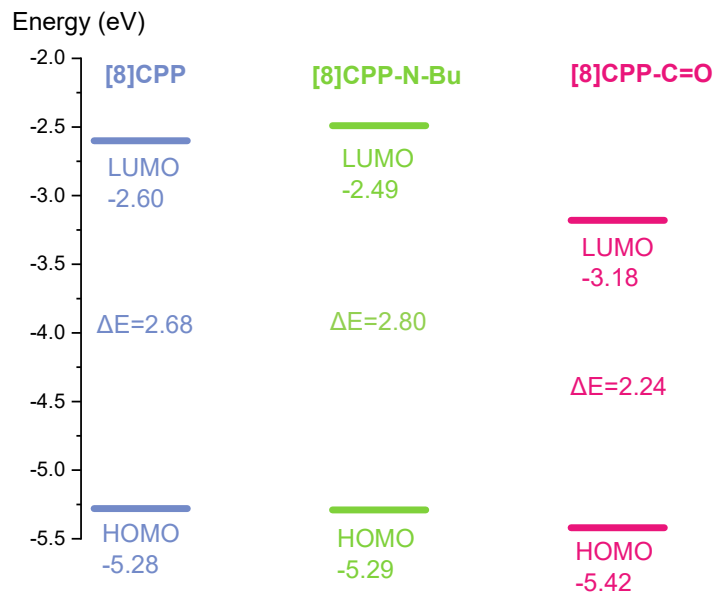


Figure S 21 HOMO and LUMO energy of studied nanohoops with electronic gap obtained from electrochemical measurements (E^{onset}).

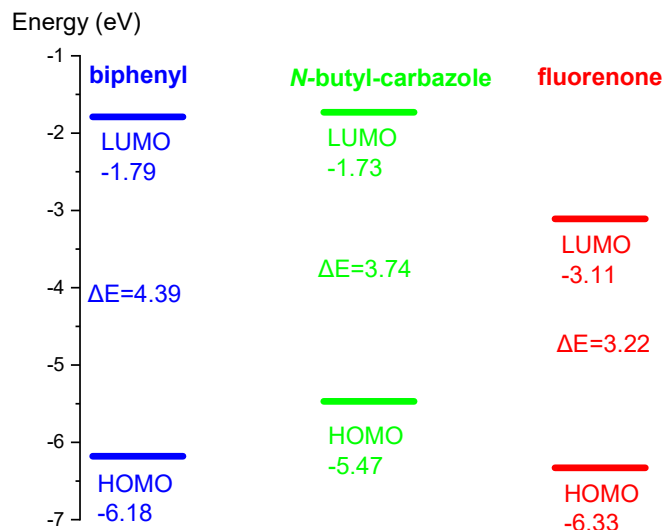


Figure S 22 HOMO and LUMO levels of studied (bridged) biphenylene fragments with electronic gap obtained from electrochemical measurement (E^{onset}).

5.2. Study of [8]CPP-N-Bu

Determination of the onset potentials E^{onset} , frontier orbital energies HOMO and LUMO, anodic potential E^a , cathodic potential E^c and inflection point potentials $E^{(i)}$.^[18]

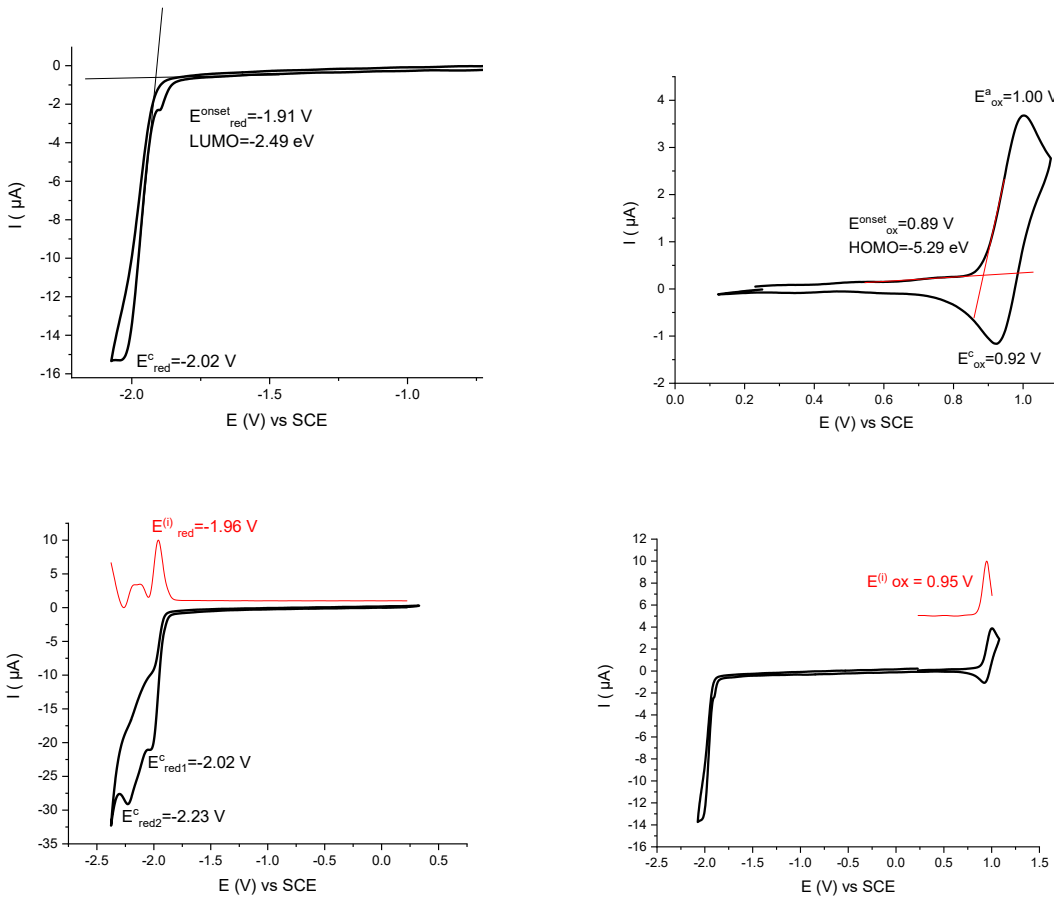


Figure S 23 Cyclic voltammograms (in black) recorded in DCM + Bu_4NPF_6 0.2 M in presence of **[8]CPP-N-Bu** 2×10^{-3} M. Platinum Working electrode, 100 mV/s. Reduction (up-left), oxidation (up-right), reduction responses between 0.32 and -2.38 V (bottom left) and combined oxidative-reductive responses (bottom right). The first derivative of the voltammograms are shown as red traces and allow estimation of the inflection potentials $E^{(i)}$.

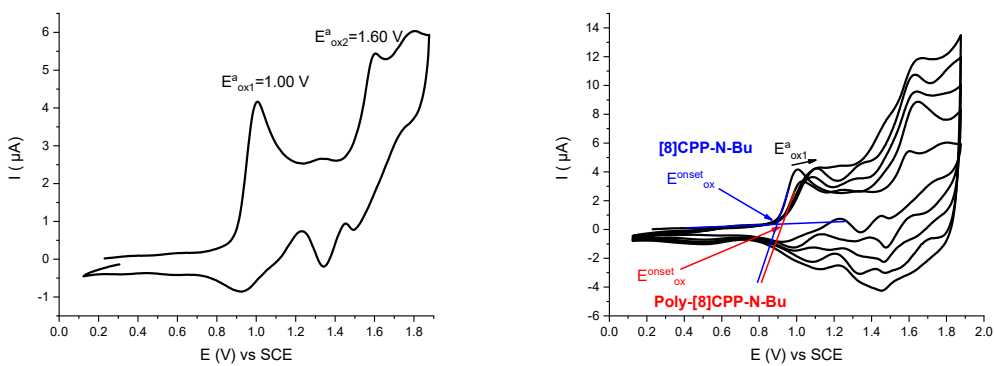


Figure S 24 Cyclic voltammograms recorded in DCM + Bu_4NPF_6 0.2 M in presence of **[8]CPP-N-Bu** 2×10^{-3} M. Platinum Working electrode, 100 mV/s. Oxidation response between 0.12 V and 2.24 V (left) and five recurrent cycles between 0.12 V and 2.24 V (right).

5.3. Study of [8]CPP-C=O

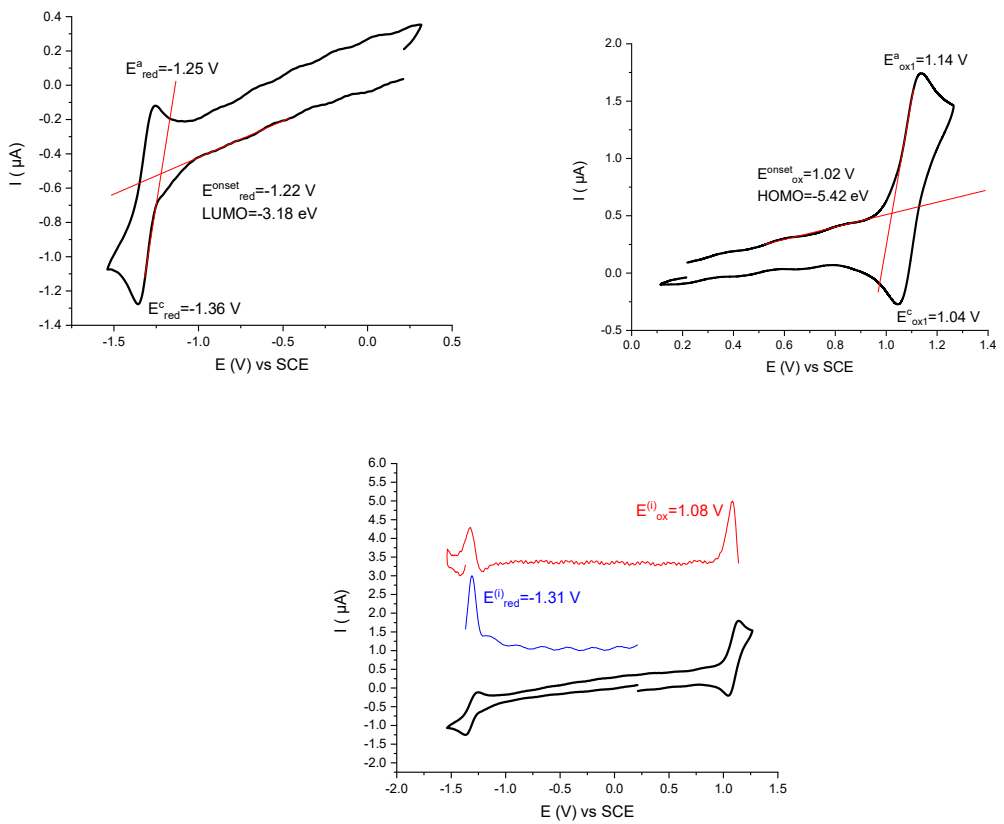


Figure S 25 Cyclic voltammograms recorded in DCM + Bu₄NPF₆ 0.2 M in presence of [8]CPP-C=O 2 × 10⁻³M. Platinum Working electrode, 100 mV/s. Reduction (up-left), oxidation (up-right) and combined oxidative-reductive responses (bottom left). The first derivative of the voltammograms are shown as red and blue traces and allow estimation of the inflection potentials E⁽ⁱ⁾.

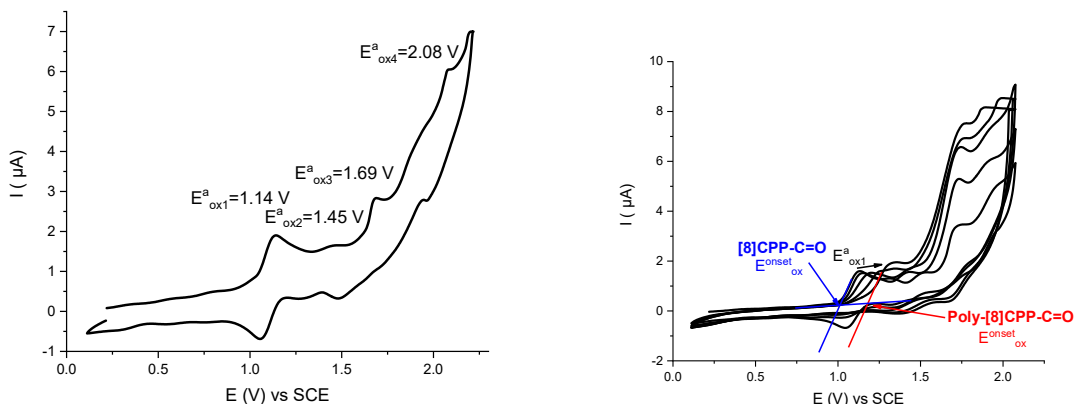


Figure S 26 Cyclic voltammograms recorded in DCM + Bu₄NPF₆ 0.2 M in presence of [8]CPP-C=O 2 × 10⁻³M. Platinum Working electrode, 100 mV/s. Oxidation response between 0.10 V and 2.05 V (left) and five recurrent cycles between 0.10 V and 2.05 V (right).

5.4 Study of [8]CPP

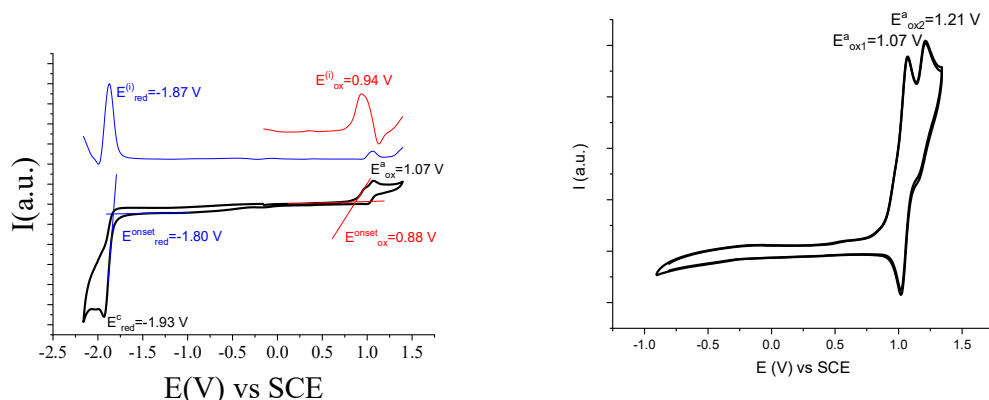


Figure S 27. Cyclic voltammograms of [8]CPP recorded in DCM + Bu₄NPF₆ 0.2 M in presence of [8]CPP. Platinum Working electrode, 100 mV/s. Combined oxidative-reductive responses (left) and two recurrent cycles between -0.90 V and 1.33 V (right). The first derivative of the voltammograms are shown as red and blue traces and allow estimation of the inflection potentials $E^{(i)}$.

5.5 Study of the (un)bridged biphenylene units

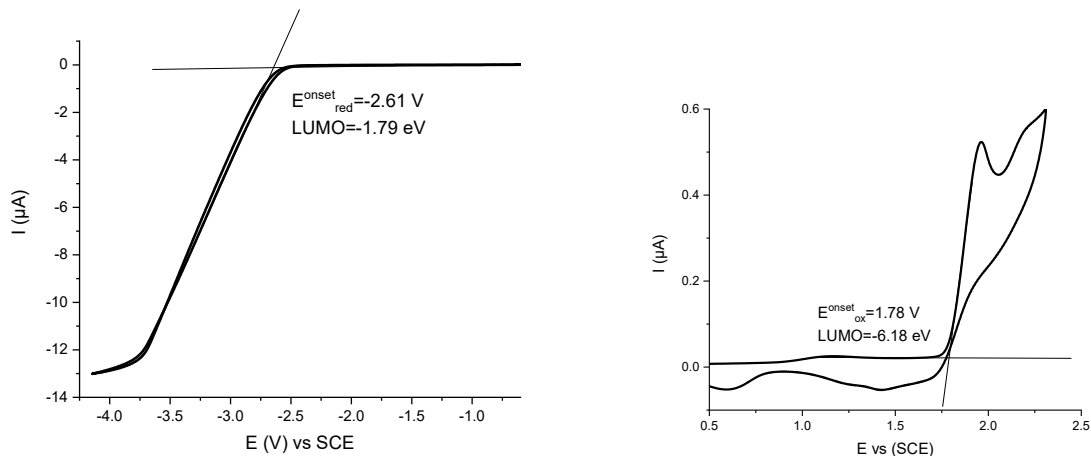


Figure S 28 Cyclic voltammograms recorded in DCM + Bu₄NPF₆ 0.2 M in presence of **biphenyl** (reduction, left). Cyclic voltammogram recorded in DMF + Bu₄NPF₆ 0.1 M in presence of **biphenyl** (oxidation, right).

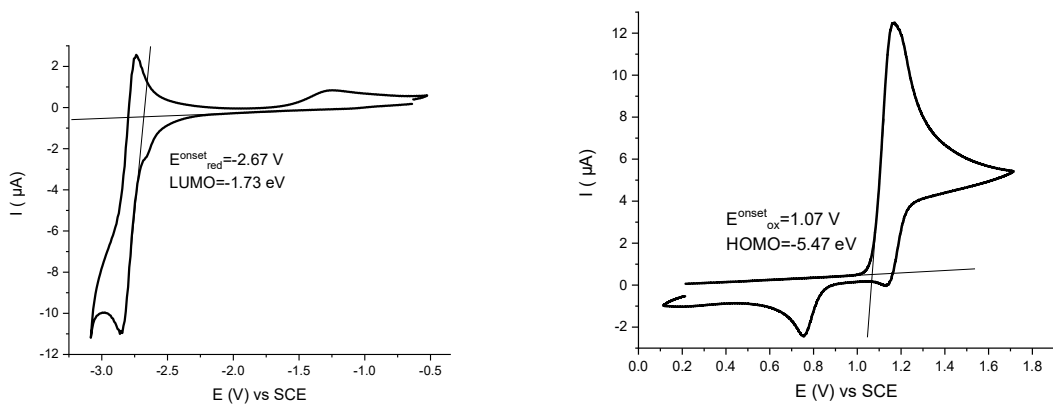


Figure S 29 Cyclic voltammogram recorded in DCM + Bu_4NPF_6 0.2 M in presence of ***N*-butyl-carbazole** (reduction, left). Cyclic voltammogram recorded in DMF + Bu_4NPF_6 0.1 M in presence of ***N*-butyl-carbazole** (oxidation, right).

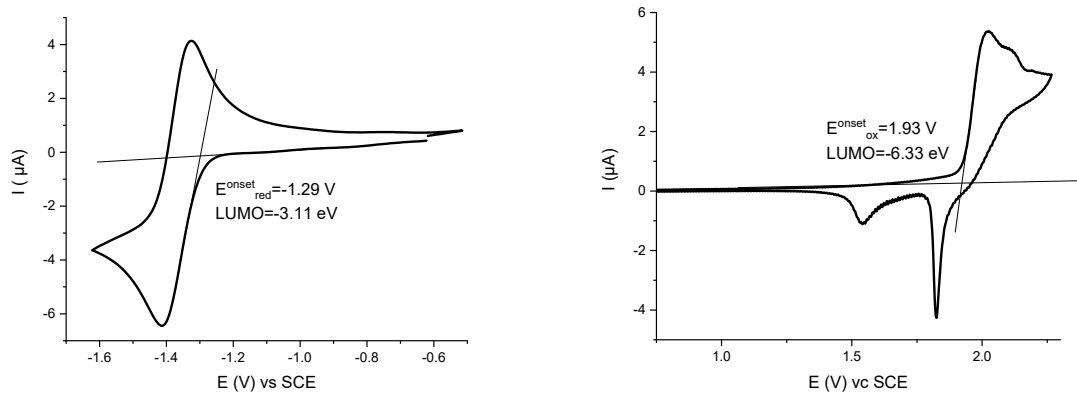


Figure S 30 Cyclic voltammogram recorded in DCM + Bu_4NPF_6 0.2 M in presence of **fluorenone** (reduction, left). Cyclic voltammogram recorded in DMF + Bu_4NPF_6 0.1 M in presence of **fluorenone** (oxidation, right).

5 Molecular modelling

5.1 TD-DFT calculations and atomic coordinates

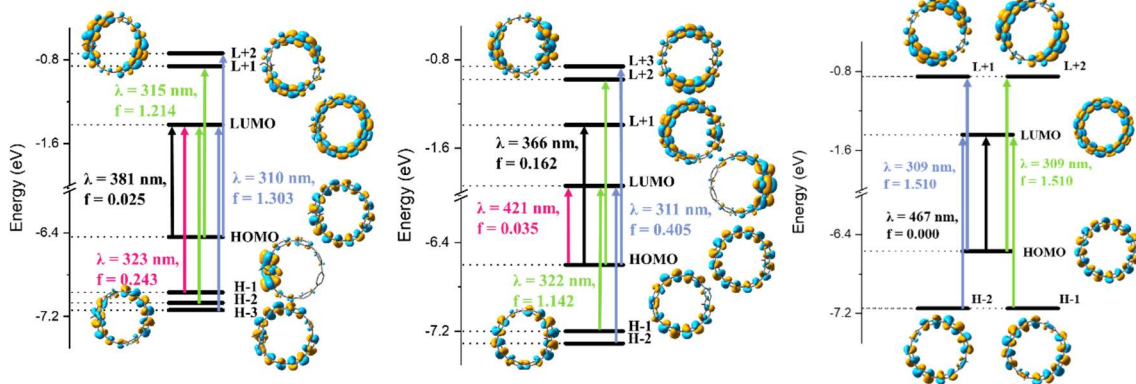


Figure S 31 Molecular diagrams of [8]CPP-N-Bu, [8]CPP-C=O and [8]CPP (TD-DFT, m062x/6-311+G(d,p)). For clarity, only the major contributions of each transition are shown.

Table S 8 Results of TD-DFT calculations for [8]CPP

λ (nm)	Oscillator strength	Major contributions	Minor contributions
372	0.00	H-2→L+1 (10%), H-1→L+2 (10%), HOMO→LUMO (78%)	
309	1.510	H-1→LUMO (45%), HOMO→L+2 (45%)	
309	1.510	H-2→LUMO (45%), HOMO→L+1 (45%)	
275	0.000	H-5→LUMO (10%), H-2→L+6 (10%), H-1→L+5 (10%), HOMO→L+4 (42%)	H-7→L+1 (4%), H-6→L+2 (4%), H-2→L+5 (3%), H-1→L+6 (3%)
273	0.007	H-1→L+4 (15%), HOMO→L+5 (29%)	H-6→LUMO (8%), H-5→L+2 (4%), H-2→LUMO (8%), H-2→L+7 (3%), H-1→L+8 (3%), HOMO→L+1 (5%), HOMO→L+6 (5%)
273	0.007	H-2→L+4 (15%), HOMO→L+6 (29%)	H-7→LUMO (8%), H-5→L+1 (4%), H-2→L+8 (3%), H-1→LUMO (8%), H-1→L+7 (3%), HOMO→L+2 (5%), HOMO→L+5 (5%)
267	0.00	HOMO→L+7 (24%)	H-8→LUMO (7%), H-4→LUMO (7%), H-3→L+4 (3%), H-2→L+1 (5%), H-2→L+2 (4%), H-2→L+5 (5%), H-2→L+17 (2%), H-1→L+1 (4%), H-1→L+2 (5%), H-1→L+6 (5%), H-1→L+16 (2%), HOMO→L+12 (4%)
267	0.00	HOMO→L+8 (24%)	H-9→LUMO (7%), H-4→L+4 (3%), H-3→LUMO (7%), H-2→L+1 (4%), H-2→L+2 (5%),

			H-2→L+6 (5%), H-2→L+16 (2%), H-1→L+1 (5%), H-1→L+2 (4%), H-1→L+5 (5%), H-1→L+17 (2%), HOMO→L+13 (4%)
265	0.003	H-2→LUMO (15%), H-1→LUMO (22%), HOMO→L+1 (12%), HOMO→L+2 (29%)	HOMO→L+5 (4%)
265	0.003	H-2→LUMO (22%), H-1→LUMO (15%), HOMO→L+1 (29%), HOMO→L+2 (12%)	HOMO→L+6 (4%)
257	0.000	H-10→LUMO (13%), HOMO→L+17 (15%)	H-12→L+2 (7%), H-11→LUMO (7%), H-9→L+1 (2%), H-8→L+2 (2%), H-2→L+7 (2%), H-2→L+8 (3%), H-2→L+13 (2%), H-1→L+7 (3%), H-1→L+8 (2%), H-1→L+12 (2%), H-1→L+20 (7%), HOMO→L+16 (7%)
257	0.000	H-11→LUMO (13%), HOMO→L+16 (15%)	H-12→L+1 (7%), H-10→LUMO (7%), H-9→L+2 (2%), H-8→L+1 (2%), H-2→L+7 (3%), H-2→L+8 (2%), H-2→L+12 (2%), H-2→L+20 (7%), H-1→L+7 (2%), H-1→L+8 (3%), H-1→L+13 (2%), HOMO→L+17 (7%)
256	0.000	H-2→L+1 (15%), H-1→L+2 (15%), HOMO→L+13 (17%)	H-9→LUMO (7%), H-3→LUMO (7%), H-2→L+2 (8%), H-2→L+6 (3%), H-1→L+1 (8%), H-1→L+5 (3%), HOMO→L+18 (3%)
256	0.000	H-2→L+2 (15%), H-1→L+1 (15%), HOMO→L+12 (17%)	H-8→LUMO (7%), H-4→LUMO (7%), H-2→L+1 (8%), H-2→L+5 (3%), H-1→L+2 (8%), H-1→L+6 (3%), HOMO→L+19 (3%)
254	0.000	H-2→L+2 (44%), H-1→L+1 (44%)	
253	0.003	H-12→LUMO (23%), HOMO→L+20 (20%)	H-11→L+1 (9%), H-10→L+2 (9%), H-4→L+7 (3%), H-3→L+8 (3%), H-2→L+16 (8%), H-1→L+17 (8%)
247	0.00	H-2→L+1 (33%), H-1→L+2 (33%), HOMO→LUMO (19%)	HOMO→L+3 (9%)
242	0.00	HOMO→L+3 (68%)	H-2→L+1 (4%), H-2→L+10 (5%), H-1→L+2 (4%), H-1→L+9 (5%), HOMO→LUMO (2%)
234	0.026	H-2→L+3 (20%), HOMO→L+10 (38%)	H-6→LUMO (7%), H-5→L+2 (2%), HOMO→L+5 (8%),

			HOMO→L+6 (7%), HOMO→L+9 (3%)
234	0.026	H-1→L+3 (20%), HOMO→L+9 (38%)	H-7→LUMO (7%), H-5→L+1 (2%), HOMO→L+5 (7%), HOMO→L+6 (8%), HOMO→L+10 (3%)

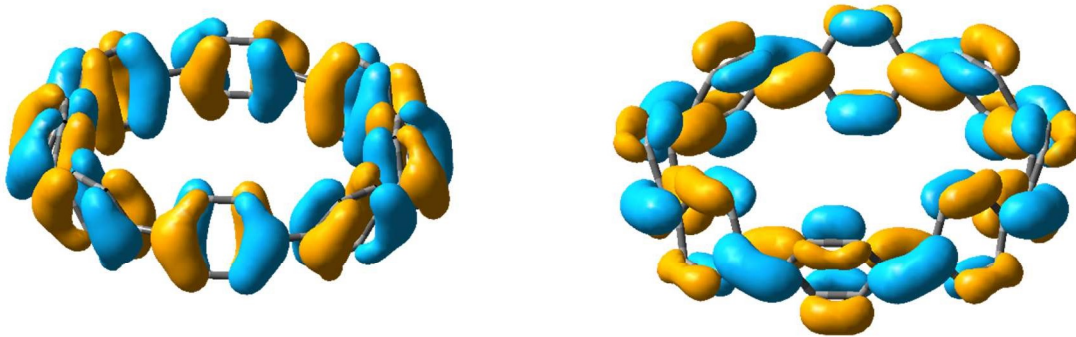


Figure S 32 Side view of the HOMO (left) and LUMO (right) orbitals of **[8]CPP** (TD-DFT, m062x/6-311+g(d,p)).

Table S 9 Atomic coordinates of **[8]CPP** at the fundamental state after geometry optimization.

Atom	X (Å)	Y (Å)	Z (Å)
C	-5.498941	1.647494	1.857566
H	-5.631352	1.985922	2.88202
C	-5.338981	0.273331	1.592377
C	-4.862953	-0.688449	2.620273
C	-3.947877	-0.228472	3.583835
H	-3.815882	0.839296	3.729472
C	-3.065869	-1.095834	4.214578
H	-2.285172	-0.662289	4.829822
C	-3.051482	-2.473112	3.923131
C	-1.805086	-3.254397	4.149062
C	-0.749462	-2.754646	4.936809
H	-0.936773	-1.974754	5.668376
C	0.567742	-3.136255	4.708327
H	1.351148	-2.605809	5.240404
C	0.90222	-4.066087	3.704727
C	-2.247541	4.045096	-3.068702
C	-2.381886	4.440037	-1.724094
H	-1.585426	4.992453	-1.237805

C	-3.427439	3.982575	-0.933117
H	-3.400478	4.192778	0.131713
C	-4.395935	3.098252	-1.440499
C	-5.100471	2.207741	-0.481953
C	-5.184054	0.834431	-0.77383
H	-4.993626	0.490359	-1.786155
C	-5.300564	-0.110997	0.239986
H	-5.197132	-1.161676	-0.014622
C	-5.00218	-2.084237	2.501583
H	-5.758454	-2.495949	1.837963
C	-4.12342	-2.954086	3.143064
H	-4.228866	-4.020028	2.962603
C	-3.345813	3.359146	-3.627382
H	-3.3511	3.111799	-4.685082
C	-4.389652	2.890669	-2.832826
H	-5.170238	2.288934	-3.291569
C	-1.492231	-4.359882	3.334335
H	-2.269392	-4.840188	2.748215
C	-0.178012	-4.765892	3.13206
H	0.00603	-5.573449	2.430262
C	-5.382219	2.593456	0.843205
H	-5.425993	3.649139	1.098561
C	5.498941	-1.647494	-1.857566
H	5.631352	-1.985922	-2.88202
C	5.338981	-0.273331	-1.592377
C	4.862953	0.688449	-2.620273
C	3.947877	0.228472	-3.583835
H	3.815882	-0.839296	-3.729472
C	3.065869	1.095834	-4.214578
H	2.285172	0.662289	-4.829822
C	3.051482	2.473112	-3.923131
C	1.805086	3.254397	-4.149062
C	0.749462	2.754646	-4.936809
H	0.936773	1.974754	-5.668376
C	-0.567742	3.136255	-4.708327
H	-1.351148	2.605809	-5.240404
C	-0.90222	4.066087	-3.704727
C	2.247541	-4.045096	3.068702
C	2.381886	-4.440037	1.724094
H	1.585426	-4.992453	1.237805
C	3.427439	-3.982575	0.933117
H	3.400478	-4.192778	-0.131713
C	4.395935	-3.098252	1.440499
C	5.100471	-2.207741	0.481953
C	5.184054	-0.834431	0.77383
H	4.993626	-0.490359	1.786155

C	5.300564	0.110997	-0.239986
H	5.197132	1.161676	0.014622
C	5.00218	2.084237	-2.501583
H	5.758454	2.495949	-1.837963
C	4.12342	2.954086	-3.143064
H	4.228866	4.020028	-2.962603
C	3.345813	-3.359146	3.627382
H	3.3511	-3.111799	4.685082
C	4.389652	-2.890669	2.832826
H	5.170238	-2.288934	3.291569
C	1.492231	4.359882	-3.334335
H	2.269392	4.840188	-2.748215
C	0.178012	4.765892	-3.13206
H	-0.00603	5.573449	-2.430262
C	5.382219	-2.593456	-0.843205
H	5.425993	-3.649139	-1.098561

No imaginary frequency.

Table S 10 Results of TD-DFT calculations for **[8]CPP-N-Bu**.

λ (nm)	Oscillator strength	Major contributions	Minor contributions
381	0.025	HOMO→LUMO (78%)	H-3→L+1 (4%), H-3→L+2 (4%), H-2→L+1 (5%), H-2→L+2 (3%)
323	0.243	H-1→LUMO (50%), H-1→L+2 (19%), HOMO→L+1 (12%)	H-1→L+1 (3%)
315	1.214	H-2→LUMO (39%), HOMO→L+1 (33%)	H-3→LUMO (6%), H-1→L+1 (3%), H-1→L+2 (3%), HOMO→L+2 (6%)
310	1.303	H-3→LUMO (38%), HOMO→L+2 (39%)	H-2→LUMO (6%), HOMO→L+1 (4%)
282	0.024	H-3→L+4 (12%), HOMO→L+4 (42%)	H-6→LUMO (8%), H-6→L+1 (4%), H-1→L+4 (2%), HOMO→L+3 (2%)
275	0.035	H-2→LUMO (30%), HOMO→L+1 (15%), HOMO→L+2 (10%)	H-3→L+4 (2%), H-2→L+2 (3%), H-1→LUMO (3%), H-1→L+1 (3%), HOMO→LUMO (2%), HOMO→L+7 (7%), HOMO→L+8 (2%)
275	0.003	H-2→L+5 (13%), HOMO→L+5 (26%)	H-7→LUMO (7%), H-7→L+1 (5%), H-3→L+5 (3%), H-3→L+7 (2%), H-3→L+9 (2%), H-2→L+6 (2%), HOMO→L+6 (4%)

271	0.020	H-3→LUMO (23%), H-1→LUMO (10%), HOMO→L+1 (25%)	H-2→L+2 (3%), H-1→L+1 (6%), HOMO→L+2 (5%), HOMO→L+7 (3%)
269	0.036	HOMO→L+9 (18%)	H-10→LUMO (2%), H-8→LUMO (3%), H-5→LUMO (2%), H-4→LUMO (2%), H-3→L+1 (5%), H-3→L+5 (3%), H-2→L+1 (6%), H-2→L+4 (3%), H-2→L+9 (3%), H-1→L+1 (6%), H-1→L+2 (2%), HOMO→L+2 (2%), HOMO→L+10 (2%)
268	0.031	H-3→LUMO (10%), HOMO→L+2 (21%)	H-4→LUMO (2%), H-3→L+1 (6%), H-2→LUMO (5%), H-1→L+1 (6%), HOMO→LUMO (2%), HOMO→L+7 (6%), HOMO→L+8 (3%), HOMO→L+9 (4%)
263	0.027		H-9→LUMO (6%), H-8→LUMO (4%), H-3→L+18 (3%), H-2→L+1 (5%), H-2→L+4 (3%), H-2→L+5 (2%), H-1→L+2 (3%), HOMO→L+2 (2%), HOMO→L+3 (3%), HOMO→L+11 (6%), HOMO→L+12 (9%), HOMO→L+14 (3%)
259	0.006	H-2→L+1 (24%)	H-9→LUMO (2%), H-5→LUMO (3%), H-3→L+1 (2%), H-1→L+1 (8%), HOMO→L+3 (5%), HOMO→L+12 (5%), HOMO→L+18 (5%)
257	0.003	H-2→L+1 (15%)	H-12→LUMO (3%), H-12→L+1 (3%), H-11→LUMO (6%), H-10→LUMO (3%), H-3→LUMO (4%), H-3→L+1 (3%), H-2→L+2 (3%), H-2→L+9 (4%), H-1→LUMO (3%), HOMO→L+3 (3%), HOMO→L+15 (2%), HOMO→L+18 (8%)
256	0.001	HOMO→L+3 (53%)	H-11→LUMO (3%), H-3→L+1 (7%), H-3→L+2 (3%), H-1→L+1 (2%)
255	0.005	H-12→LUMO (11%)	H-11→LUMO (5%), H-11→L+1 (7%), H-10→L+2 (2%), H-3→L+2 (6%), H-3→L+18 (2%), H-2→L+1 (3%), H-2→L+2 (4%), H-2→L+18 (2%), H-1→L+2 (4%), HOMO→L+15 (2%), HOMO→L+19 (6%)

254	0.001	H-3→L+1 (10%), H-1→LUMO (13%), H-1→L+2 (23%)	H-3→LUMO (3%), H-2→L+2 (5%), HOMO→L+3 (4%), HOMO→L+12 (3%)
253	0.002	H-2→L+2 (22%), H-1→L+1 (19%)	H-12→LUMO (2%), H-3→L+2 (4%), H-2→L+1 (7%), H-1→LUMO (5%), H-1→L+2 (5%), HOMO→L+3 (4%)
252	0.009	H-3→L+1 (18%), H-3→L+2 (21%)	H-12→LUMO (4%), H-5→LUMO (2%), H-3→LUMO (2%), H-2→L+1 (3%), H-2→L+2 (4%), H-1→LUMO (8%), H-1→L+1 (5%)
249	0.004	H-3→L+1 (11%), H-3→L+2 (11%), H-1→L+1 (11%)	H-4→LUMO (3%), H-2→LUMO (2%), H-2→L+1 (2%), H-2→L+2 (6%), HOMO→LUMO (7%), HOMO→L+2 (2%), HOMO→L+3 (4%), HOMO→L+4 (4%), HOMO→L+6 (3%), HOMO→L+7 (3%), HOMO→L+21 (2%)
245	0.034	H-3→L+2 (12%), H-2→L+2 (11%)	H-4→LUMO (5%), H-3→L+1 (4%), H-2→L+1 (7%), HOMO→LUMO (6%), HOMO→L+3 (3%), HOMO→L+4 (5%), HOMO→L+7 (6%), HOMO→L+26 (2%)

Table S 11 Atomic coordinates of [8]CPP-N-Bu at the fundamental state after geometry optimization.

Atom	X (Å)	Y (Å)	Z (Å)
C	-4.13004	-1.32	0.004595
C	-4.705242	-0.992434	-1.25123
C	-4.865896	-2.025149	-2.189437
H	-5.345127	-1.830726	-3.14559
C	-4.321732	-3.281101	-1.936287
H	-4.39577	-4.049217	-2.700652
C	-3.596559	-3.550647	-0.7474
C	-3.59343	-2.578934	0.264928
H	-3.012839	-2.738432	1.165581
C	-4.242828	0.92382	-0.066912
C	-4.771441	0.456099	-1.301197
C	-5.008972	1.393445	-2.319886
H	-5.445227	1.078458	-3.264443
C	-4.586732	2.710373	-2.160378
H	-4.697349	3.409016	-2.985116

C	-3.935321	3.135631	-0.976913
C	-3.855006	2.250931	0.107855
H	-3.314695	2.553665	0.997631
C	-2.565146	-4.620314	-0.655028
C	-1.86291	-5.021956	-1.807047
H	-2.273449	-4.809082	-2.789522
C	-0.568442	-5.525765	-1.7254
H	-0.037715	-5.732976	-2.649866
C	0.101954	-5.621471	-0.490372
C	-0.698609	-5.474971	0.659814
H	-0.260729	-5.603903	1.644924
C	-2.004662	-5.004774	0.578394
H	-2.551509	-4.823701	1.499736
C	1.582954	-5.509608	-0.391954
C	2.295589	-4.921653	-1.454357
H	1.822024	-4.800337	-2.422505
C	3.526253	-4.310276	-1.253518
H	3.959147	-3.739355	-2.069313
C	4.111352	-4.247361	0.023507
C	3.513362	-5.031477	1.02857
H	3.976399	-5.09365	2.010231
C	2.2837	-5.653306	0.823186
H	1.828017	-6.187348	1.652441
C	5.059012	-3.138079	0.306754
C	5.896443	-2.583062	-0.680553
H	6.13726	-3.161436	-1.568835
C	6.339869	-1.266267	-0.591503
H	6.917691	-0.848365	-1.411854
C	5.965568	-0.443293	0.488536
C	5.329211	-1.073701	1.573107
H	5.035769	-0.485014	2.437116
C	4.887311	-2.389419	1.484871
H	4.263935	-2.783111	2.282265
C	5.89807	1.03819	0.384211
C	5.557537	1.609562	-0.855213
H	5.604647	1.003651	-1.754962
C	4.973005	2.86851	-0.933575
H	4.584132	3.200313	-1.8915
C	4.700018	3.619688	0.223709
C	5.24984	3.144644	1.430557
H	5.149132	3.735304	2.33747
C	5.834264	1.882993	1.509297
H	6.175055	1.51977	2.475502
C	3.607078	4.626444	0.17777
C	3.253928	5.321958	-0.99514
H	3.97375	5.413419	-1.804505

C	1.962821	5.809596	-1.183809
H	1.70934	6.269283	-2.135557
C	0.962514	5.621004	-0.209903
C	1.386923	5.138365	1.041714
H	0.659596	4.990814	1.833925
C	2.675746	4.654197	1.231158
H	2.906494	4.148253	2.163739
C	-0.487392	5.562527	-0.537244
C	-0.879406	5.095119	-1.805045
H	-0.153264	5.058623	-2.611545
C	-2.113601	4.481908	-1.998746
H	-2.310296	3.989313	-2.946634
C	-3.006819	4.299472	-0.928753
C	-2.718607	4.989667	0.264061
H	-3.429545	4.958111	1.086195
C	-1.487599	5.611977	0.454066
H	-1.269333	6.062217	1.419006
C	-3.314217	-0.119801	2.061487
H	-2.415234	-0.748985	2.028555
H	-5.06566	1.377585	3.661857
C	-6.329949	-0.110749	4.593343
H	-6.736893	-1.108888	4.390514
H	-7.176214	0.569628	4.739656
N	-3.95983	-0.162761	0.757359
H	-2.970597	0.903659	2.233604
C	-4.229262	-0.563548	3.213702
H	-3.617712	-0.616291	4.125823
H	-4.583588	-1.584647	3.018443
C	-5.428969	0.361969	3.448062
H	-6.016394	0.434253	2.524185
H	-5.777649	-0.164351	5.539767

No imaginary frequency.

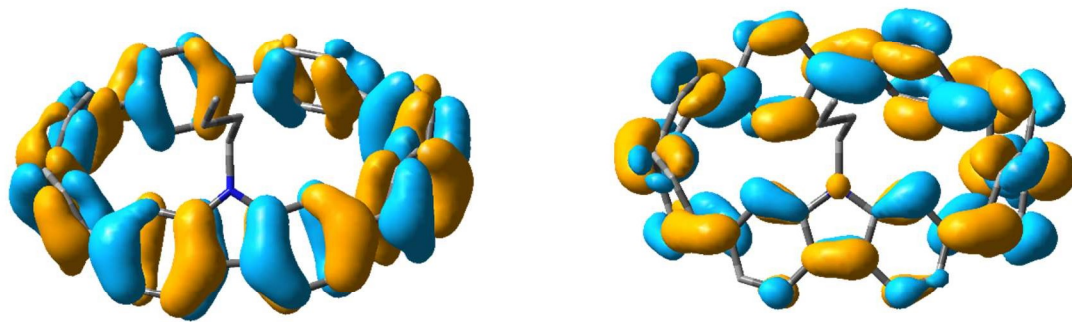


Figure S 33 Side view of the HOMO (left) and LUMO (right) orbitals of **[8]CPP-N-Bu** (TD-DFT, m062x/6-311+g(d,p)).

Table S 12 Results of TD-DFT calculations for **[8]CPP-C=O**.

λ (nm)	Oscillator strength	Major contributions	Minor contributions
421	0.035	H-2→LUMO (26%), HOMO→LUMO (60%)	H-3→LUMO (2%), H-2→L+1 (4%), H-1→L+2 (2%)
381	0.000	H-13→LUMO (67%), H-13→L+1 (16%)	
366	0.162	H-2→LUMO (13%), HOMO→L+1 (62%)	H-3→LUMO (3%), H-2→L+3 (6%), H-1→L+2 (7%), HOMO→LUMO (2%)
322	1.143	H-1→LUMO (56%), HOMO→L+2 (25%)	H-1→L+1 (6%)
311	0.406	H-2→LUMO (23%), H-2→L+1 (11%), HOMO→L+3 (23%)	H-11→LUMO (8%), H-3→LUMO (4%), H-2→L+3 (6%), HOMO→LUMO (9%), HOMO→L+1 (5%)
303	0.456	H-2→L+1 (10%), HOMO→LUMO (18%), HOMO→L+1 (11%), HOMO→L+2 (10%), HOMO→L+3 (15%)	H-3→LUMO (2%), H-2→LUMO (8%), H-1→LUMO (6%), H-1→L+1 (9%)
296	0.319	H-1→LUMO (21%), H-1→L+1 (19%), HOMO→L+2 (19%)	H-3→LUMO (2%), H-2→LUMO (6%), H-2→L+1 (6%), HOMO→LUMO (4%), HOMO→L+3 (9%)
285	0.008	H-1→L+4 (15%), HOMO→L+4 (48%)	H-5→L+1 (3%), H-4→L+1 (4%)
280	0.541	H-11→LUMO (29%), H-3→LUMO (10%), H-2→LUMO (10%), H-1→L+2 (10%)	H-11→L+1 (2%), H-2→L+1 (9%), H-2→L+3 (4%), HOMO→L+5 (2%)

			HOMO→L+6 (3%), HOMO→L+7 (2%)
273	0.030	H-1→L+6 (12%), HOMO→L+6 (24%)	H-7→L+2 (3%), H-6→LUMO (3%), H-6→L+1 (3%), H-6→L+2 (2%), H-5→L+1 (2%), H-5→L+2 (2%), H-1→L+3 (3%), H-1→L+7 (6%), HOMO→L+7 (7%)
270	0.004	H-1→L+1 (31%), HOMO→L+2 (26%)	H-12→LUMO (9%), H-1→LUMO (6%), HOMO→L+13 (2%)
268	0.003		H-11→LUMO (2%), H-8→L+2 (4%), H-7→LUMO (4%), H-7→L+1 (7%), H-4→L+1 (2%), H-2→L+1 (2%), H-2→L+4 (6%), H-1→L+6 (4%), H-1→L+13 (3%), HOMO→L+7 (3%), HOMO→L+8 (3%), HOMO→L+9 (8%), HOMO→L+10 (7%), HOMO→L+11 (8%), HOMO→L+13 (4%)
263	0.012	H-1→L+3 (12%), HOMO→L+13 (14%)	H-8→LUMO (4%), H-8→L+1 (4%), H-6→L+1 (2%), H-2→L+1 (5%), H-2→L+6 (3%), H-1→L+1 (7%), H-1→L+11 (2%), HOMO→L+2 (3%), HOMO→L+3 (4%)
262	0.023	H-2→L+1 (18%), HOMO→L+3 (19%)	H-12→LUMO (8%), H-11→LUMO (4%), H-8→L+1 (2%), H-7→LUMO (2%), H-2→L+2 (5%), H-1→L+3 (4%), HOMO→L+13 (4%), HOMO→L+15 (3%)
260	0.009	H-12→LUMO (18%), H-2→L+1 (12%), H-1→L+1 (11%), HOMO→L+3 (15%)	H-2→L+2 (5%), H-1→L+3 (3%), HOMO→L+2 (4%)
258	0.024	H-2→L+2 (12%), H-1→L+2 (14%)	H-11→LUMO (6%), H-10→L+1 (3%), H-9→LUMO (2%), H-9→L+2 (4%), H-5→L+1 (2%), H-2→L+1 (2%), H-2→L+3 (2%), HOMO→L+17 (6%)
255	0.006	H-2→L+2 (15%), HOMO→L+17 (11%)	H-9→LUMO (7%), H-9→L+1 (4%), H-9→L+2 (7%), H-8→L+1 (5%), H-1→L+2 (4%), H-1→L+3 (3%), H-1→L+17 (5%), HOMO→L+18 (2%)
254	0.043	H-10→L+1 (10%), H-2→L+2 (15%)	H-12→LUMO (2%), H-11→LUMO (4%), H-

			10→LUMO (4%), H-10→L+2 (4%), H-9→LUMO (2%), H-1→L+3 (4%), H-1→L+17 (3%), HOMO→L+11 (3%), HOMO→L+22 (7%), HOMO→L+23 (3%)
252	0.101	H-1→L+2 (25%)	H-11→LUMO (6%), H-10→LUMO (8%), H-10→L+1 (5%), H-10→L+2 (2%), H-8→L+1 (2%), H-2→L+2 (3%), H-1→L+3 (3%), HOMO→L+1 (3%), HOMO→L+5 (3%), HOMO→L+7 (2%), HOMO→L+22 (2%), HOMO→L+23 (2%)
248	0.022	H-2→L+3 (24%), H-1→L+3 (14%)	H-12→LUMO (7%), H-3→LUMO (6%), H-3→L+1 (2%), H-2→L+1 (4%), H-2→L+2 (7%), H-1→L+2 (7%), HOMO→L+1 (6%), HOMO→L+7 (3%)

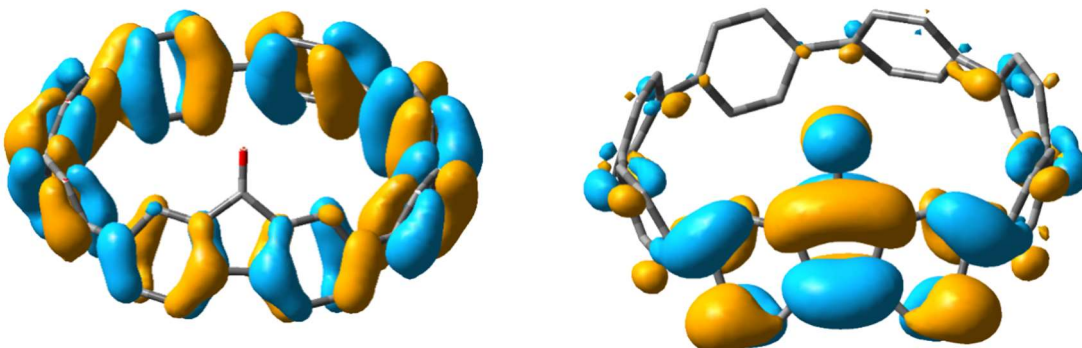


Figure S 34 Side view of the HOMO (left) and LUMO (right) orbitals of [8]CPP-C=O (TD-DFT, m062x/6-311+g(d,p)).

Table S 13 Atomic coordinates of [8]CPP-C=O at the fundamental state after geometry optimization.

Atom	X (Å)	Y (Å)	Z (Å)
O	-3.864866	0.092412	2.852529
C	-4.366292	0.111602	1.743393
C	-4.729342	-1.057292	0.879053
C	-4.663168	1.307163	0.890322
C	-5.325036	0.892149	-0.283707
C	-4.098555	2.56293	1.01266
C	-4.158147	3.459159	-0.076685
C	-4.967114	3.102505	-1.173226
C	-3.103767	4.505943	-0.153355

C	-5.555704	1.833596	-1.285405
C	-5.368067	-0.594218	-0.290059
C	-5.656714	-1.512076	-1.298549
C	-5.140744	-2.812967	-1.199458
C	-4.346786	-3.223988	-0.110549
C	-4.23454	-2.343725	0.987528
C	-3.35119	-4.324004	-0.208297
C	-2.843358	-4.998726	0.916919
C	-2.629025	-4.463705	-1.40652
C	-1.36313	-5.03536	-1.421495
C	-0.750501	-5.501504	-0.24198
C	-1.579767	-5.583025	0.896106
C	0.735232	-5.562334	-0.152261
C	1.387781	-5.467404	1.092907
C	1.552281	-5.385064	-1.286352
C	2.837797	-4.866701	-1.179201
C	3.394098	-4.529332	0.069561
C	2.685727	-4.98145	1.199983
C	-2.580935	5.139505	0.989319
C	-2.357117	4.615354	-1.340059
C	-1.28628	5.651518	0.996874
C	-1.060324	5.116981	-1.328597
C	-0.451016	5.536832	-0.13193
C	1.032223	5.493919	-0.027131
C	1.607688	4.988075	1.152698
C	1.882362	5.612455	-1.144072
C	2.87749	4.423961	1.152015
C	3.15362	5.043073	-1.146236
C	3.635115	4.333174	-0.029581
C	4.656851	3.257573	-0.129036
C	5.359475	2.772178	0.991086
C	4.687689	2.463362	-1.289403
C	5.853127	1.470999	1.021287
C	5.182274	1.163723	-1.259874
C	5.667661	0.597231	-0.067782
C	5.615434	-0.879536	0.090795
C	5.77112	-1.780933	-0.979272
C	5.064056	-1.397971	1.275597
C	4.493736	-2.663514	1.31263
C	5.20762	-3.05416	-0.937512
C	4.448035	-3.484309	0.169976
H	-3.477339	2.779027	1.876505
H	-5.070185	3.799566	-2.000998
H	-6.097509	1.574468	-2.191306
H	-6.187263	-1.214811	-2.19943
H	-5.286414	-3.495713	-2.032626

H	-3.624239	-2.60306	1.84735
H	-3.406592	-4.994871	1.846704
H	-2.991304	-3.981644	-2.309778
H	-0.796904	-4.979325	-2.344388
H	-1.204534	-6.026158	1.813491
H	0.842481	-5.662657	2.010543
H	1.14979	-5.546072	-2.28132
H	3.360771	-4.605949	-2.093982
H	3.107658	-4.857065	2.192593
H	-3.162089	5.15708	1.907825
H	-2.729835	4.156454	-2.25116
H	-0.891494	6.06562	1.920651
H	-0.465272	5.031145	-2.232486
H	1.001123	4.890367	2.0475
H	1.517934	6.085451	-2.052248
H	3.215255	3.9078	2.04529
H	3.747322	5.083166	-2.055927
H	5.447832	3.390492	1.880646
H	4.175863	2.803794	-2.184576
H	6.314724	1.102543	1.933773
H	5.040619	0.532942	-2.132504
H	6.273635	-1.4573	-1.887334
H	4.939603	-0.748607	2.13676
H	3.948506	-2.946948	2.206175
H	5.295558	-3.688993	-1.814723

No imaginary frequency.

5.2 Strain energies calculations

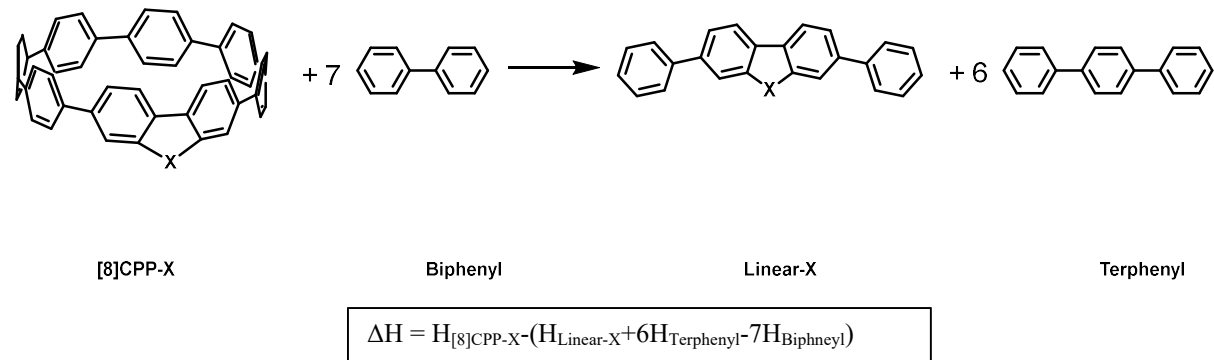
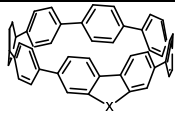
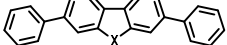
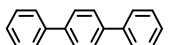


Figure S 35 Strain energy (ΔH) calculation (B3LYP/6-31g(d)).

Table S 14 Strain energies of **[8]CPP-N-Bu** and **[8]CPP-C=O**. Energies are given in kcal.mol⁻¹.

					ΔH
[8]CPP-N-Bu	-1292019.65	-290608.64	-713078.78	-435545.78	73
[8]CPP-C=O	-1229794.69	-290608.64	-650852.89	-290608.64	72

6 NMR study

Protons on the carbazole part and butyl chain are easily identified by 1D and 2D NMR (Fig. S40).

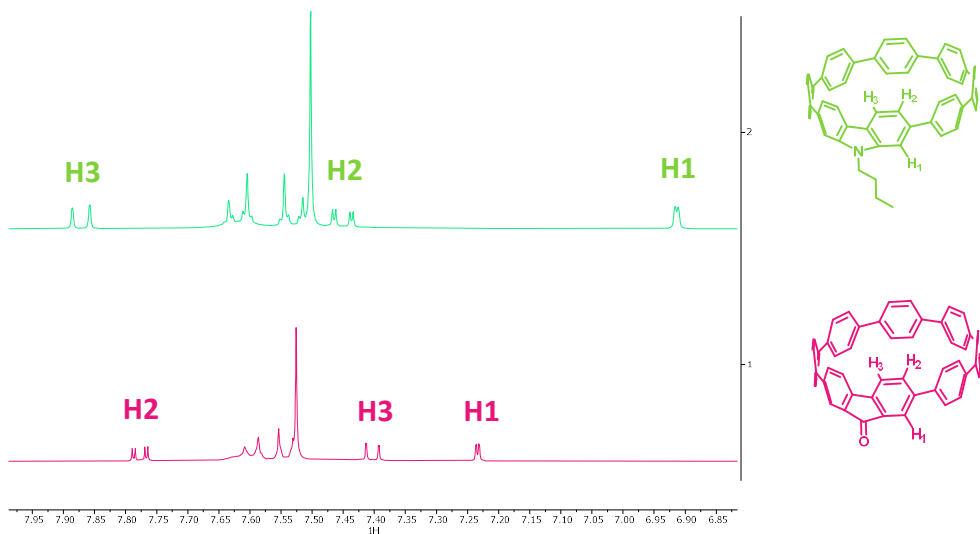


Figure S 36 ¹H NMR spectrum of [8]CPP-N-Bu (top) and [8]CPP-C=O (bottom) in CD₂Cl₂ (aromatic protons region, 400 MHz).

However, protons on the unbridged phenylene units are harder to assign. In order to identify H₄ and H₅ located on the phenyl linked to the carbazole moiety (Fig. S37), we performed NMR at variable temperatures from 303 to 253 K.

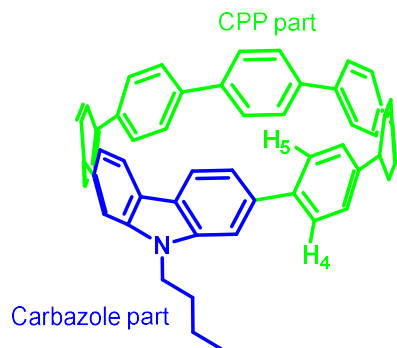


Figure S 37 Representation of [8]CPP-N-Bu with H₄ and H₅.

At room temperature, the nitrogen bridge prevents the tilt of the two bridged phenylene units, whereas the unbridged phenylene units can be more tilted. It is therefore not possible to precisely identify each proton of the unbridged phenylene units. Nevertheless, by lowering the temperature, it is possible to gradually freeze one conformation and observe new proton signals at 7.05 and 7.87 ppm (Fig. S38). H₄ and H₅ which were not observable at room temperature become observable by decreasing the temperature.

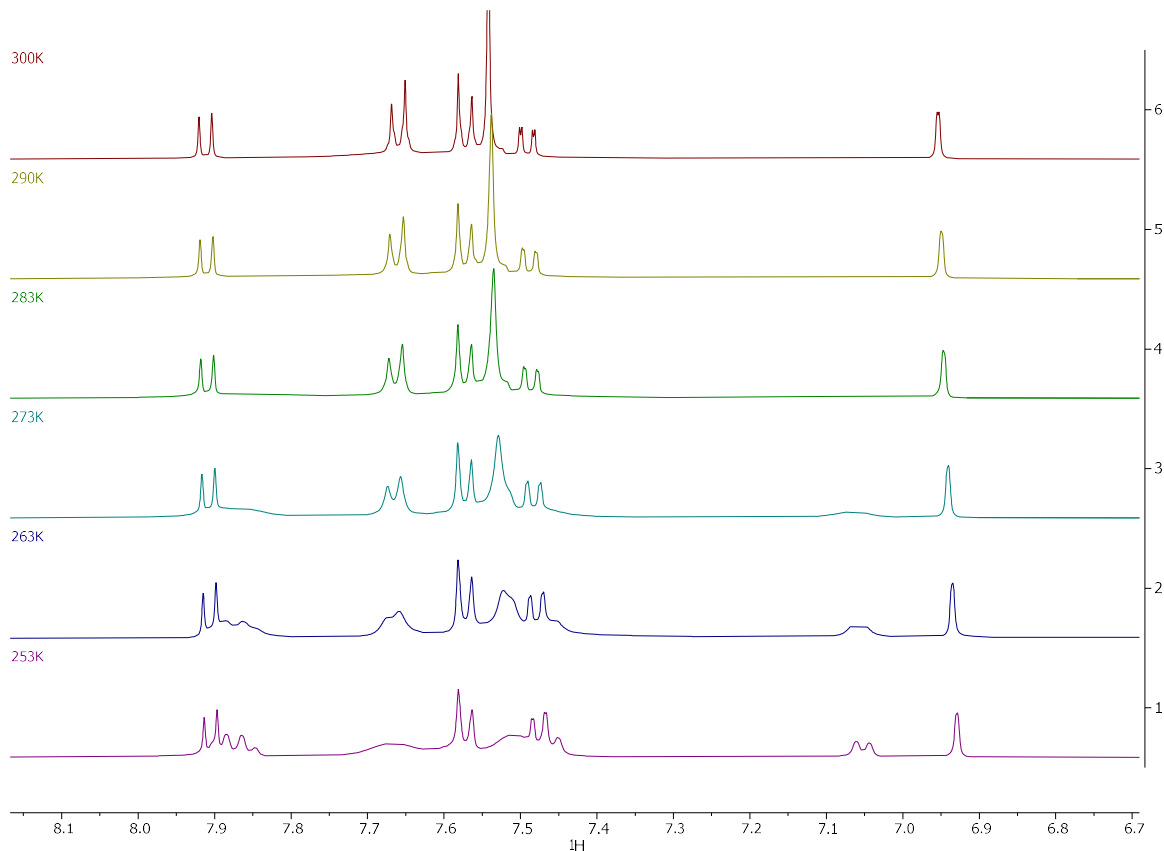


Figure S 38 ^1H NMR performed from 300 to 253K (aromatic protons region, 500 MHz).

Selective NOESY technique at low temperature allowed us to identify H_4 and H_5 thanks to the dipolar coupling with nearby protons (Fig. S39). H_1 is coupled with the butyl chain (H_a), H_4 and H_5 . However, we can't discriminate H_4 and H_5 .

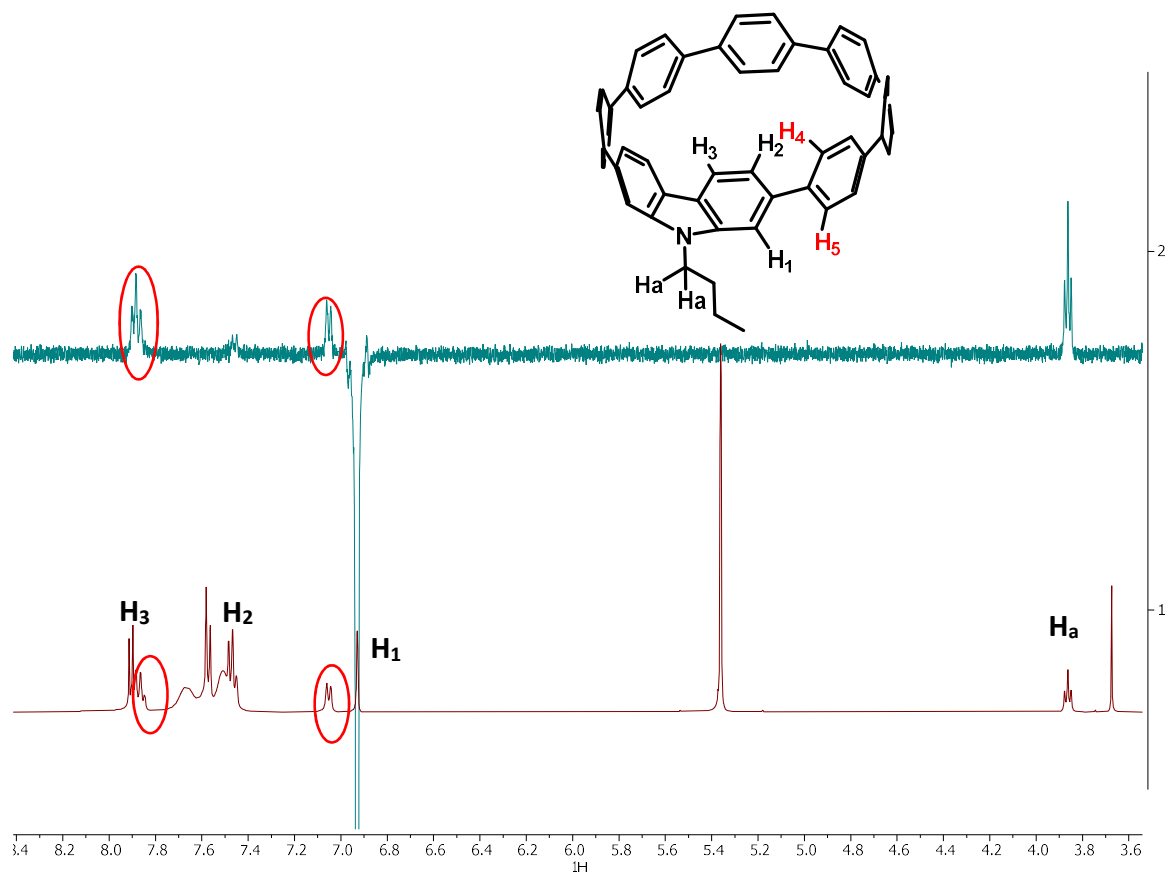


Figure S 39 Selective (irradiated on H_1) NOESY at 253K (up) and ^1H spectra at 253K (bottom), H_4 and H_5 are encircled in red (500 MHz).

7 Copy of NMR spectra

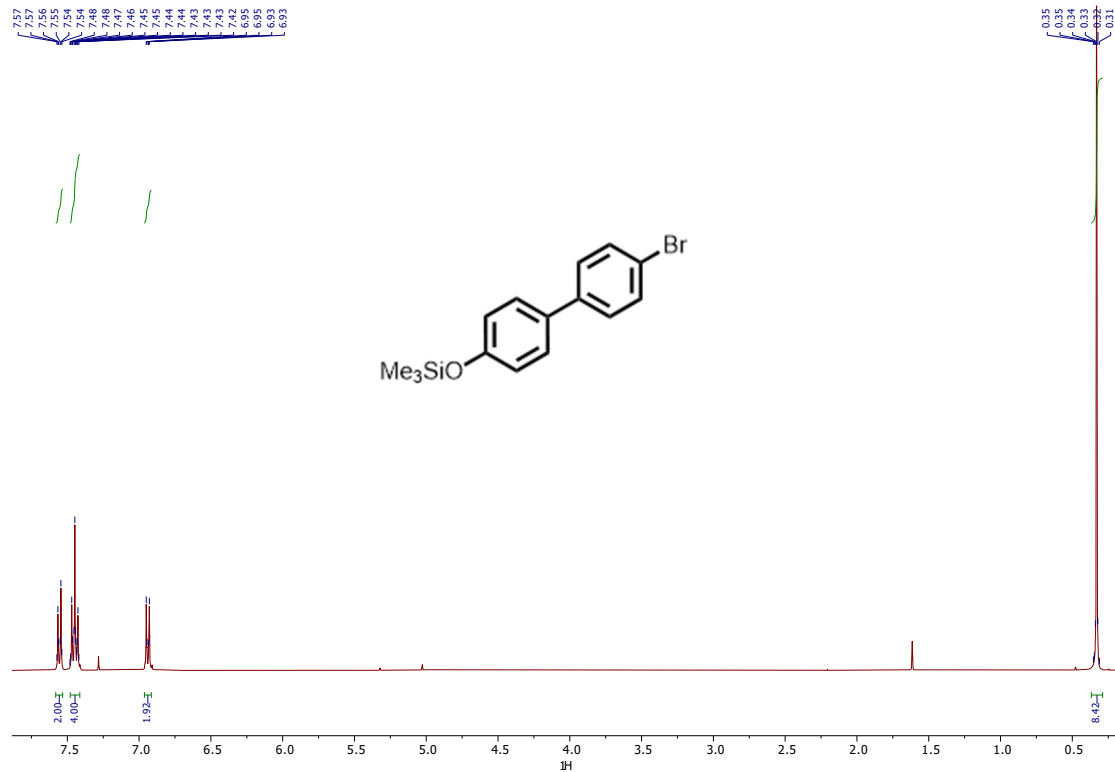


Figure S 40 ^1H -NMR of A (400 MHz).

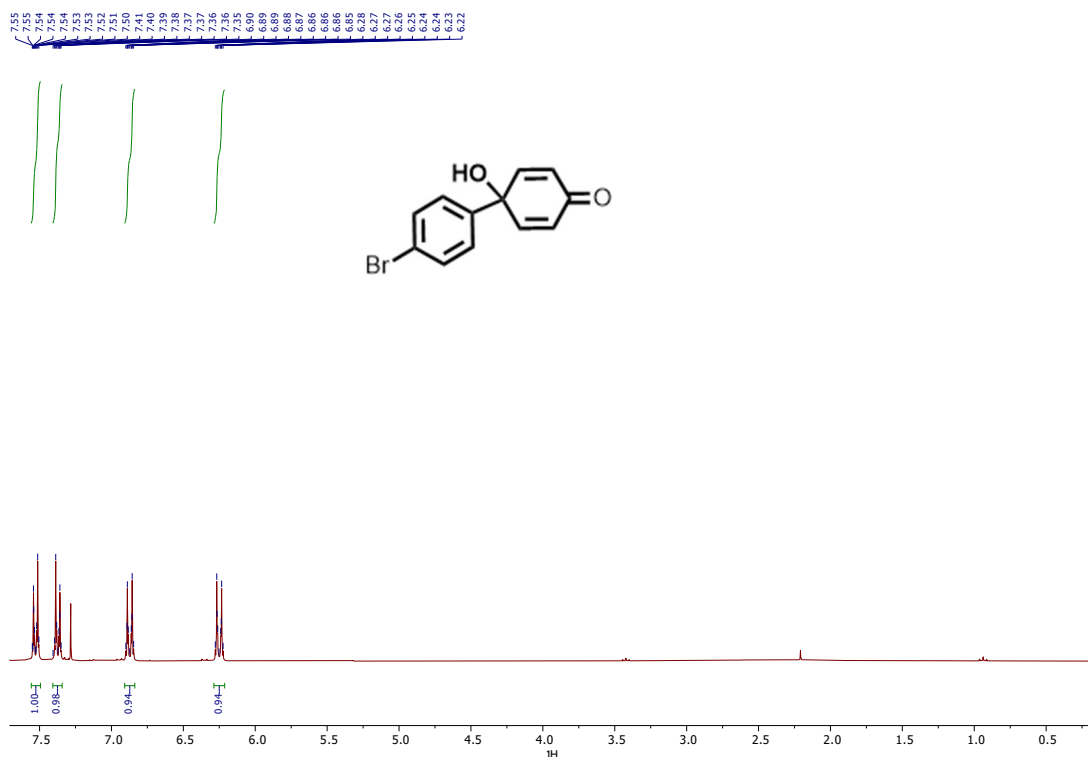


Figure S 41 ^1H -NMR of B (300 MHz).

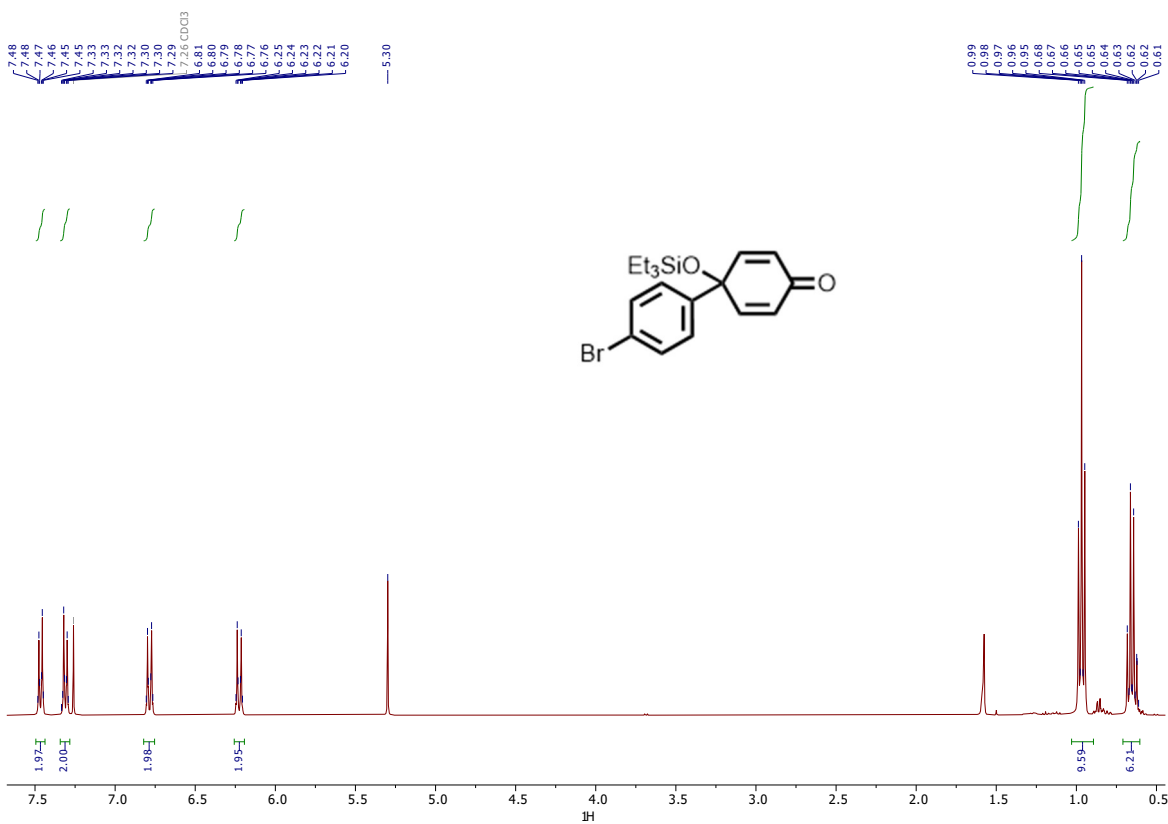


Figure S 42 ^1H -NMR of **C** (400 MHz).

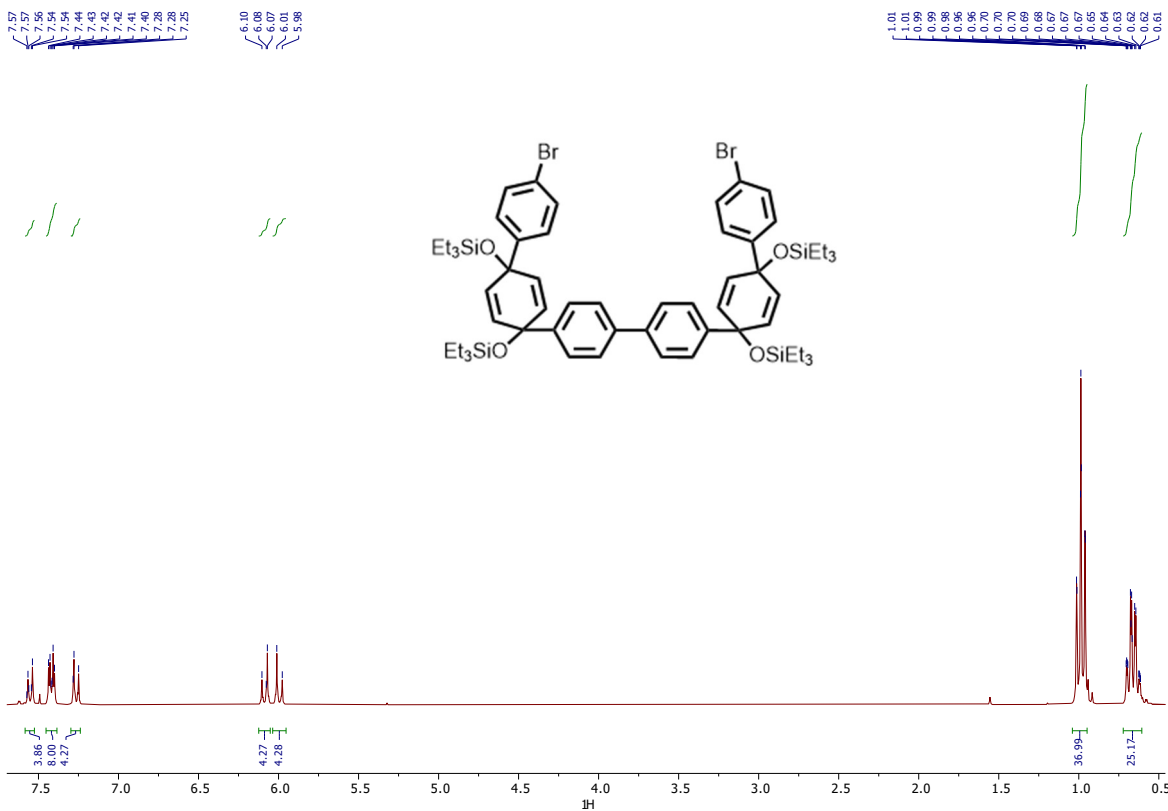


Figure S 43 ^1H -NMR of **1** (300 MHz).

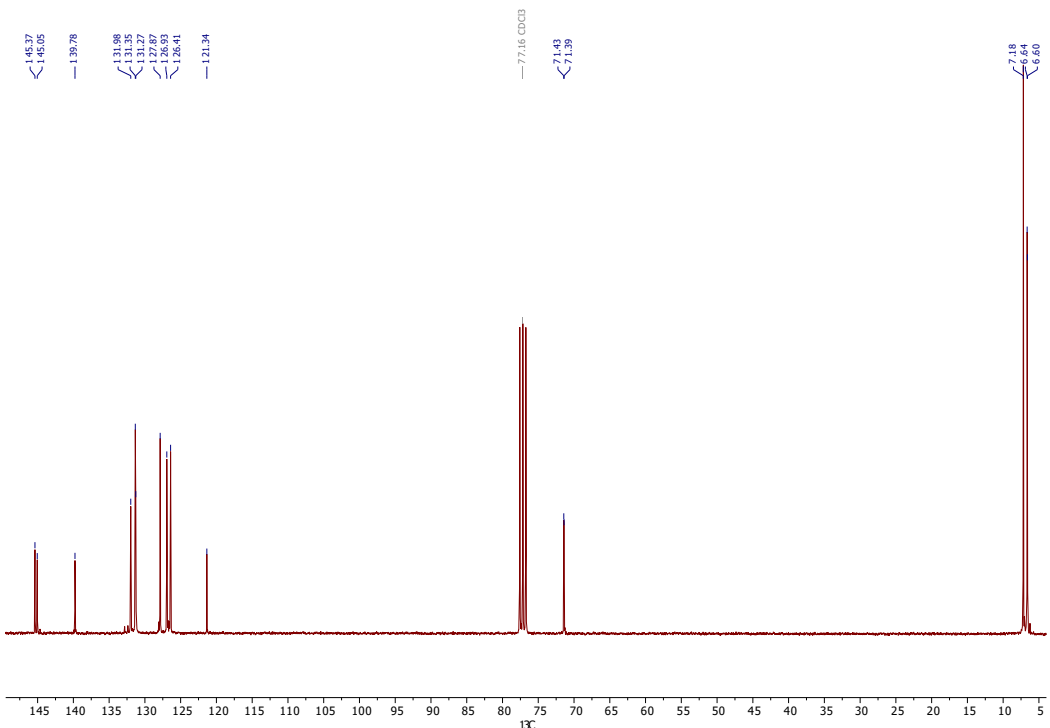


Figure S 44 ^{13}C -NMR of **1** (300 MHz).

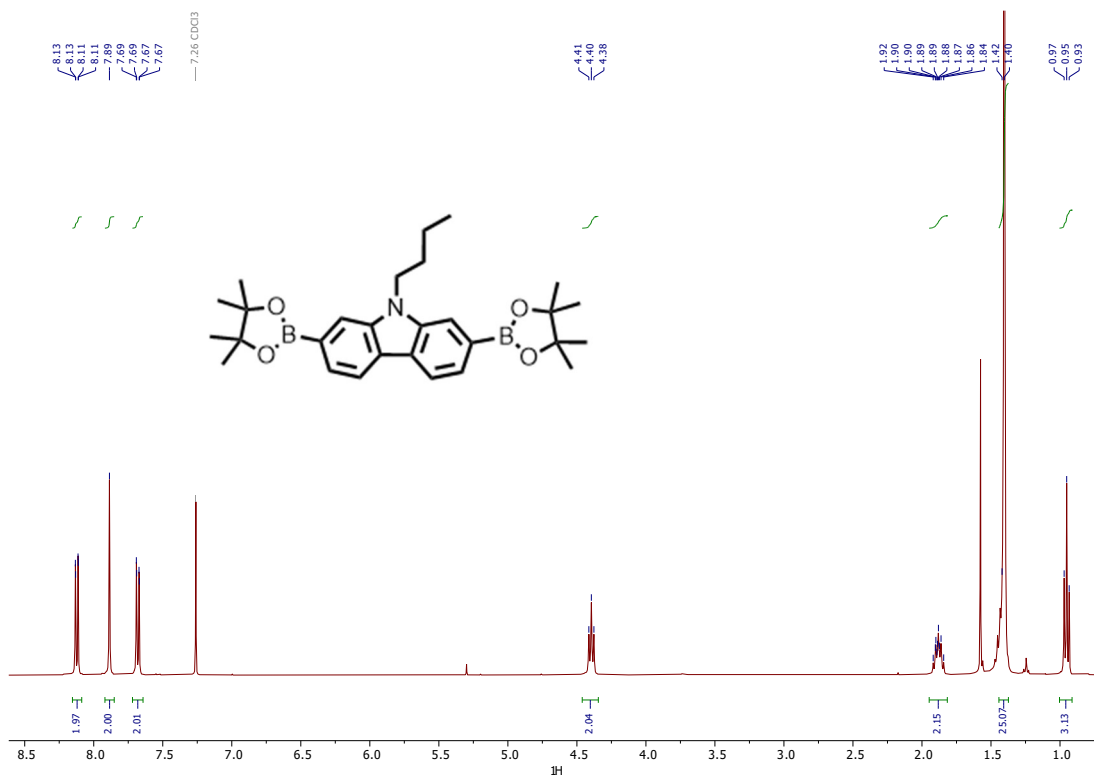


Figure S 45 ^1H -NMR of **2a** (400 MHz).

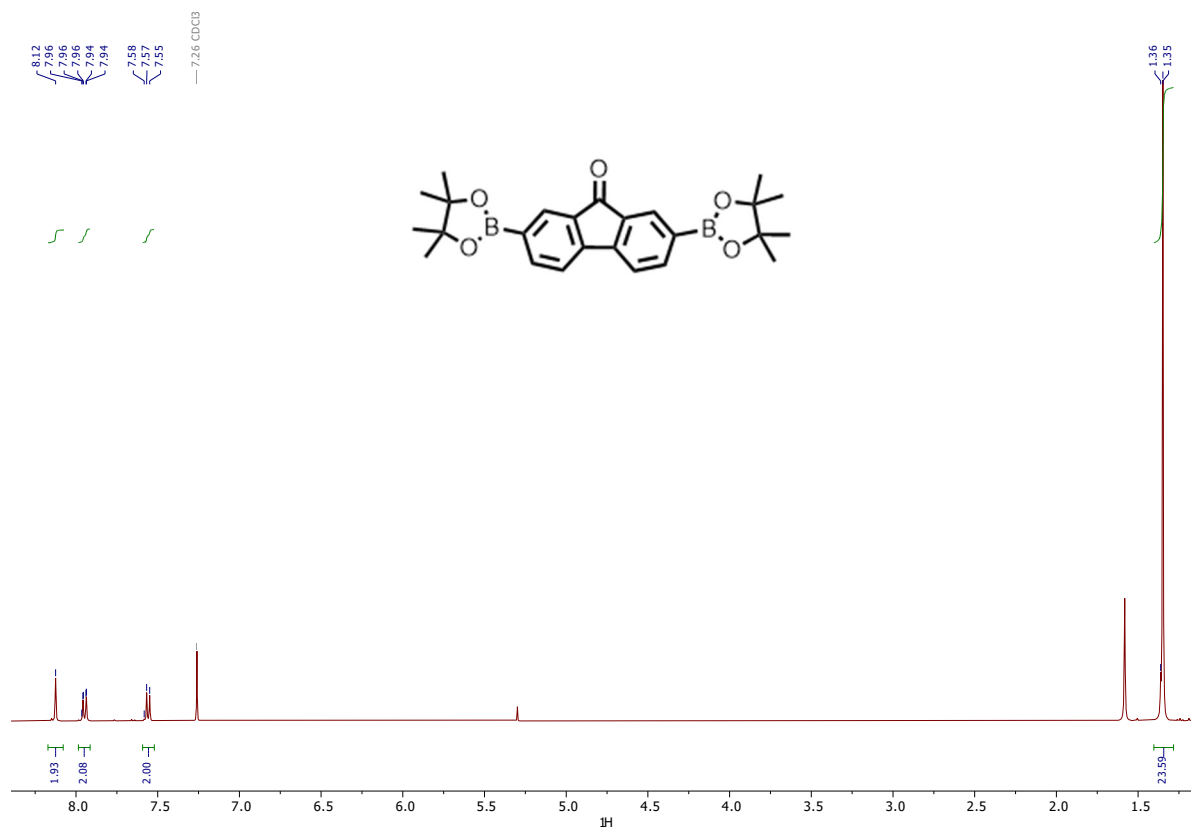


Figure S 46 ¹H-NMR of **2b** (400 MHz).

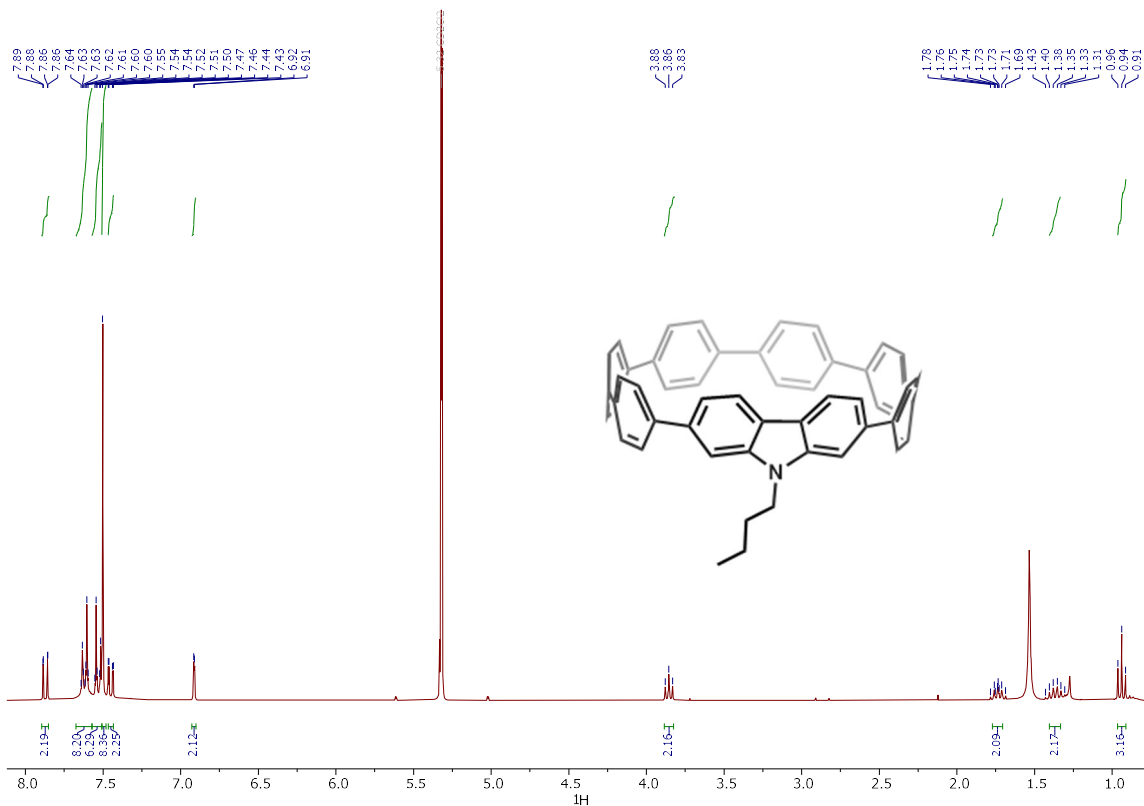
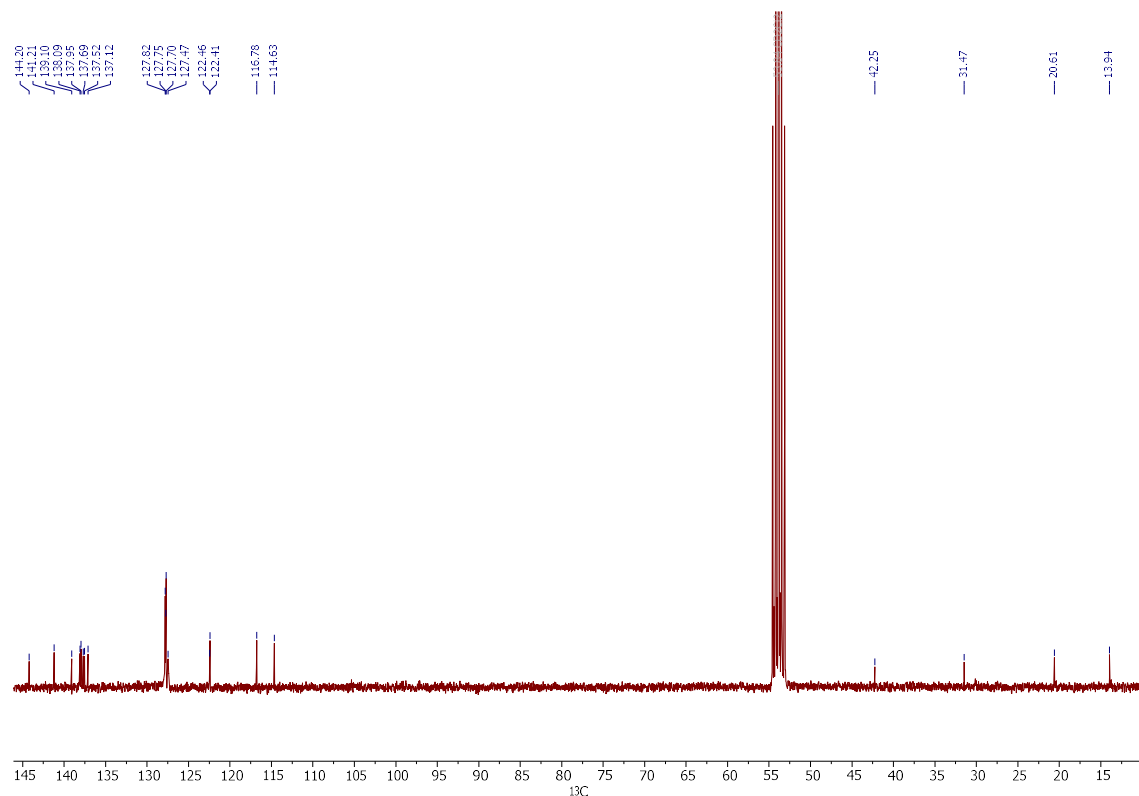
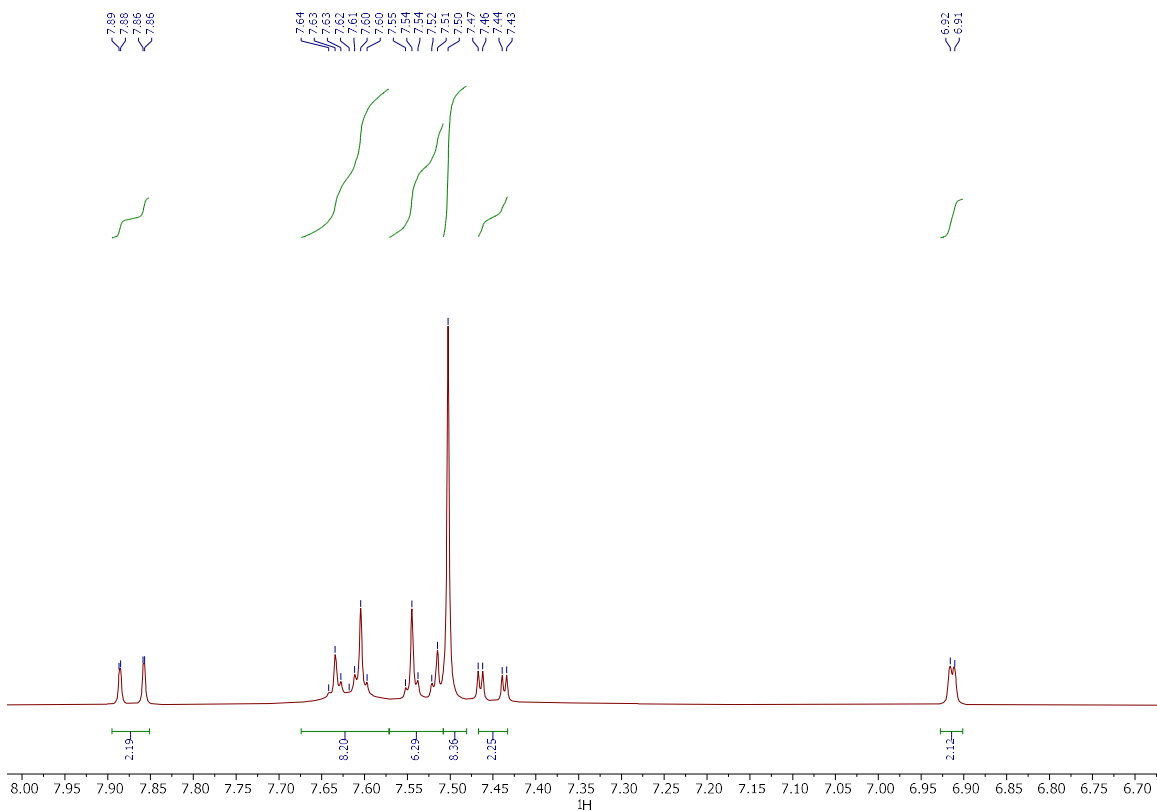


Figure S 47 ¹H-NMR of [8]CPP-N-Bu (400 MHz).



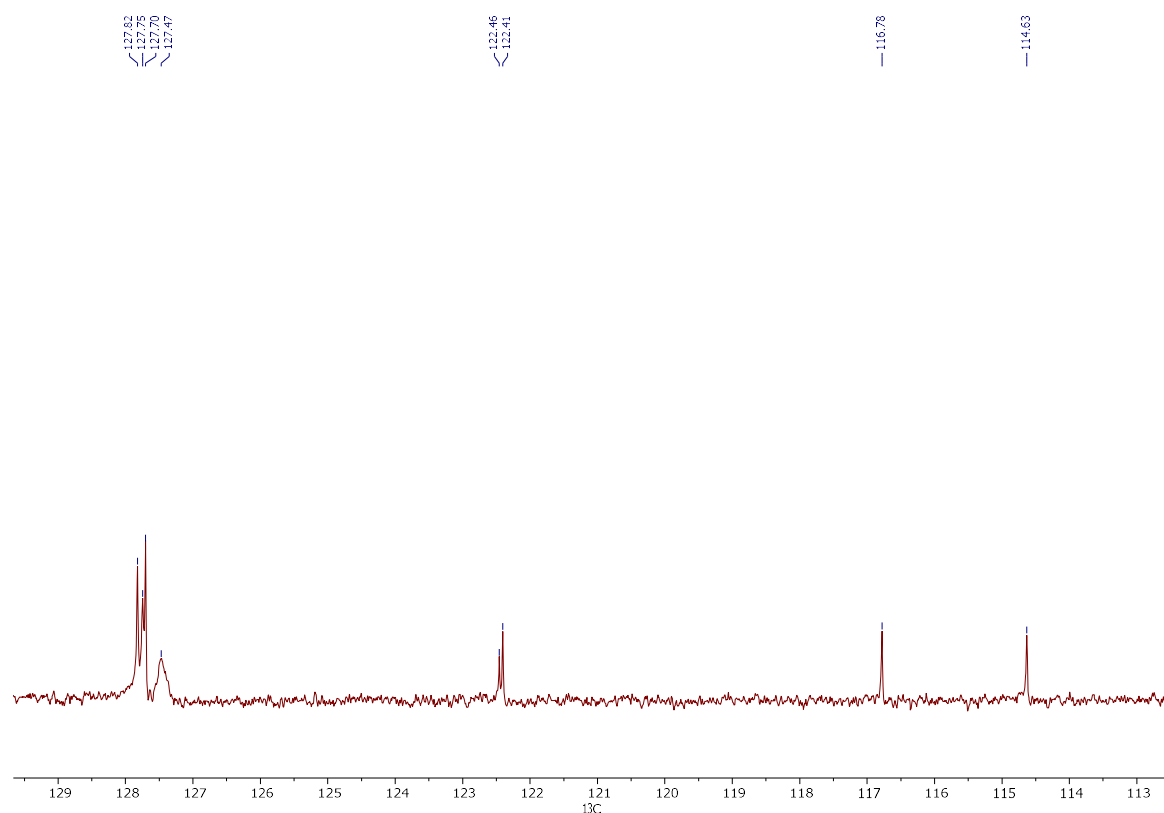


Figure S 50 ^{13}C -NMR of **[8]CPP-N-Bu** (aromatic CH region, quaternary C at 122.46 ppm, 400 MHz).

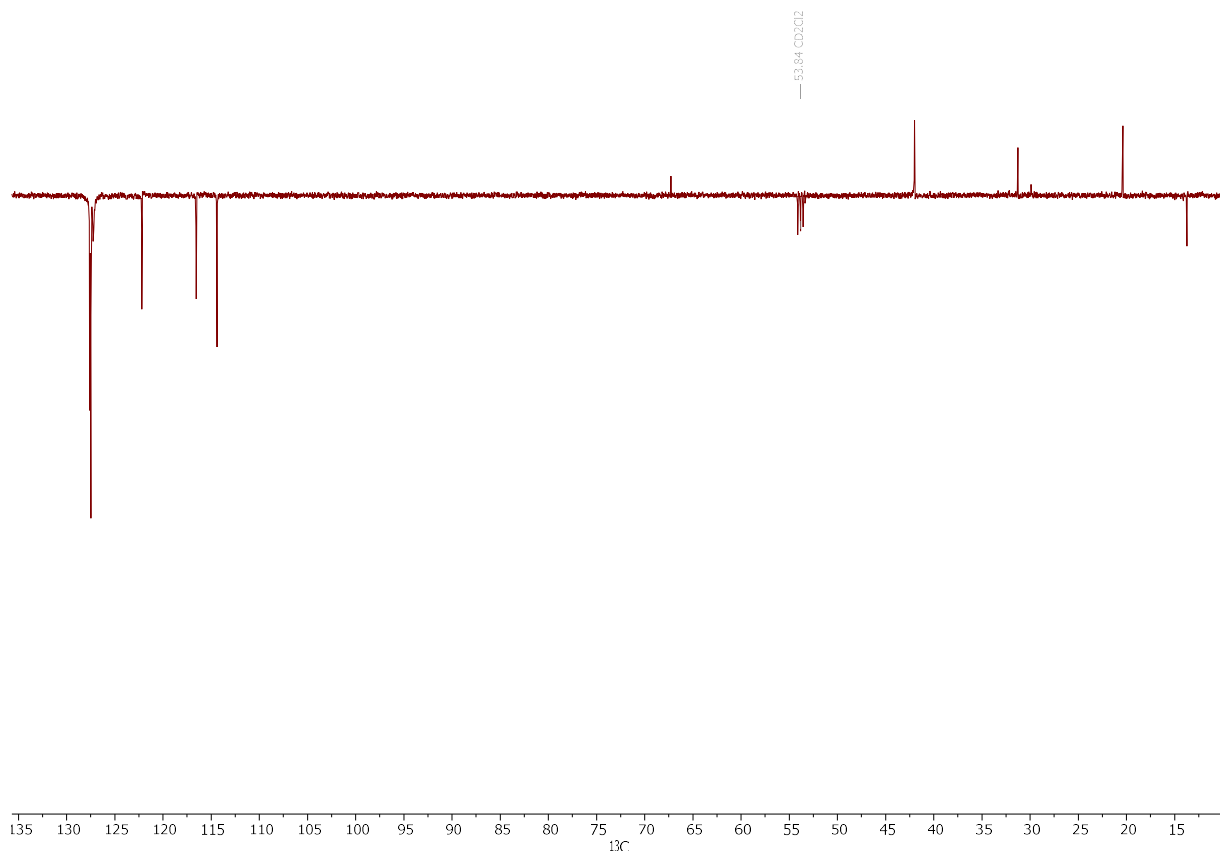


Figure S 51 DEPT-135 of **[8]CPP-N-Bu** (400 MHz).

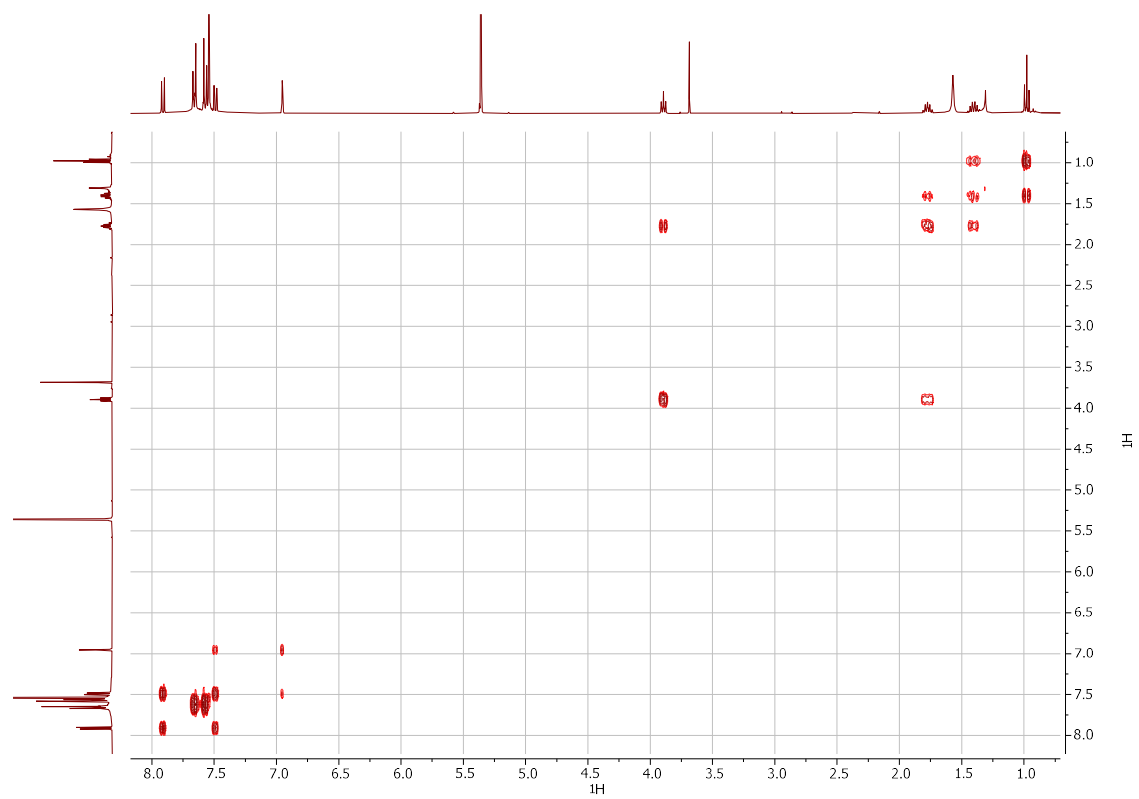


Figure S 52 COSY-DQF of **[8]CPP-N-Bu** (400 MHz).

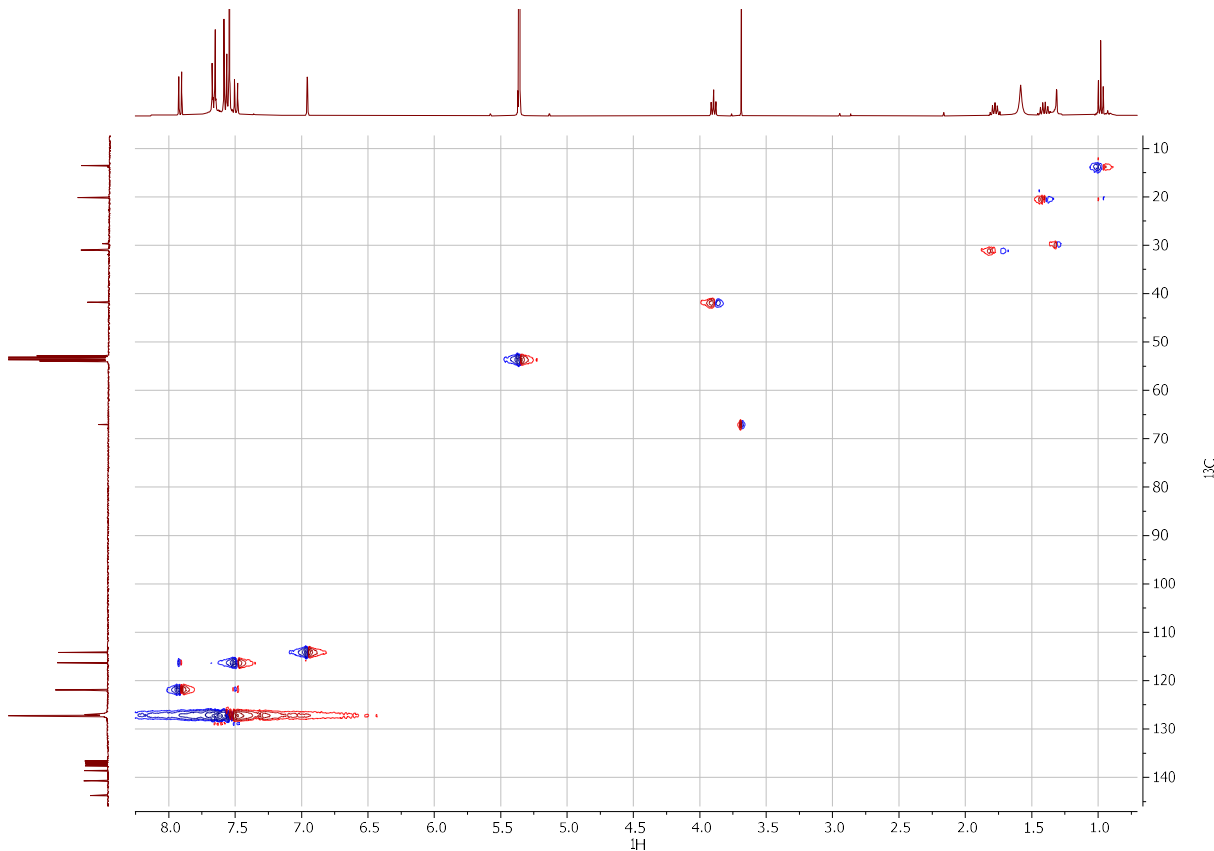


Figure S 53 HSQC of **[8]CPP-N-Bu** (400 MHz).

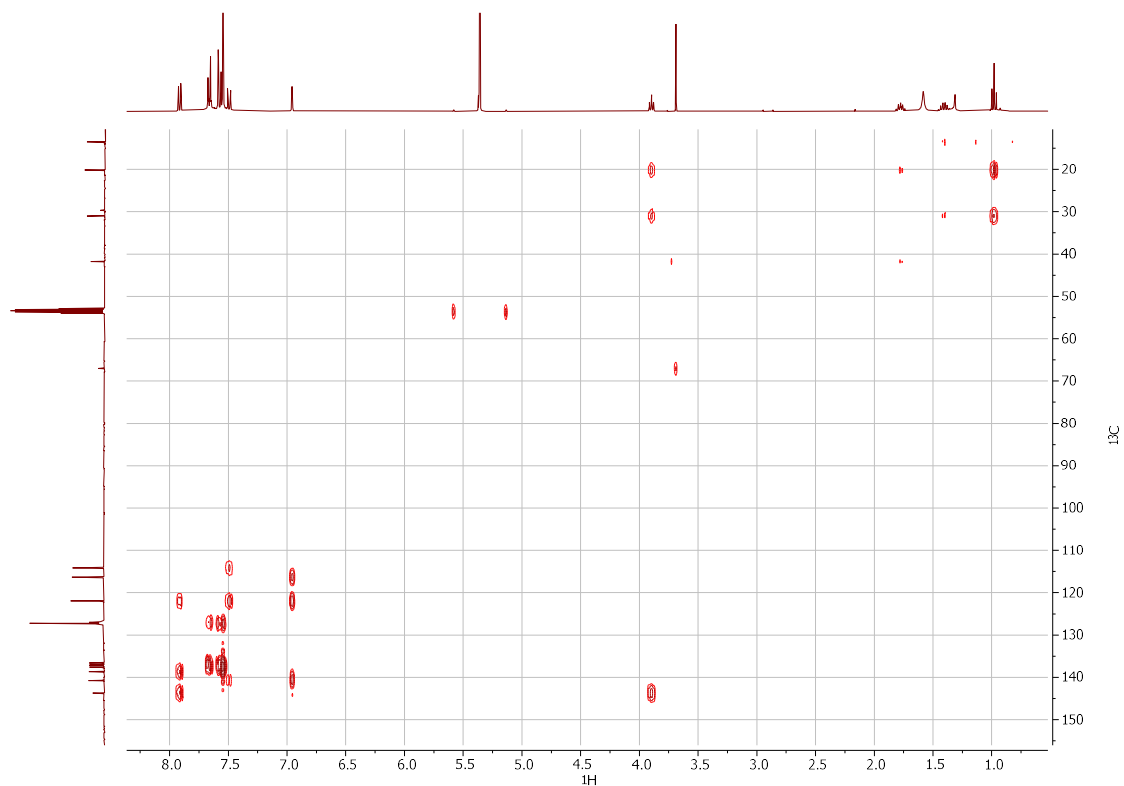


Figure S 54 HMBC of [8]CPP-N-Bu (400 MHz).

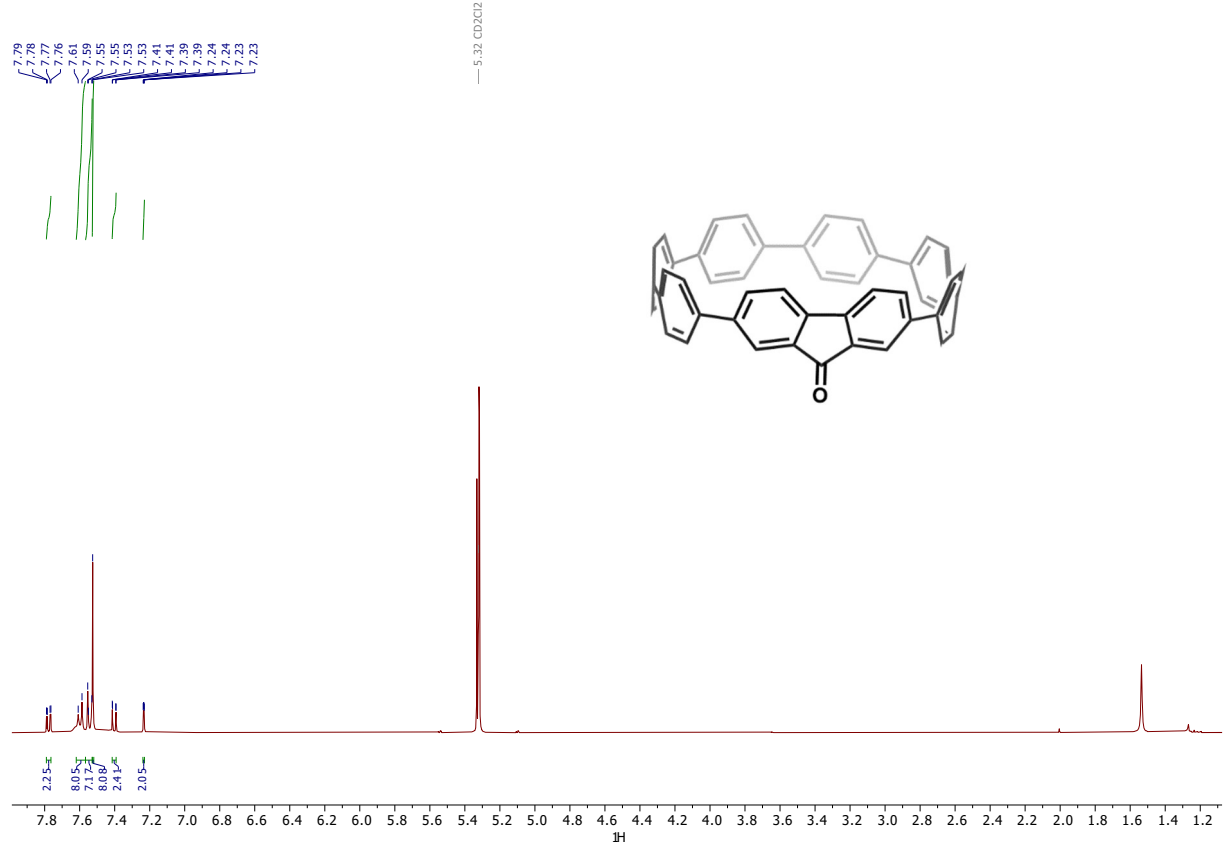


Figure S 55 ¹H-NMR of [8]CPP-C=O (400 MHz).

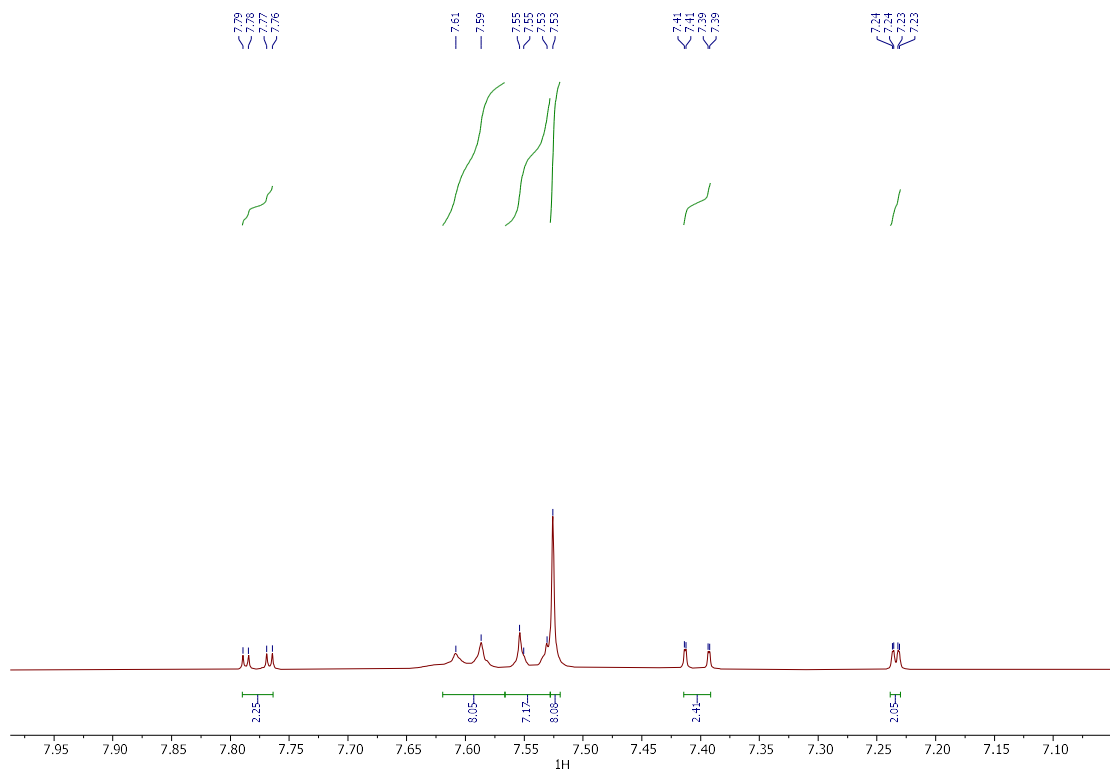


Figure S 56 ^1H -NMR of [8]CPP-C=O (aromatic protons region, 400 MHz).

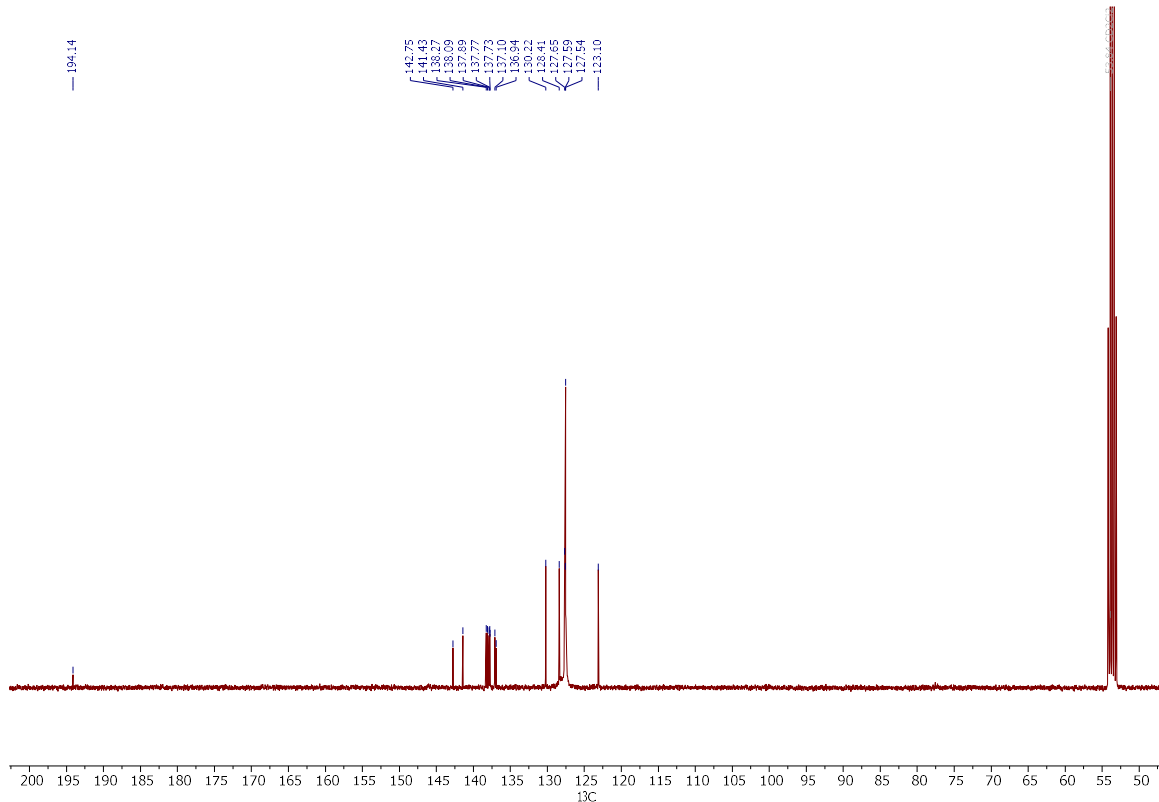


Figure S 57 ^{13}C -NMR of [8]CPP-C=O (400 MHz).

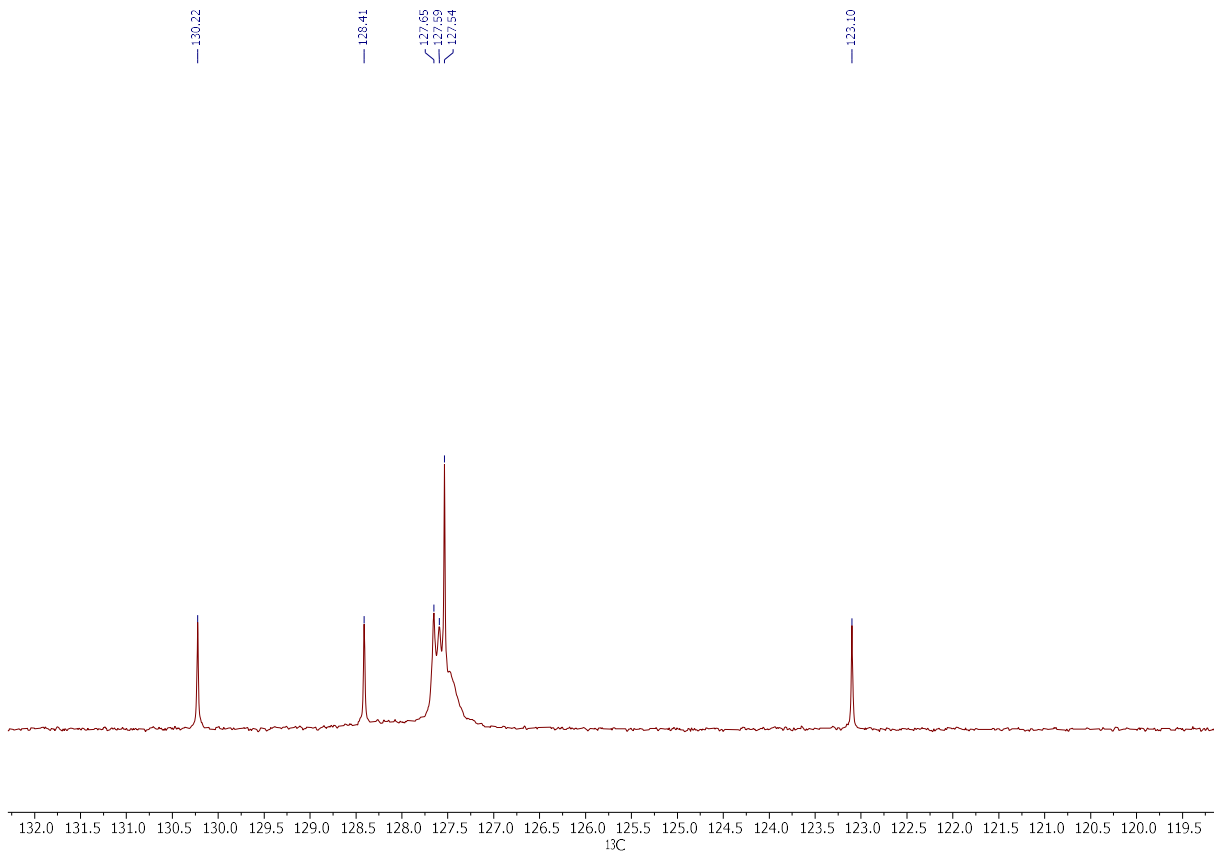


Figure S 58 ¹³C-NMR of [8]CPP-C=O (aromatic CH region, 400 MHz).

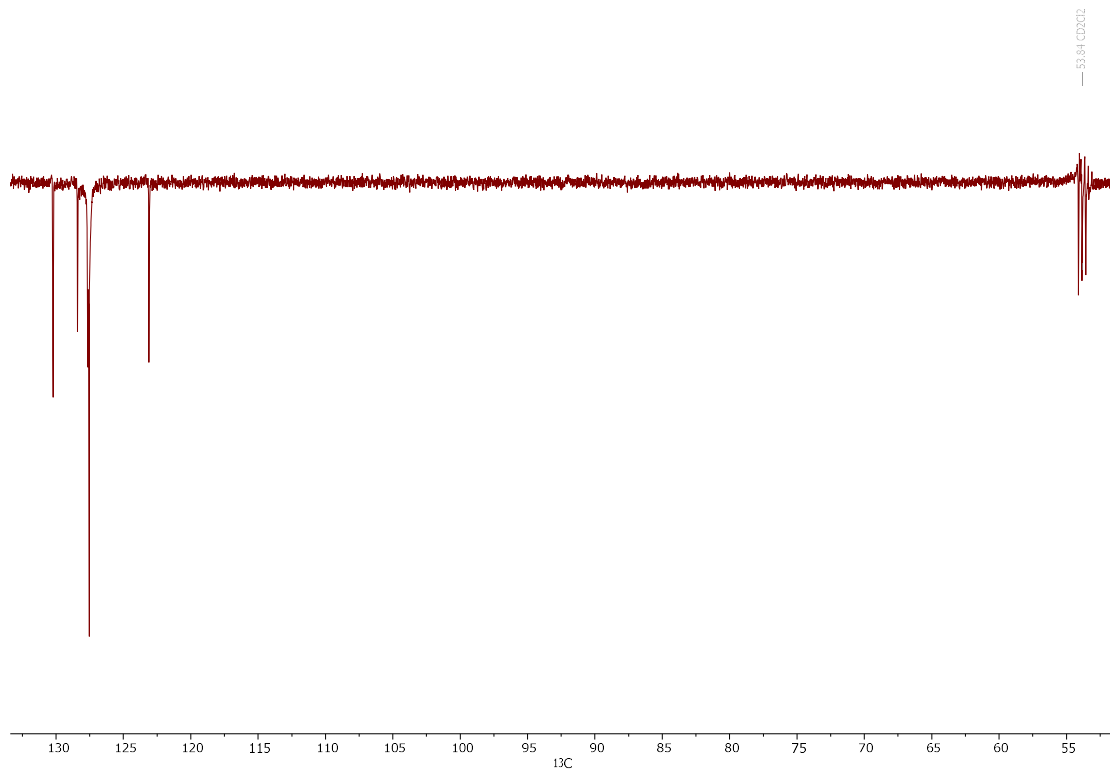
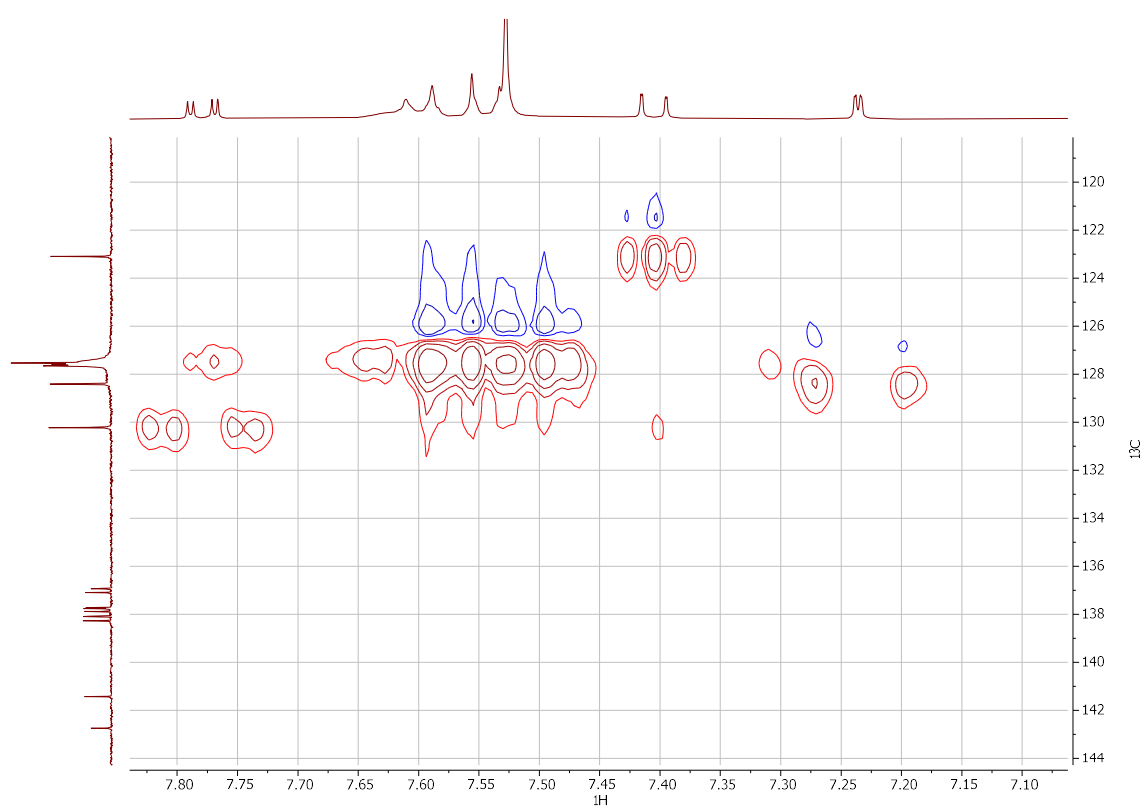
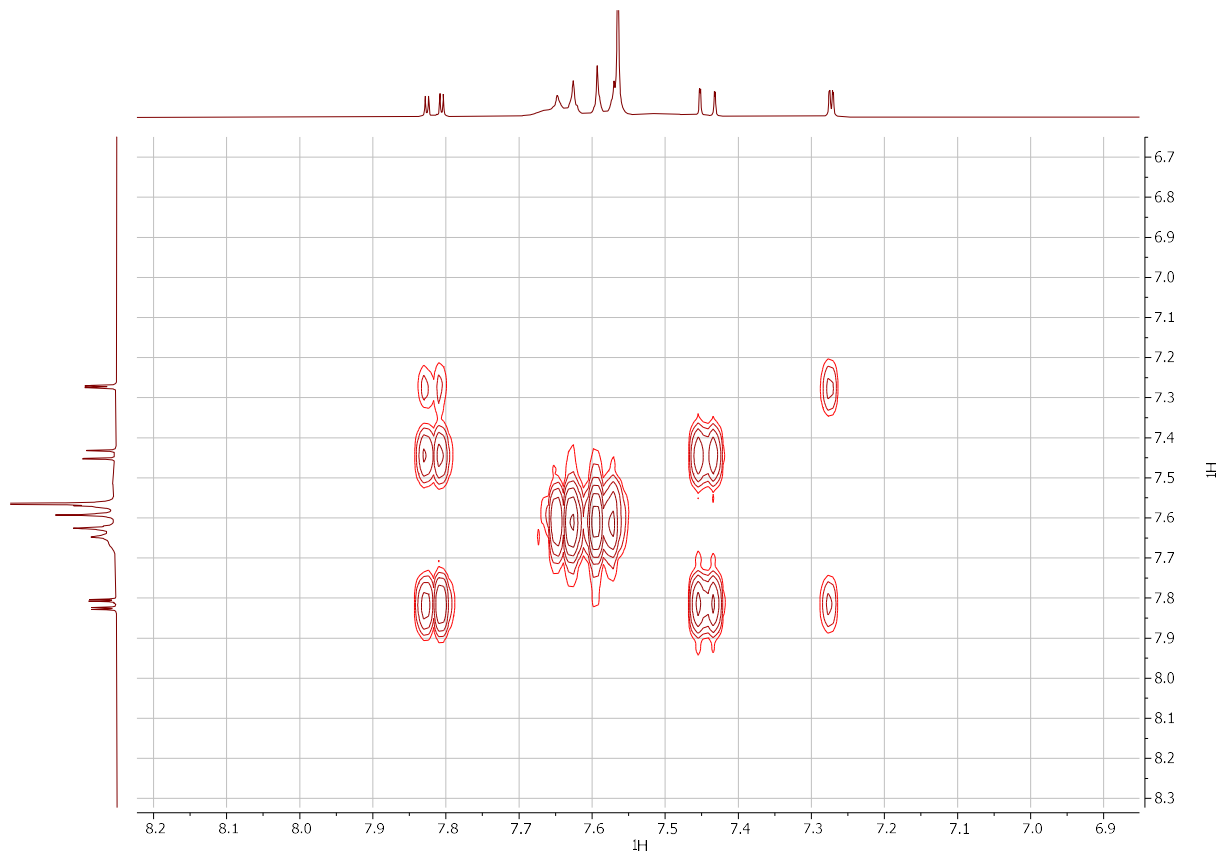


Figure S 59 DEPT-135 of [8]CPP-C=O (400 MHz).



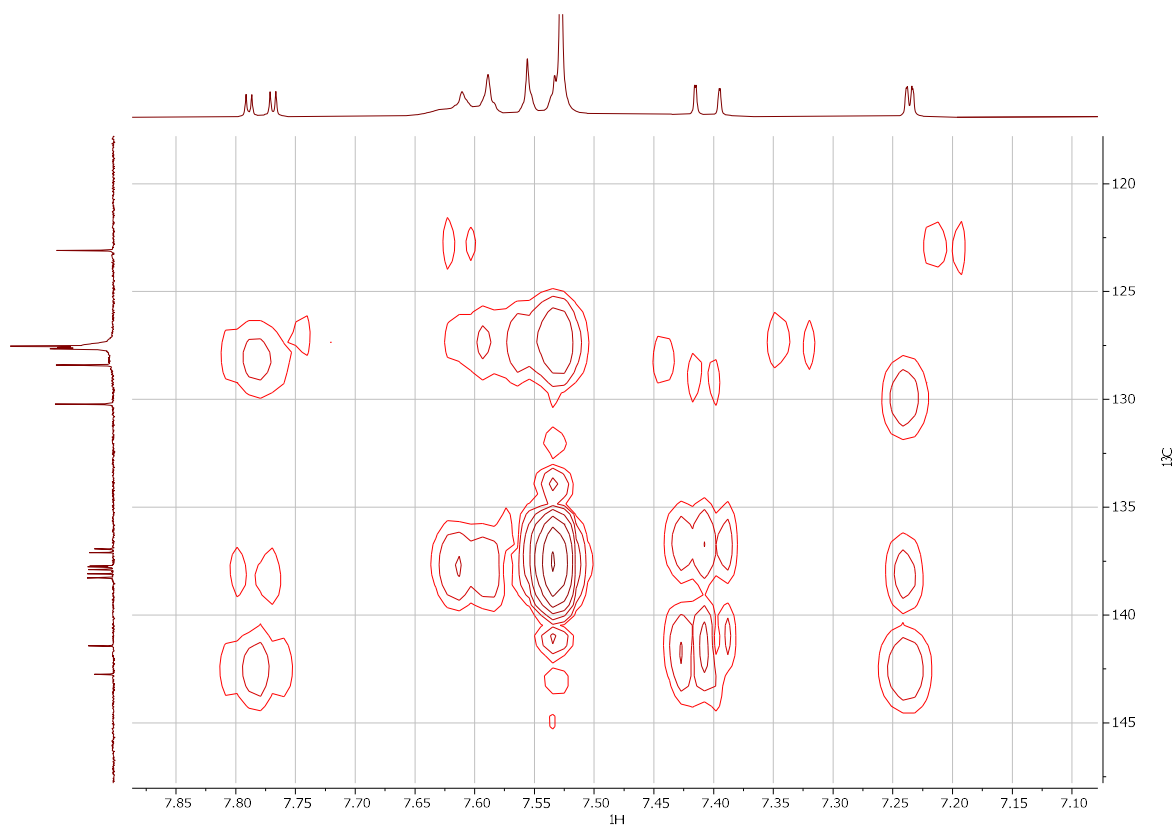


Figure S 62 HMBC of [8]CPP-C=O (400 MHz).

8 Copy of infrared spectra

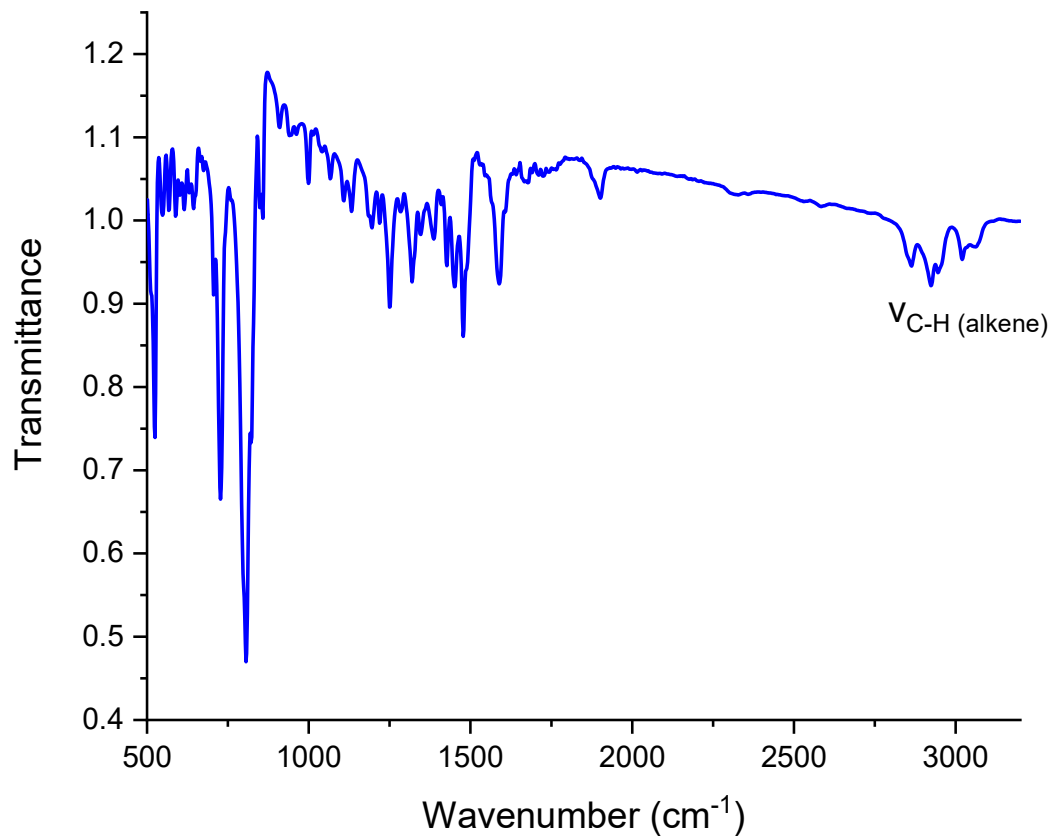


Figure S 63 Infrared spectra of **[8]CPP-N-Bu**.

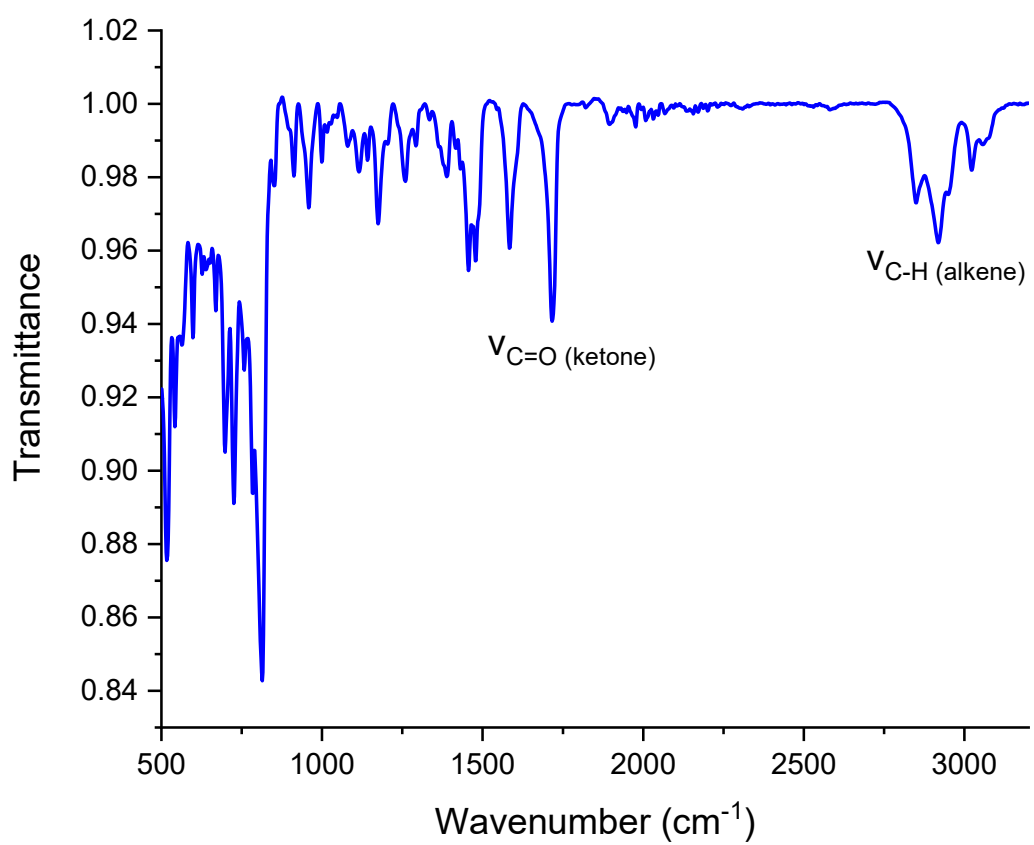


Figure S 64 Infrared spectra of **[8]CPP-C=O**.

9 X-ray diffraction

The crystals were obtained by ethanol vapor diffusion in chloroform. The X-Ray structures have been registered to the CCDC data base on the following numbers: CCDC 2294551 for [8]CPP-N-Bu and CCDC 2294552 [8]CPP-C=O. The X-Ray structure of [8]CPP has been previously reported (CCDC 871414).^[20]

Axes and mean diameter \varnothing

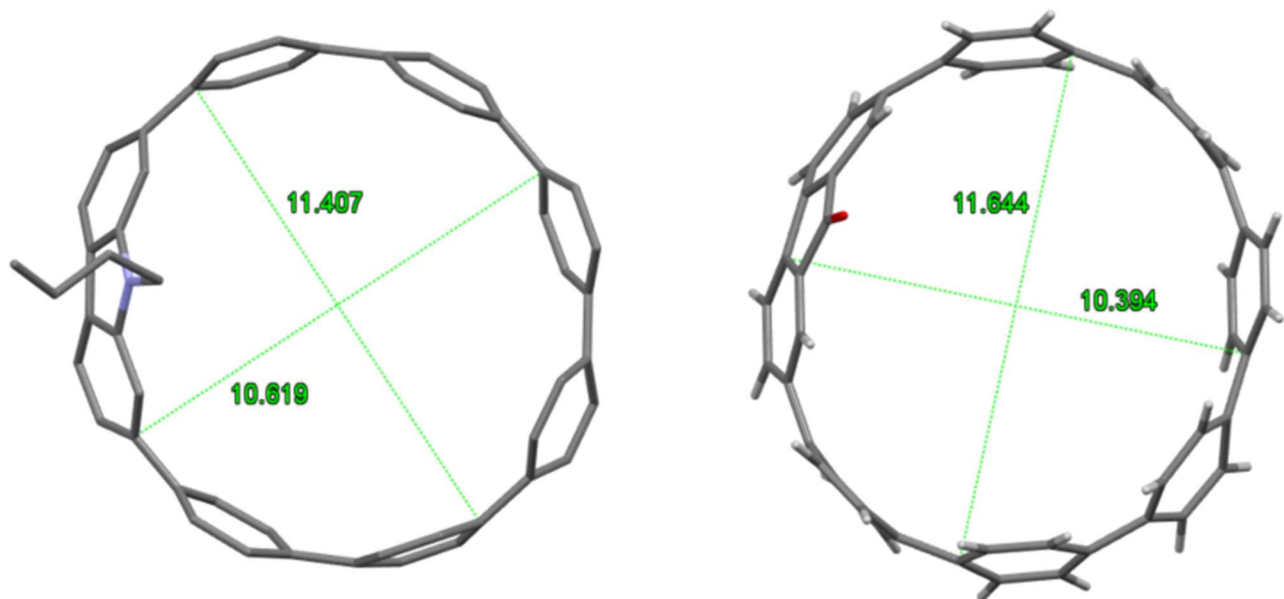


Figure S 65 Minimal and maximal C-C axes in [8]CPP-N-Bu and [8]CPP-C=O.

Table S 15 Axes and mean diameter values

	Axes (Å)	Mean diameter (Å)
[8]CPP-N-Bu	11.147	11.0
	11.345	
	11.407	
	11.231	
	11.019	
	10.670	
	10.932	
	10.619	
[8]CPP-C=O	10.394	11.0
	10.664	
	11.239	
	11.512	
	11.644	
	11.480	

	10.866	
	10.500	

Torsion angle

Definition of a torsion angle: The external torsion angle (θ_{ext}) is the dihedral angle between two unbridged phenylene units. Two angles are measured for each C2-C7 link (C8-C7-C2-C3 and C6-C7-C2-C1). The internal torsion angles (θ_{int}) are the dihedral angles within a bridged biphenyl unit (C4-C β -C γ -C5 and C α -C β -C γ -C δ)

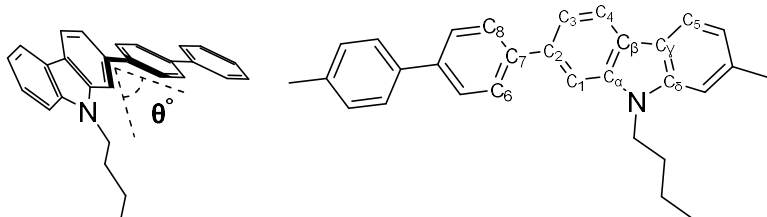


Table S 16 Torsion angle values

	$\theta_{\text{Ext}} (\circ)$		$\theta_{\text{Int}} (\circ)$		$\theta (\circ)$
	Values	Average	Values	Average	
[8]CPP-N-Bu	38.71	27.74	0.00	1.17	24.4
	41.01		2.33		
	13.90				
	14.56				
	12.59				
	9.82				
	32.90				
	34.04				
	35.37				
	37.19				
	25.42				
	22.79				
	34.19				
[8]CPP-C=O	35.87				
	27.60	18.41	3.40	3.96	16.6
	22.06		4.52		
	7.72				
	7.22				

	27.73				
	26.51				
	31.45				
	28.24				
	0.23				
	9.86				
	7.22				
	7.72				
	26.51				
	27.73				

Displacement angle

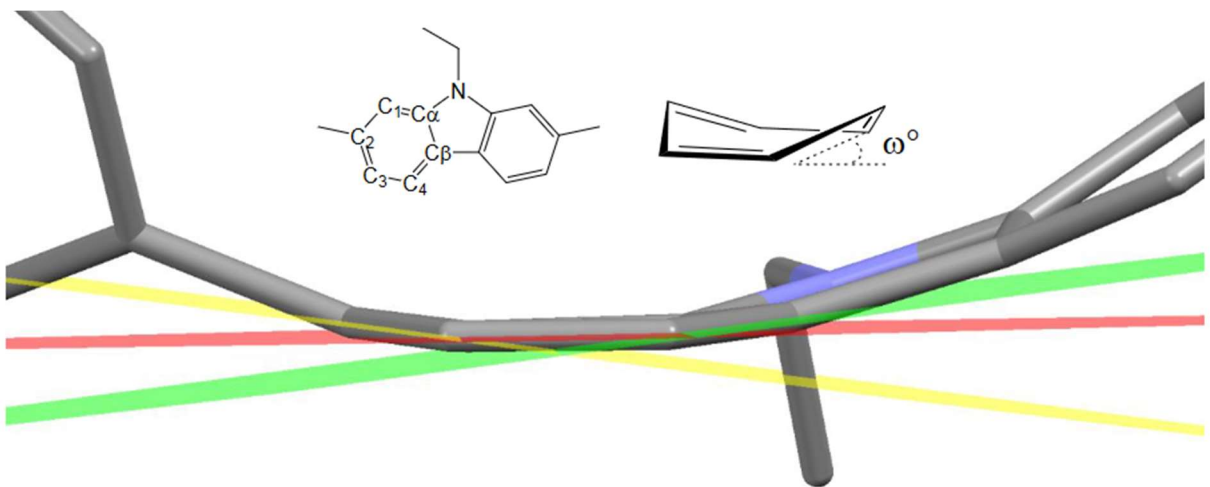


Figure S 66 Measurement of a displacement angle

Definition of a displacement angle: The mean planes passing by $C\alpha$ -C1-C3-C4 (red), C1-C2-C3 (yellow) and $C\alpha$ -C β -C4 (green) are drawn. The external displacement angle (ω_{ext}) is measured between red and yellow planes, and, the internal displacement angle (ω_{int}) between red and green planes. Then, the mean displacement angle is calculated taking into account two ω_{ext} and two ω_{int} for a bridged biphenyl unit.

Table S 17. Displacement angle values

	$\omega_{\text{Ext}} (\circ)$		$\omega_{\text{Int}} (\circ)$		$\omega (\circ)$
	Values	Average	Values	Average	
[8]CPP-N-Bu	9.26	9.0	6.57	6.4	8.7
	9.17		6.22		
	7.31				
	10.04				
	8.79				
	7.75				
	11.02				
	10.79				
	9.73				
	11.69				
	9.33				
	8.69				
[8]CPP-C=O	6.17	9.0		3.3	8.7
	6.25				
	11.46		1.10		
	9.91		5.57		
	9.96				
	9.56				
	5.57				
	5.26				
	9.44				
	14.96				
	9.91				
	11.46				
	9.56				

In the two structures, the voids contain solvent molecules that have been fully (for **[8]CPP-C=O**) or partially (for **[8]CPP-N-Bu**) squeezed in the crystal structure refinements. The porous volume of the structure has been investigated using Mercury 2023.2.0 (Build 382240) software. When default parameters are used, *ie.* a probe radius of 1.2 Å and a grid spacing of 0.3 Å, the voids represent 21.1 % (229.07 Å³/molecule) and 18.5% (178.36 Å³/molecule) of the unit cell volume for **[8]CPP-N-Bu** and **[8]CPP-C=O**, respectively. When using the sodium ionic radius (probe radius of 1.02 Å with a grid spacing of 0.1 Å) to probe the voids, the voids represent 24.1 % (262.50 Å³/molecule) and 21.0% (202.32 Å³/molecule) of the unit cell volume for **[8]CPP-N-Bu** and **[8]CPP-C=O**, respectively, whereas when using the ionic radius of the lithium cation (probe radius of 0.76 Å with a grid spacing of 0.1 Å), the values increased to 29.9 % (325.61 Å³/molecule) and 24.9% (240.00 Å³/molecule).

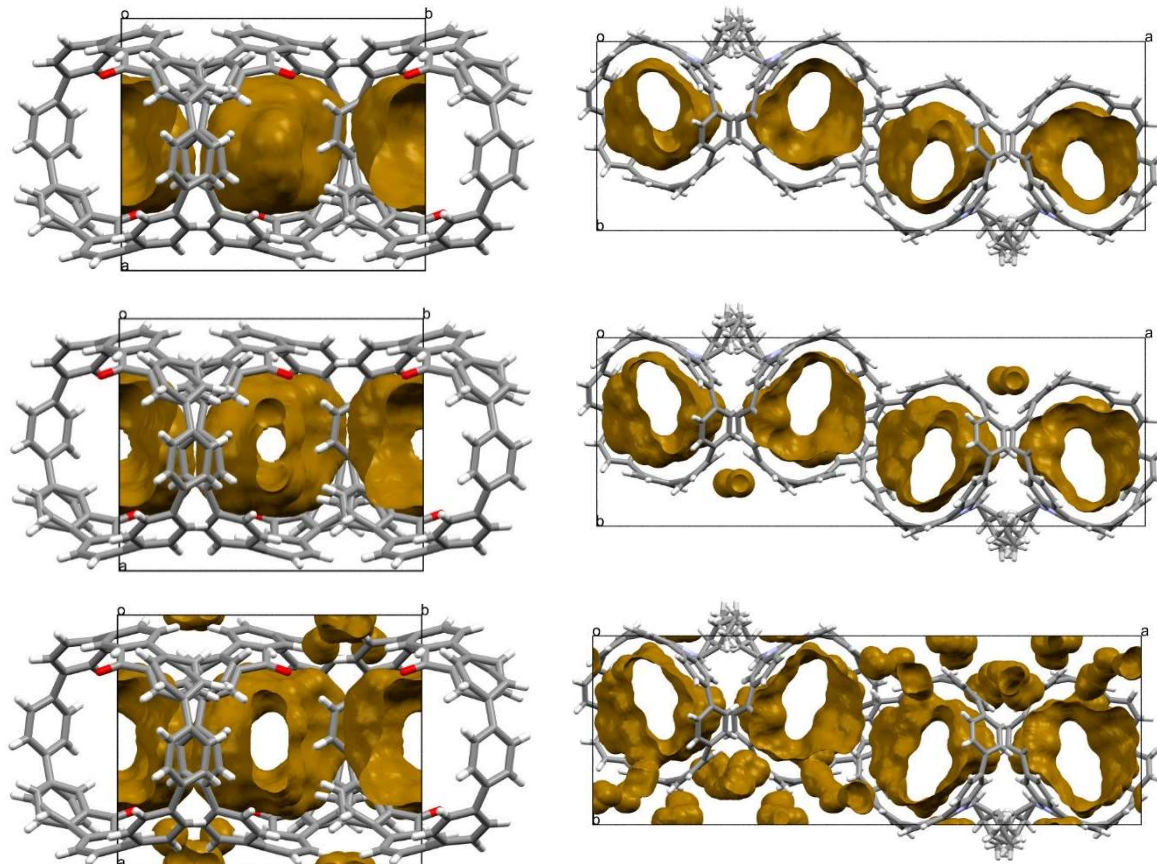


Figure S 67. View of the voids along the channels in the structures of **[8]CPP-C=O** (left) and **[8]CPP-N-Bu** (right) with 1.2 Å (top), 1.02 Å (middle) and 0.76 Å (bottom) probe radii.

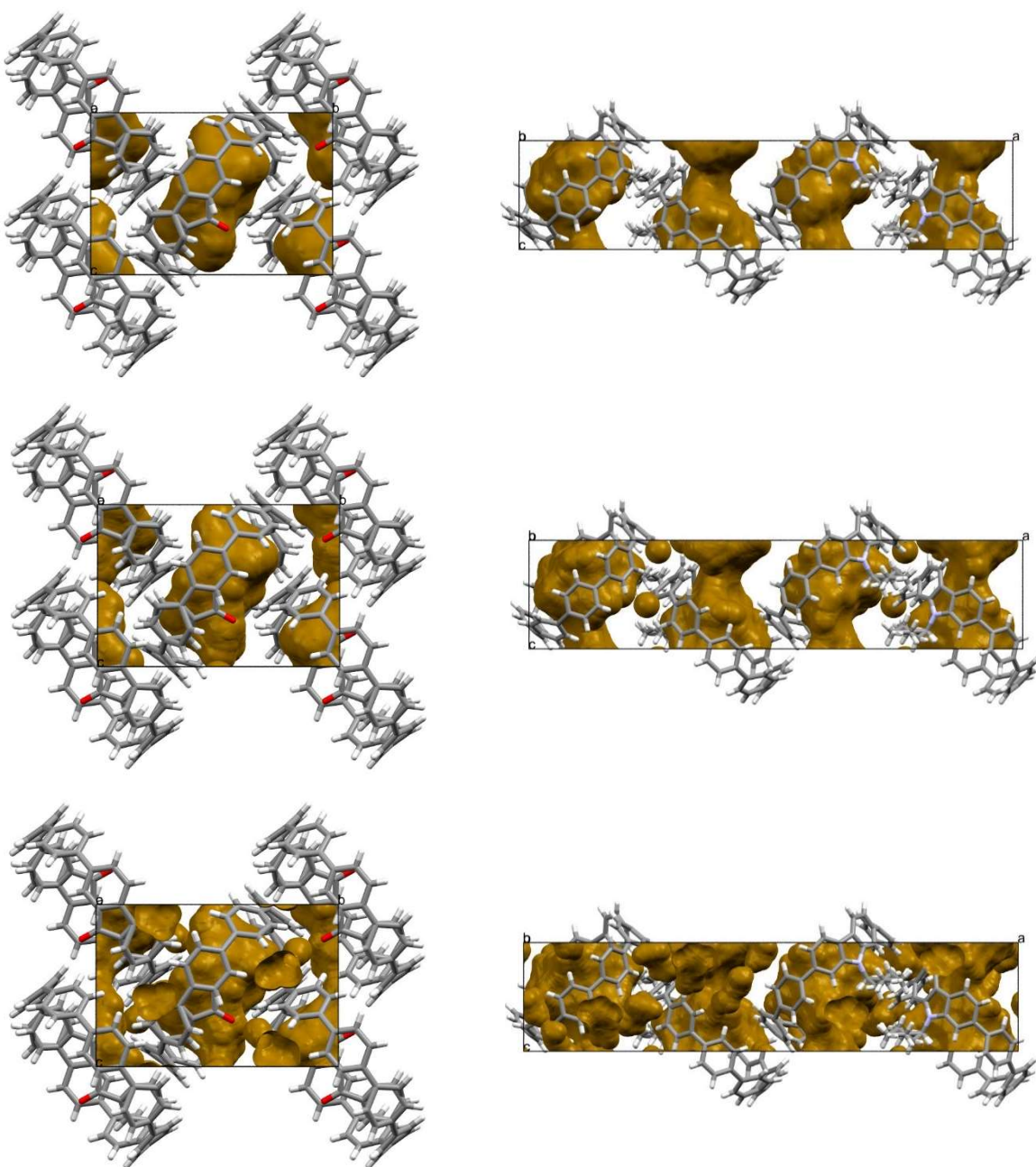


Figure S 68. View of the voids across the channels in the structures of **[8]CPP-C=O** (left) and **[8]CPP-N-Bu** (right) with 1.2 Å (top), 1.02 Å (middle) and 0.76 Å (bottom) probe radii.

Definitions of the mean plane, tilt angle and lateral displacement:

The mean plan of a nanohoop is calculated as the mean plan including all the bridging carbon atoms. The tilt angle is the angle between the mean planes of the two molecules in a chevron of the herring bone pattern (Fig. S68).

The lateral displacement is defined as the distance between the projection of the centroid of a nanohoop in the mean plane of the neighboring coplanar nanohoop and the centroid of this nanohoop (the centroid of a nanohoop is calculated from the coordinates of the bridging carbon atoms of the nanohoop) (Fig. S69).

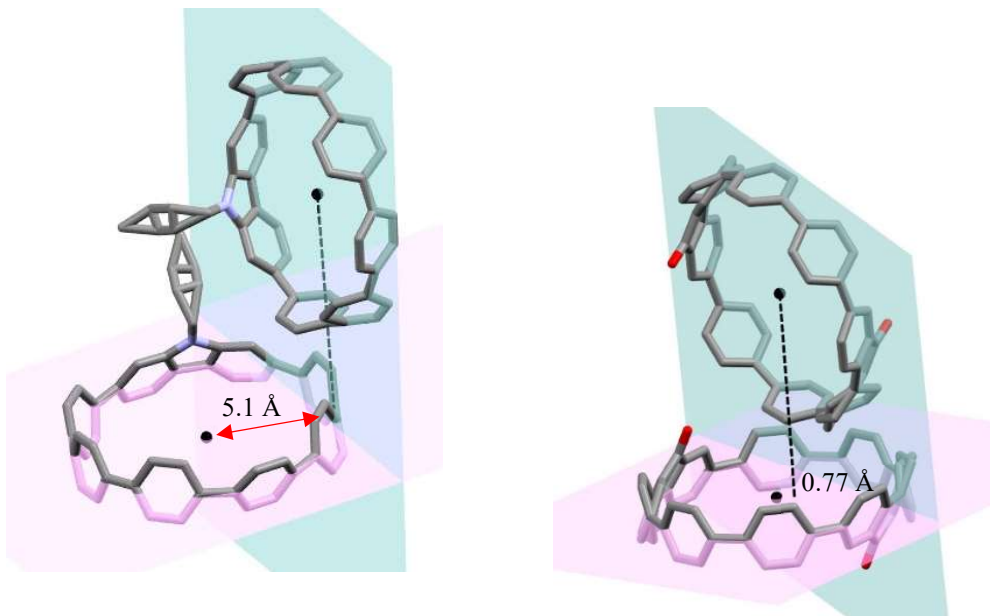


Figure S 69 Tilt in a chevron of the herring bone pattern in **[8]CPP-N-Bu** (left) and **[8]CPP-C=O** (right).

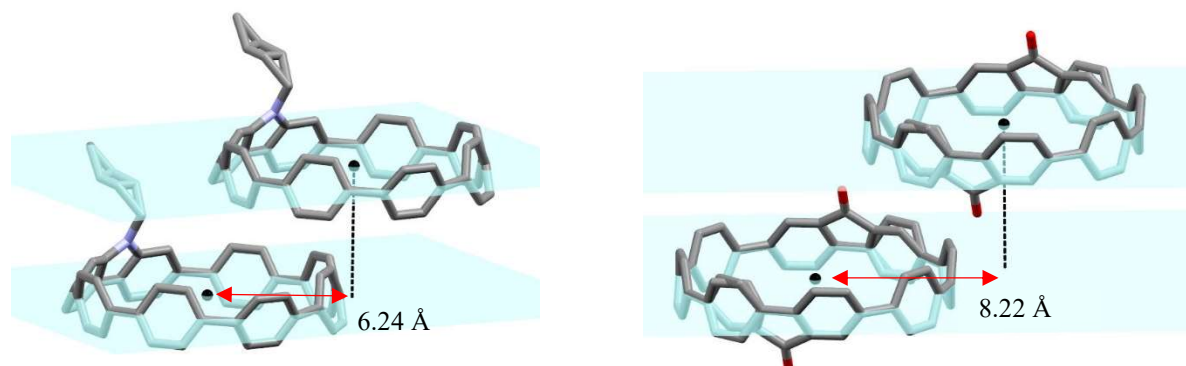


Figure S 70 Lateral displacement in **[8]CPP-N-Bu** (left) and **[8]CPP-C=O** (right).

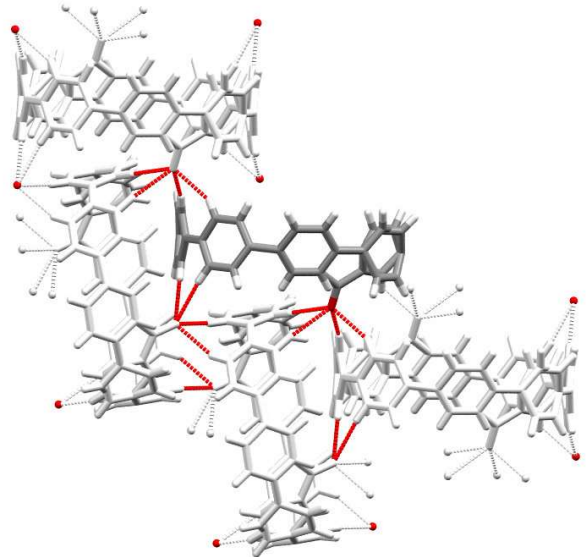


Figure S 71 Representation of the C=O ... H short contact observed in [8]CPP-C=O.

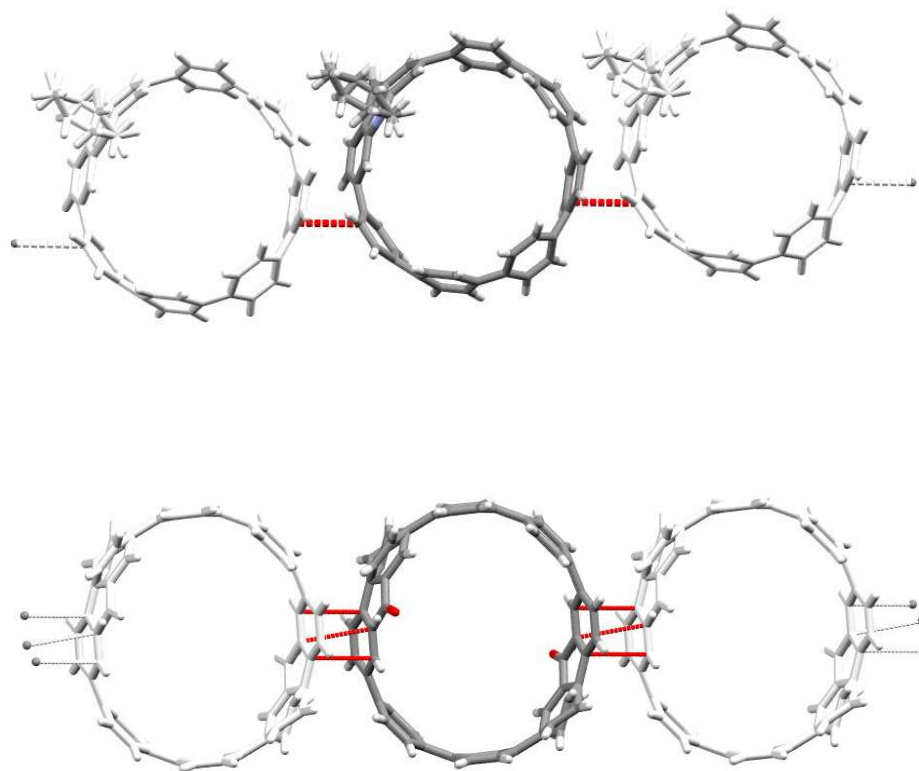


Figure S 72 Representation of the C ... C short contact observed in [8]CPP-N-Bu (upper) and [8]CPP-C=O (lower).

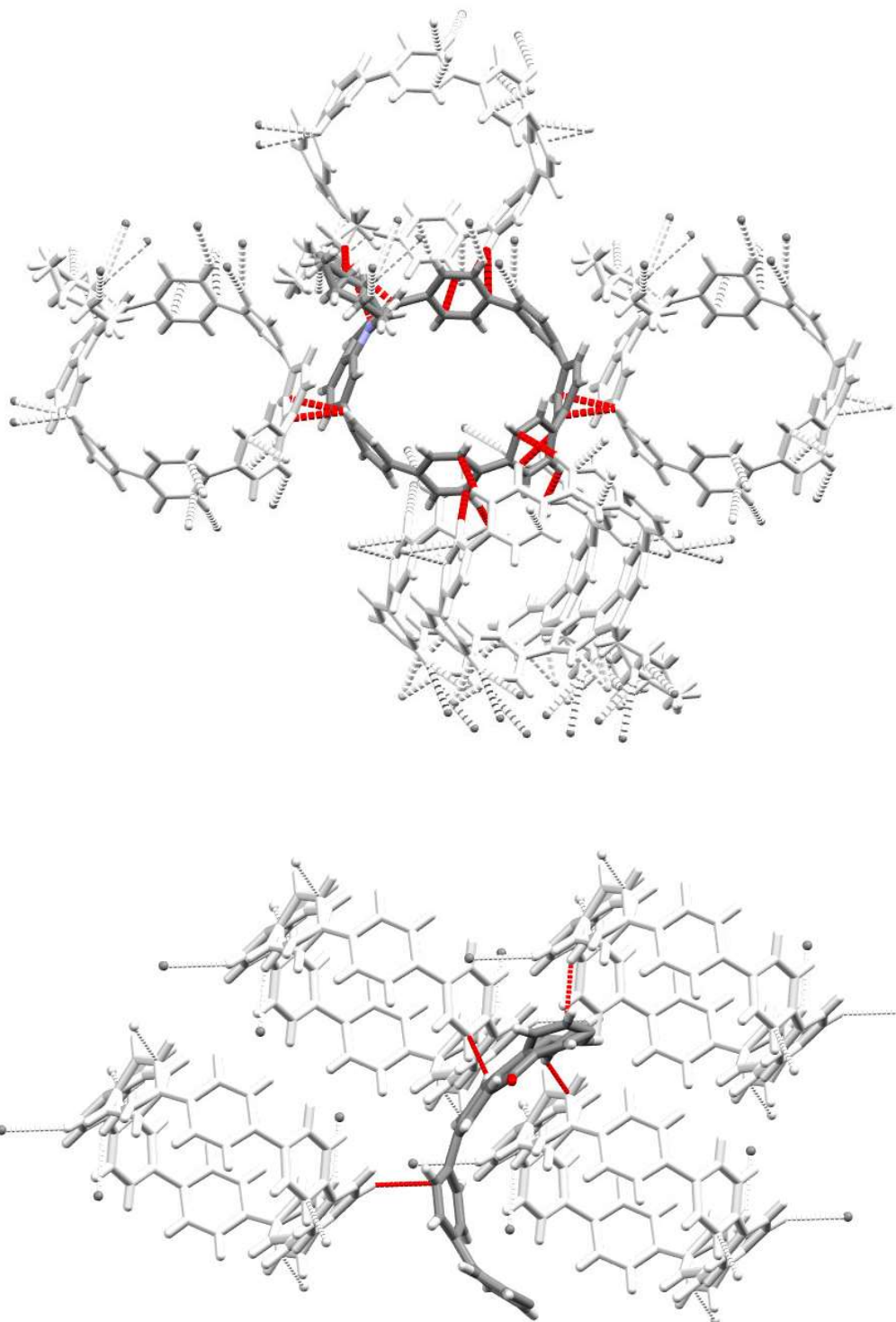


Figure S 73 Representation of the C ... H short contact observed in **[8]CPP-N-Bu** (upper) and **[8]CPP-C=O** (lower).

Table S 18 Short contact list for **[8]CPP-N-Bu** (short contacts involving the disordered butyl chain omitted) and for **[8]CPP-C=O** (within the asymmetric unit).

[8]CPP-N-Bu		[8]CPP-C=O	
contact	Distance (Å)	contact	Distance (Å)
C32 … C18 (x, 1-y, z)	2 * 3.396(7)	C13A … C13A (2-x, 1-y, 1-z)	3.337(4)
C18 … C32 (x, -1+y, z)		C8A … C12A (2-x, 1-y, 1-z)	2 * 3.399(4)
C43 … H41 (1/2-x, y, -1/2+z)	2 * 2.834 (5)	C12A … C8A (2-x, 1-y, 1-z)	
H41 … C43 (1/2-x, y, z)		C3B … H6B (x, 3/2-y, -1/2+z)	2 * 2.596 (7)
C45 … H48 (1/2-x, y, -1/2+z)	2 * 2.862 (5)	H6B … C3B (x, 3/2-y, 1/2+z)	
H48 … C45 (1/2-x, y, z)		C19 … H9A (2-x, -1/2+y, 3/2-z)	2 * 2.893 (7)
C48 … H41 (1/2-x, y, -1/2+z)	2 * 2.684 (5)	H9A … C19 (2-x, 1/2+y, 3/2-z)	
H41 … C48 (1/2-x, y, z)		H3B … H6B (x, 3/2-y, -1/2+z)	2 * 2.308(1)
C32 … H18 (x, 1+y, z)	2 * 2.805 (5)	H6B … H3B (x, 3/2-y, 1/2+z)	
H18 … C32 (x, -1+y, z)		H19 … H9A (2-x, -1/2+y, 3/2-z)	2 * 2.372 (1)
C33 … H18 (x, 1+y, z)	2 * 2.830 (5)	H9A … H19 (2-x, 1/2+y, 3/2-z)	
H18 … C33 (x, -1+y, z)		O1A … H21 (x, y, -1+z)	2 * 2.336(4)
C30 … H21 (1-x, 1-y, 1/2+z)	2 * 2.847 (5)	H21 … O1A (x, y, 1+z)	
H21 … C30 (1-x, 1-y, -1/2+z)		O1A … H16 (x, y, -1+z)	2 * 2.386(4)
C23 … H27 (1-x, 1-y, 1/2+z)	2 * 2.894 (5)	H16 … O1A (x, y, 1+z)	
H27 … C23 (1-x, 1-y, -1/2+z)		O1A … H25 (x, 1/2-y, -1/2+z)	2 * 2.515(4)
C21 … H32 (1-x, 1-y, 1/2+z)	2 * 2.739 (5)	H25 … O1A (x, 1/2-y, 1/2+z)	
H32 … C21 (1-x, 1-y, -1/2+z)		O1A … H18 (x, 1/2-y, -1/2+z)	2 * 2.560(4)
H3 … H17 (x, y, -1+z)	2 * 2.367(1)	H18 … O1A (x, 1/2-y, 1/2+z)	
H17 … H3 (x, y, 1+z)			

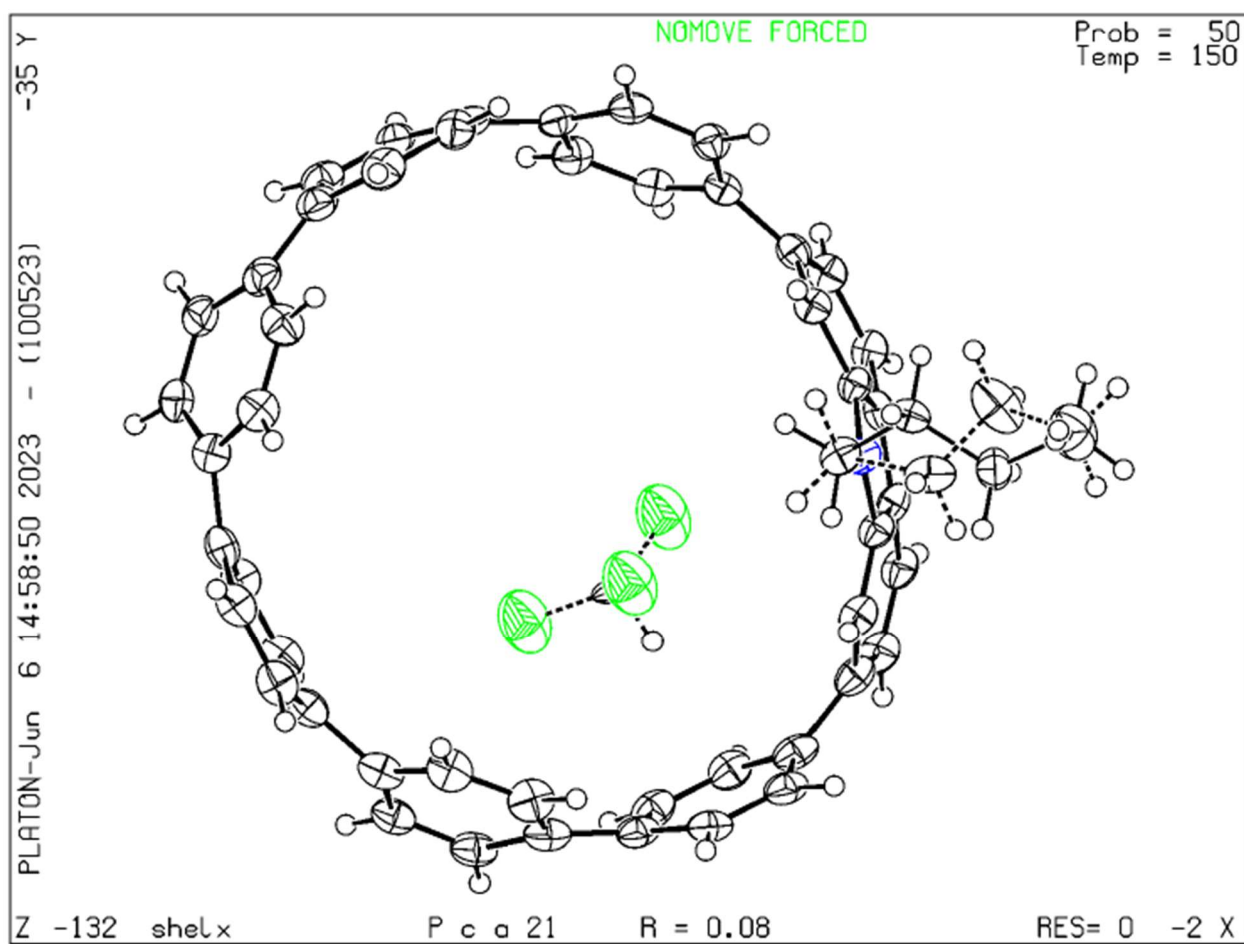


Figure S 74 Crystallographic structure of **[8]CPP-N-Bu** (CCDC: 2294551).

Table S 19 Crystal data of **[8]CPP-N-Bu**.

$C_{52}H_{39}N \cdot 0.471(\text{CHCl}_3)[+\text{solvent}]$	$F(000) = 1541.3$
$M_r = 734.06$	$D_x = 1.121 \text{ Mg m}^{-3}$
Orthorhombic, $Pca2_1$	Mo $K\alpha$ radiation, $\lambda = 0.71073 \text{ \AA}$
Hall symbol: P 2c -2ac	Cell parameters from 9955 reflections
$a = 38.622 (5) \text{ \AA}$	$\theta = 2.6\text{--}25.4^\circ$
$b = 13.2653 (15) \text{ \AA}$	$\mu = 0.15 \text{ mm}^{-1}$
$c = 8.4911 (10) \text{ \AA}$	$T = 150 \text{ K}$
$V = 4350.3 (9) \text{ \AA}^3$	Needle, yellow
$Z = 4$	$0.15 \times 0.03 \times 0.02 \text{ mm}$

Table S 20 Data collection of **[8]CPP-N-Bu**.

D8 VENTURE diffractometer	Bruker AXS	9916 independent reflections
Radiation source: Incoatec microfocus sealed tube		8733 reflections with $I > 2\sigma(I)$

Multilayer monochromator	$R_{\text{int}} = 0.062$
Detector resolution: 7.39 pixels mm ⁻¹	$\theta_{\text{max}} = 27.5^\circ$, $\theta_{\text{min}} = 2.1^\circ$
rotation images scans	$h = -49 \rightarrow 50$
Absorption correction: multi-scan [Sheldrick, G.M. (2014). <i>SADABS</i> Bruker AXS Inc., Madison, Wisconsin, USA]	$k = -17 \rightarrow 17$
$T_{\text{min}} = 0.998$, $T_{\text{max}} = 0.999$	$l = -11 \rightarrow 11$
77156 measured reflections	

Table S 21 Refinement of [8]CPP-N-Bu.

Refinement on F^2	Hydrogen site location: inferred from neighbouring sites
Least-squares matrix: full	H-atom parameters constrained
$R[F^2 > 2\sigma(F^2)] = 0.081$	$w = 1/[\sigma^2(F_o^2) + (0.1264P)^2 + 4.0501P]$ where $P = (F_o^2 + 2F_c^2)/3$
$wR(F^2) = 0.226$	$(\Delta/\sigma)_{\text{max}} = 0.001$
$S = 1.07$	$\Delta\rho_{\text{max}} = 1.27 \text{ e \AA}^{-3}$
9916 reflections	$\Delta\rho_{\text{min}} = -1.10 \text{ e \AA}^{-3}$
522 parameters	Absolute structure: Flack x determined using 3397 quotients $[(I+)-(I-)]/[(I+)+(I-)]$ (Parsons, Flack and Wagner, Acta Cryst. B69 (2013) 249-259).
1 restraint	Absolute structure parameter: 0.11 (3)
0 constraints	

Table S 22 Special details of [8]CPP-N-Bu.

Geometry. All esds (except the esd in the dihedral angle between two l.s. planes) are estimated using the full covariance matrix. The cell esds are taken into account individually in the estimation of esds in distances, angles and torsion angles; correlations between esds in cell parameters are only used when they are defined by crystal symmetry. An approximate (isotropic) treatment of cell esds is used for estimating esds involving l.s. planes.

Table S 23 Fractional atomic coordinates and isotropic or equivalent isotropic displacement parameters (\AA^2) for (shelx) of [8]CPP-N-Bu.

	x	y	z	$U_{\text{iso}}^*/U_{\text{eq}}$	Occ. (<1)
C1	0.35325 (11)	0.0443 (3)	0.6663 (5)	0.0287 (9)	
C2	0.36116 (12)	0.0394 (3)	0.5047 (6)	0.0294 (9)	
C3	0.39321 (13)	-0.0009 (4)	0.4585 (6)	0.0326 (10)	
H3	0.398003	-0.012927	0.35035	0.039*	
C4	0.41764 (13)	-0.0227 (4)	0.5719 (6)	0.0340 (10)	

H4	0.439491	-0.04871	0.540411	0.041*	
C5	0.41090 (12)	-0.0071 (4)	0.7355 (6)	0.0304 (9)	
C6	0.37750 (12)	0.0210 (3)	0.7819 (5)	0.0291 (9)	
H6	0.371495	0.024017	0.890306	0.035*	
C7	0.31253 (12)	0.1359 (4)	0.5415 (5)	0.0297 (9)	
C8	0.33493 (12)	0.0984 (4)	0.4244 (5)	0.0326 (10)	
C9	0.33278 (13)	0.1393 (4)	0.2712 (5)	0.0350 (10)	
H9	0.345401	0.110005	0.186847	0.042*	
C10	0.31195 (13)	0.2229 (4)	0.2458 (6)	0.0374 (11)	
H10	0.310891	0.251998	0.143699	0.045*	
C11	0.29225 (13)	0.2656 (4)	0.3697 (6)	0.0371 (11)	
C12	0.29084 (12)	0.2186 (4)	0.5144 (6)	0.0350 (10)	
H12	0.275489	0.241879	0.593957	0.042*	
C13	0.43900 (12)	0.0073 (4)	0.8513 (6)	0.0309 (9)	
C14	0.46799 (12)	0.0641 (4)	0.8099 (6)	0.0340 (10)	
H14	0.474091	0.070528	0.701955	0.041*	
C15	0.48815 (13)	0.1117 (4)	0.9237 (6)	0.0366 (11)	
H15	0.507347	0.151586	0.892055	0.044*	
C16	0.48051 (12)	0.1015 (4)	1.0845 (6)	0.0331 (10)	
C17	0.45559 (13)	0.0298 (4)	1.1250 (6)	0.0357 (11)	
H17	0.4529	0.011431	1.232426	0.043*	
C18	0.43472 (12)	-0.0150 (4)	1.0128 (6)	0.0333 (10)	
H18	0.417315	-0.061299	1.044613	0.04*	
C19	0.49112 (12)	0.1811 (4)	1.1974 (6)	0.0353 (11)	
C20	0.51506 (12)	0.2563 (4)	1.1549 (6)	0.0330 (10)	
H20	0.532527	0.241096	1.079824	0.04*	
C21	0.51379 (13)	0.3517 (4)	1.2196 (6)	0.0382 (11)	
H21	0.53	0.40104	1.186027	0.046*	
C22	0.48873 (13)	0.3777 (4)	1.3356 (6)	0.0382 (11)	
C23	0.47026 (15)	0.2958 (5)	1.3984 (6)	0.0413 (12)	
H23	0.456444	0.306204	1.489527	0.05*	
C24	0.47146 (14)	0.2018 (4)	1.3333 (6)	0.0377 (11)	
H24	0.458677	0.148747	1.38104	0.045*	
C25	0.47709 (14)	0.4831 (4)	1.3510 (6)	0.0386 (11)	
C26	0.49407 (14)	0.5649 (4)	1.2775 (6)	0.0371 (11)	
H26	0.518152	0.559786	1.256124	0.045*	
C27	0.47703 (13)	0.6510 (4)	1.2362 (6)	0.0362 (11)	
H27	0.48932	0.703832	1.185346	0.043*	
C28	0.44137 (13)	0.6628 (4)	1.2680 (6)	0.0350 (10)	
C29	0.42625 (14)	0.5917 (4)	1.3703 (7)	0.0418 (12)	

H29	0.403863	0.603986	1.412532	0.05*	
C30	0.44366 (15)	0.5046 (4)	1.4098 (6)	0.0405 (12)	
H30	0.432865	0.457673	1.478485	0.049*	
C31	0.41881 (13)	0.7252 (4)	1.1686 (6)	0.0345 (10)	
C32	0.42617 (14)	0.7302 (4)	1.0072 (6)	0.0372 (11)	
H32	0.449137	0.71758	0.972322	0.045*	
C33	0.40118 (14)	0.7529 (4)	0.8981 (6)	0.0375 (11)	
H33	0.4072	0.755573	0.789738	0.045*	
C34	0.36717 (14)	0.7720 (4)	0.9431 (6)	0.0360 (11)	
C35	0.36077 (14)	0.7832 (4)	1.1058 (6)	0.0383 (11)	
H35	0.338906	0.807121	1.140827	0.046*	
C36	0.38610 (14)	0.7594 (4)	1.2146 (6)	0.0380 (11)	
H36	0.381156	0.766611	1.323641	0.046*	
C37	0.33892 (14)	0.7568 (4)	0.8253 (6)	0.0387 (11)	
C38	0.34303 (14)	0.7773 (4)	0.6659 (7)	0.0384 (11)	
H38	0.360263	0.82406	0.633631	0.046*	
C39	0.32266 (13)	0.7314 (4)	0.5534 (6)	0.0376 (11)	
H39	0.325311	0.749626	0.445872	0.045*	
C40	0.29802 (13)	0.6579 (4)	0.5951 (6)	0.0377 (11)	
C41	0.29055 (14)	0.6495 (5)	0.7568 (7)	0.0420 (12)	
H41	0.271402	0.609902	0.790058	0.05*	
C42	0.31054 (14)	0.6977 (4)	0.8668 (6)	0.0414 (12)	
H42	0.304843	0.690505	0.975031	0.05*	
C43	0.28657 (12)	0.5758 (4)	0.4877 (6)	0.0349 (11)	
C44	0.30845 (13)	0.5426 (4)	0.3669 (6)	0.0396 (12)	
H44	0.324664	0.588588	0.323096	0.047*	
C45	0.30729 (14)	0.4445 (4)	0.3086 (6)	0.0386 (11)	
H45	0.322658	0.42406	0.227284	0.046*	
C46	0.28306 (13)	0.3759 (5)	0.3715 (6)	0.0388 (11)	
C47	0.25738 (12)	0.4143 (4)	0.4715 (6)	0.0388 (12)	
H47	0.238446	0.372463	0.50039	0.047*	
C48	0.25901 (12)	0.5109 (4)	0.5285 (6)	0.0373 (11)	
H48	0.241277	0.534639	0.596565	0.045*	
C491	0.30523 (13)	0.1163 (4)	0.8370 (5)	0.0341 (10)	0.419 (17)
H49A	0.300737	0.189438	0.847427	0.041*	0.419 (17)
H49B	0.320373	0.094941	0.924989	0.041*	0.419 (17)
C501	0.2688 (4)	0.0538 (12)	0.8422 (16)	0.041 (4)	0.419 (17)
H50A	0.255707	0.075254	0.936692	0.049*	0.419 (17)
H50B	0.254909	0.072843	0.748769	0.049*	0.419 (17)
C511	0.2721 (5)	-0.0575 (12)	0.845 (2)	0.055 (5)	0.419 (17)

H51A	0.284536	-0.081163	0.750305	0.066*	0.419 (17)
H51B	0.285435	-0.078714	0.939324	0.066*	0.419 (17)
C521	0.23720 (18)	-0.1014 (6)	0.8502 (11)	0.067 (2)	0.419 (17)
H52A	0.238924	-0.175095	0.852357	0.1*	0.419 (17)
H52B	0.225146	-0.077964	0.944919	0.1*	0.419 (17)
H52C	0.22425	-0.080405	0.75653	0.1*	0.419 (17)
C492	0.30523 (13)	0.1163 (4)	0.8370 (5)	0.0341 (10)	0.581 (17)
H49C	0.288248	0.171372	0.82228	0.041*	0.581 (17)
H49D	0.322916	0.139959	0.912847	0.041*	0.581 (17)
C502	0.2870 (2)	0.0265 (6)	0.9053 (10)	0.030 (2)	0.581 (17)
H50C	0.277386	0.043876	1.009853	0.036*	0.581 (17)
H50D	0.303651	-0.029585	0.919044	0.036*	0.581 (17)
C512	0.2577 (3)	-0.0063 (9)	0.7946 (12)	0.039 (3)	0.581 (17)
H51C	0.267646	-0.020261	0.689386	0.047*	0.581 (17)
H51D	0.241234	0.050416	0.783014	0.047*	0.581 (17)
C522	0.23720 (18)	-0.1014 (6)	0.8502 (11)	0.067 (2)	0.581 (17)
H52D	0.21906	-0.117171	0.773363	0.1*	0.581 (17)
H52E	0.253078	-0.158748	0.859156	0.1*	0.581 (17)
H52F	0.226617	-0.08794	0.952958	0.1*	0.581 (17)
C53	0.3535 (3)	0.4065 (10)	0.6730 (12)	0.041 (3)	0.471 (5)
H53	0.336013	0.416609	0.587713	0.049*	0.471 (5)
N1	0.32202 (10)	0.0951 (3)	0.6861 (5)	0.0307 (8)	
Cl1	0.37759 (11)	0.3093 (3)	0.5926 (7)	0.0851 (12)	0.471 (5)
Cl2	0.37091 (11)	0.5129 (3)	0.6750 (8)	0.0851 (12)	0.471 (5)
Cl3	0.32686 (11)	0.3959 (3)	0.8327 (8)	0.0851 (12)	0.471 (5)

Table S 24 Atomic displacement parameters (\AA^2) for [8]CPP-N-Bu.

	U^{11}	U^{22}	U^{33}	U^{12}	U^{13}	U^{23}
C1	0.028 (2)	0.033 (2)	0.025 (2)	-0.0033 (17)	0.0001 (17)	-0.0008 (18)
C2	0.034 (2)	0.027 (2)	0.027 (2)	-0.0073 (17)	0.0059 (18)	-0.0034 (18)
C3	0.036 (2)	0.039 (3)	0.023 (2)	-0.002 (2)	0.0039 (18)	-0.0058 (19)
C4	0.038 (2)	0.035 (2)	0.029 (2)	0.002 (2)	0.0037 (19)	-0.0018 (19)
C5	0.035 (2)	0.026 (2)	0.030 (2)	-0.0025 (17)	0.0038 (19)	0.0037 (17)
C6	0.032 (2)	0.032 (2)	0.023 (2)	-0.0003 (18)	0.0032 (17)	0.0020 (18)
C7	0.030 (2)	0.038 (2)	0.021 (2)	-0.0037 (18)	-0.0006 (16)	0.0022 (18)
C8	0.031 (2)	0.043 (3)	0.024 (2)	-0.0052 (19)	-0.0040 (17)	-0.0041 (19)
C9	0.041 (2)	0.046 (3)	0.0172 (19)	-0.005 (2)	-0.0025 (18)	-0.0029 (19)
C10	0.042 (3)	0.050 (3)	0.019 (2)	-0.007 (2)	0.0005 (19)	0.005 (2)
C11	0.034 (2)	0.052 (3)	0.025 (2)	-0.002 (2)	-0.0054 (19)	0.001 (2)

C12	0.031 (2)	0.048 (3)	0.025 (2)	-0.005 (2)	0.0023 (18)	0.000 (2)
C13	0.032 (2)	0.028 (2)	0.032 (2)	0.0037 (17)	0.0039 (19)	0.0021 (18)
C14	0.033 (2)	0.037 (2)	0.031 (2)	0.0021 (19)	0.0067 (19)	0.002 (2)
C15	0.030 (2)	0.041 (3)	0.038 (3)	0.000 (2)	0.003 (2)	0.006 (2)
C16	0.027 (2)	0.037 (2)	0.035 (3)	0.0039 (18)	-0.0029 (19)	0.006 (2)
C17	0.040 (3)	0.038 (3)	0.030 (2)	0.005 (2)	-0.0025 (19)	0.0112 (19)
C18	0.032 (2)	0.033 (2)	0.035 (2)	-0.0020 (18)	0.0014 (19)	0.006 (2)
C19	0.034 (2)	0.042 (3)	0.030 (2)	0.0043 (19)	-0.0078 (19)	0.007 (2)
C20	0.030 (2)	0.034 (2)	0.035 (2)	0.0028 (18)	-0.0054 (19)	0.006 (2)
C21	0.031 (2)	0.049 (3)	0.034 (3)	-0.002 (2)	-0.0017 (19)	0.010 (2)
C22	0.037 (2)	0.043 (3)	0.034 (3)	0.000 (2)	-0.008 (2)	0.006 (2)
C23	0.046 (3)	0.053 (3)	0.025 (2)	-0.004 (2)	-0.001 (2)	0.008 (2)
C24	0.043 (3)	0.041 (3)	0.029 (2)	-0.005 (2)	-0.002 (2)	0.005 (2)
C25	0.043 (3)	0.044 (3)	0.029 (2)	-0.004 (2)	-0.009 (2)	0.001 (2)
C26	0.041 (3)	0.039 (3)	0.032 (2)	-0.003 (2)	-0.006 (2)	-0.003 (2)
C27	0.038 (3)	0.038 (3)	0.032 (2)	-0.007 (2)	0.001 (2)	-0.005 (2)
C28	0.036 (2)	0.038 (2)	0.031 (2)	0.000 (2)	0.003 (2)	-0.002 (2)
C29	0.041 (3)	0.046 (3)	0.038 (3)	-0.002 (2)	0.003 (2)	0.002 (2)
C30	0.051 (3)	0.040 (3)	0.030 (2)	-0.001 (2)	0.005 (2)	0.005 (2)
C31	0.042 (3)	0.029 (2)	0.033 (2)	-0.0060 (19)	0.010 (2)	-0.0044 (19)
C32	0.040 (3)	0.038 (3)	0.033 (2)	0.000 (2)	0.008 (2)	-0.003 (2)
C33	0.048 (3)	0.036 (3)	0.029 (2)	0.001 (2)	0.012 (2)	0.004 (2)
C34	0.042 (3)	0.029 (2)	0.037 (3)	0.000 (2)	0.007 (2)	0.004 (2)
C35	0.039 (2)	0.038 (3)	0.038 (3)	0.002 (2)	0.015 (2)	-0.006 (2)
C36	0.043 (3)	0.034 (3)	0.036 (3)	0.000 (2)	0.013 (2)	-0.003 (2)
C37	0.043 (3)	0.034 (3)	0.040 (3)	0.008 (2)	0.010 (2)	0.007 (2)
C38	0.041 (3)	0.034 (3)	0.040 (3)	0.005 (2)	0.007 (2)	0.009 (2)
C39	0.038 (2)	0.039 (3)	0.036 (3)	0.005 (2)	0.005 (2)	0.016 (2)
C40	0.034 (2)	0.044 (3)	0.036 (3)	0.010 (2)	0.004 (2)	0.014 (2)
C41	0.039 (3)	0.053 (3)	0.034 (3)	-0.002 (2)	0.011 (2)	0.010 (2)
C42	0.046 (3)	0.047 (3)	0.032 (3)	0.000 (2)	0.012 (2)	0.006 (2)
C43	0.030 (2)	0.041 (3)	0.033 (2)	0.0026 (19)	-0.0030 (19)	0.014 (2)
C44	0.033 (2)	0.056 (3)	0.030 (2)	-0.004 (2)	-0.0018 (19)	0.008 (2)
C45	0.040 (3)	0.051 (3)	0.024 (2)	0.000 (2)	0.0004 (19)	0.005 (2)
C46	0.036 (2)	0.055 (3)	0.025 (2)	0.002 (2)	-0.0049 (19)	0.010 (2)
C47	0.028 (2)	0.048 (3)	0.040 (3)	-0.001 (2)	-0.0035 (19)	0.019 (2)
C48	0.029 (2)	0.043 (3)	0.040 (3)	0.0066 (19)	0.001 (2)	0.015 (2)
C491	0.037 (2)	0.044 (3)	0.022 (2)	0.002 (2)	0.0020 (18)	-0.0001 (19)
C501	0.043 (8)	0.052 (9)	0.028 (6)	0.016 (7)	0.009 (6)	0.005 (6)
C511	0.058 (9)	0.044 (9)	0.064 (10)	-0.003 (7)	0.039 (8)	0.002 (8)

C521	0.055 (4)	0.057 (4)	0.088 (6)	-0.012 (3)	0.013 (4)	0.003 (4)
C492	0.037 (2)	0.044 (3)	0.022 (2)	0.002 (2)	0.0020 (18)	-0.0001 (19)
C502	0.036 (5)	0.031 (4)	0.023 (4)	0.005 (3)	0.007 (3)	0.004 (3)
C512	0.042 (5)	0.035 (6)	0.040 (5)	-0.007 (4)	-0.003 (4)	-0.003 (4)
C522	0.055 (4)	0.057 (4)	0.088 (6)	-0.012 (3)	0.013 (4)	0.003 (4)
C53	0.033 (5)	0.065 (7)	0.023 (5)	0.008 (5)	-0.005 (4)	0.024 (5)
N1	0.0283 (18)	0.040 (2)	0.0243 (18)	0.0005 (16)	0.0041 (15)	0.0043 (16)
Cl1	0.0617 (14)	0.0659 (16)	0.128 (3)	-0.0096 (11)	0.0240 (15)	-0.0071 (15)
Cl2	0.0617 (14)	0.0659 (16)	0.128 (3)	-0.0096 (11)	0.0240 (15)	-0.0071 (15)
Cl3	0.0617 (14)	0.0659 (16)	0.128 (3)	-0.0096 (11)	0.0240 (15)	-0.0071 (15)

Table S 25 Geometric parameters (\AA , $^{\circ}$) for **[8]CPP-N-Bu**.

C1—C6	1.391 (6)	C32—H32	0.95
C1—N1	1.392 (6)	C33—C34	1.391 (7)
C1—C2	1.407 (7)	C33—H33	0.95
C2—C3	1.404 (7)	C34—C35	1.411 (7)
C2—C8	1.451 (7)	C34—C37	1.494 (8)
C3—C4	1.379 (7)	C35—C36	1.382 (8)
C3—H3	0.95	C35—H35	0.95
C4—C5	1.428 (7)	C36—H36	0.95
C4—H4	0.95	C37—C38	1.390 (8)
C5—C6	1.399 (6)	C37—C42	1.393 (8)
C5—C13	1.478 (7)	C38—C39	1.379 (8)
C6—H6	0.95	C38—H38	0.95
C7—N1	1.391 (6)	C39—C40	1.408 (7)
C7—C12	1.399 (7)	C39—H39	0.95
C7—C8	1.409 (7)	C40—C41	1.407 (7)
C8—C9	1.412 (7)	C40—C43	1.487 (8)
C9—C10	1.387 (8)	C41—C42	1.370 (9)
C9—H9	0.95	C41—H41	0.95
C10—C11	1.416 (7)	C42—H42	0.95
C10—H10	0.95	C43—C44	1.400 (8)
C11—C12	1.379 (7)	C43—C48	1.412 (7)
C11—C46	1.506 (8)	C44—C45	1.392 (8)
C12—H12	0.95	C44—H44	0.95
C13—C14	1.395 (7)	C45—C46	1.410 (8)
C13—C18	1.412 (7)	C45—H45	0.95
C14—C15	1.392 (7)	C46—C47	1.401 (8)
C14—H14	0.95	C47—C48	1.372 (8)

C15—C16	1.403 (7)	C47—H47	0.95
C15—H15	0.95	C48—H48	0.95
C16—C17	1.396 (7)	C491—N1	1.463 (6)
C16—C19	1.484 (7)	C491—C501	1.634 (16)
C17—C18	1.383 (7)	C491—H49A	0.99
C17—H17	0.95	C491—H49B	0.99
C18—H18	0.95	C501—C511	1.48 (2)
C19—C20	1.407 (7)	C501—H50A	0.99
C19—C24	1.408 (7)	C501—H50B	0.99
C20—C21	1.380 (8)	C511—C521	1.469 (17)
C20—H20	0.95	C511—H51A	0.99
C21—C22	1.423 (7)	C511—H51B	0.99
C21—H21	0.95	C521—H52A	0.98
C22—C23	1.405 (8)	C521—H52B	0.98
C22—C25	1.475 (8)	C521—H52C	0.98
C23—C24	1.365 (8)	C492—N1	1.463 (6)
C23—H23	0.95	C492—C502	1.499 (9)
C24—H24	0.95	C492—H49C	0.99
C25—C26	1.413 (8)	C492—H49D	0.99
C25—C30	1.413 (8)	C502—C512	1.535 (14)
C26—C27	1.364 (8)	C502—H50C	0.99
C26—H26	0.95	C502—H50D	0.99
C27—C28	1.412 (7)	C512—C522	1.562 (12)
C27—H27	0.95	C512—H51C	0.99
C28—C29	1.409 (8)	C512—H51D	0.99
C28—C31	1.469 (7)	C522—H52D	0.98
C29—C30	1.378 (8)	C522—H52E	0.98
C29—H29	0.95	C522—H52F	0.98
C30—H30	0.95	C53—Cl2	1.562 (13)
C31—C36	1.398 (7)	C53—Cl3	1.709 (12)
C31—C32	1.401 (7)	C53—Cl1	1.729 (13)
C32—C33	1.371 (8)	C53—H53	1
C6—C1—N1	127.3 (4)	C36—C35—C34	120.5 (5)
C6—C1—C2	122.1 (4)	C36—C35—H35	119.8
N1—C1—C2	109.2 (4)	C34—C35—H35	119.8
C3—C2—C1	118.8 (4)	C35—C36—C31	121.8 (5)
C3—C2—C8	133.6 (4)	C35—C36—H36	119.1
C1—C2—C8	106.4 (4)	C31—C36—H36	119.1
C4—C3—C2	119.2 (4)	C38—C37—C42	116.5 (5)

C4—C3—H3	120.4	C38—C37—C34	122.8 (5)
C2—C3—H3	120.4	C42—C37—C34	118.8 (5)
C3—C4—C5	121.6 (5)	C39—C38—C37	121.5 (5)
C3—C4—H4	119.2	C39—C38—H38	119.2
C5—C4—H4	119.2	C37—C38—H38	119.2
C6—C5—C4	118.7 (4)	C38—C39—C40	121.2 (5)
C6—C5—C13	117.1 (4)	C38—C39—H39	119.4
C4—C5—C13	122.2 (4)	C40—C39—H39	119.4
C1—C6—C5	118.7 (4)	C41—C40—C39	116.0 (5)
C1—C6—H6	120.6	C41—C40—C43	118.6 (5)
C5—C6—H6	120.6	C39—C40—C43	123.6 (5)
N1—C7—C12	127.4 (4)	C42—C41—C40	120.9 (5)
N1—C7—C8	108.9 (4)	C42—C41—H41	119.6
C12—C7—C8	121.9 (4)	C40—C41—H41	119.6
C7—C8—C9	118.6 (5)	C41—C42—C37	122.3 (5)
C7—C8—C2	106.7 (4)	C41—C42—H42	118.9
C9—C8—C2	133.0 (5)	C37—C42—H42	118.9
C10—C9—C8	119.0 (5)	C44—C43—C48	116.3 (5)
C10—C9—H9	120.5	C44—C43—C40	120.0 (4)
C8—C9—H9	120.5	C48—C43—C40	121.3 (5)
C9—C10—C11	121.0 (5)	C45—C44—C43	122.3 (5)
C9—C10—H10	119.5	C45—C44—H44	118.8
C11—C10—H10	119.5	C43—C44—H44	118.8
C12—C11—C10	120.2 (5)	C44—C45—C46	119.3 (5)
C12—C11—C46	114.9 (5)	C44—C45—H45	120.3
C10—C11—C46	121.5 (5)	C46—C45—H45	120.3
C11—C12—C7	118.5 (5)	C47—C46—C45	117.7 (5)
C11—C12—H12	120.8	C47—C46—C11	121.7 (5)
C7—C12—H12	120.8	C45—C46—C11	117.9 (5)
C14—C13—C18	116.9 (5)	C48—C47—C46	121.4 (5)
C14—C13—C5	119.4 (4)	C48—C47—H47	119.3
C18—C13—C5	122.2 (4)	C46—C47—H47	119.3
C15—C14—C13	121.2 (5)	C47—C48—C43	121.2 (5)
C15—C14—H14	119.4	C47—C48—H48	119.4
C13—C14—H14	119.4	C43—C48—H48	119.4
C14—C15—C16	121.0 (5)	N1—C491—C501	107.9 (6)
C14—C15—H15	119.5	N1—C491—H49A	110.1
C16—C15—H15	119.5	C501—C491—H49A	110.1
C17—C16—C15	116.8 (5)	N1—C491—H49B	110.1
C17—C16—C19	121.0 (5)	C501—C491—H49B	110.1

C15—C16—C19	120.1 (5)	H49A—C491—H49B	108.4
C18—C17—C16	121.7 (5)	C511—C501—C491	115.5 (11)
C18—C17—H17	119.2	C511—C501—H50A	108.4
C16—C17—H17	119.2	C491—C501—H50A	108.4
C17—C18—C13	120.7 (5)	C511—C501—H50B	108.4
C17—C18—H18	119.6	C491—C501—H50B	108.4
C13—C18—H18	119.6	H50A—C501—H50B	107.5
C20—C19—C24	115.2 (5)	C521—C511—C501	108.4 (14)
C20—C19—C16	121.4 (5)	C521—C511—H51A	110
C24—C19—C16	121.3 (5)	C501—C511—H51A	110
C21—C20—C19	121.6 (5)	C521—C511—H51B	110
C21—C20—H20	119.2	C501—C511—H51B	110
C19—C20—H20	119.2	H51A—C511—H51B	108.4
C20—C21—C22	121.5 (5)	C511—C521—H52A	109.5
C20—C21—H21	119.3	C511—C521—H52B	109.5
C22—C21—H21	119.3	H52A—C521—H52B	109.5
C23—C22—C21	114.9 (5)	C511—C521—H52C	109.5
C23—C22—C25	123.0 (5)	H52A—C521—H52C	109.5
C21—C22—C25	119.9 (5)	H52B—C521—H52C	109.5
C24—C23—C22	122.4 (5)	N1—C492—C502	113.2 (5)
C24—C23—H23	118.8	N1—C492—H49C	108.9
C22—C23—H23	118.8	C502—C492—H49C	108.9
C23—C24—C19	121.9 (5)	N1—C492—H49D	108.9
C23—C24—H24	119.1	C502—C492—H49D	108.9
C19—C24—H24	119.1	H49C—C492—H49D	107.8
C26—C25—C30	115.2 (5)	C492—C502—C512	109.6 (7)
C26—C25—C22	123.2 (5)	C492—C502—H50C	109.8
C30—C25—C22	120.1 (5)	C512—C502—H50C	109.8
C27—C26—C25	122.2 (5)	C492—C502—H50D	109.8
C27—C26—H26	118.9	C512—C502—H50D	109.8
C25—C26—H26	118.9	H50C—C502—H50D	108.2
C26—C27—C28	120.9 (5)	C502—C512—C522	114.7 (8)
C26—C27—H27	119.5	C502—C512—H51C	108.6
C28—C27—H27	119.5	C522—C512—H51C	108.6
C29—C28—C27	116.6 (5)	C502—C512—H51D	108.6
C29—C28—C31	119.1 (4)	C522—C512—H51D	108.6
C27—C28—C31	122.1 (5)	H51C—C512—H51D	107.6
C30—C29—C28	120.6 (5)	C512—C522—H52D	109.5
C30—C29—H29	119.7	C512—C522—H52E	109.5
C28—C29—H29	119.7	H52D—C522—H52E	109.5

C29—C30—C25	121.9 (5)	C512—C522—H52F	109.5
C29—C30—H30	119	H52D—C522—H52F	109.5
C25—C30—H30	119	H52E—C522—H52F	109.5
C36—C31—C32	116.2 (5)	Cl2—C53—Cl3	108.9 (8)
C36—C31—C28	124.0 (5)	Cl2—C53—Cl1	116.5 (7)
C32—C31—C28	117.9 (5)	Cl3—C53—Cl1	125.1 (7)
C33—C32—C31	121.9 (5)	Cl2—C53—H53	100.2
C33—C32—H32	119.1	Cl3—C53—H53	100.2
C31—C32—H32	119.1	Cl1—C53—H53	100.2
C32—C33—C34	121.3 (5)	C7—N1—C1	108.1 (4)
C32—C33—H33	119.4	C7—N1—C492	125.6 (4)
C34—C33—H33	119.4	C1—N1—C492	125.6 (4)
C33—C34—C35	116.9 (5)	C7—N1—C491	125.6 (4)
C33—C34—C37	118.7 (5)	C1—N1—C491	125.6 (4)
C35—C34—C37	122.8 (5)		

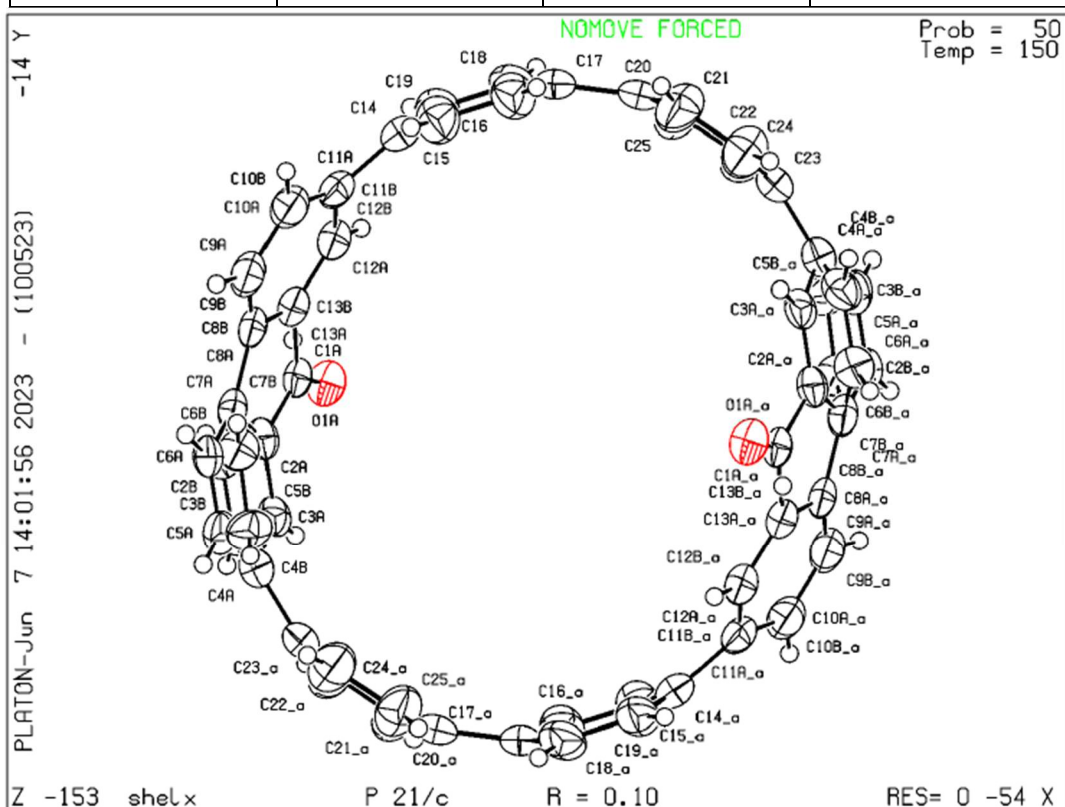


Figure S 75 Crystallographic structure of [8]CPP-C=O (CCDC: 2294552).

Table S 26 Crystal data of [8]CPP-C=O.

C ₄₉ H ₃₀ O	$F(000) = 664$
$M_r = 634.73$	$D_x = 1.092 \text{ Mg m}^{-3}$
Monoclinic, $P2_1/c$	Mo $K\alpha$ radiation, $\lambda = 0.71073 \text{ \AA}$

Hall symbol: -P 2ybc	Cell parameters from 9512 reflections
$a = 12.8766 (13) \text{ \AA}$	$\theta = 2.7\text{--}27.5^\circ$
$b = 14.9692 (16) \text{ \AA}$	$\mu = 0.06 \text{ mm}^{-1}$
$c = 10.3986 (10) \text{ \AA}$	$T = 150 \text{ K}$
$\beta = 105.590 (4)^\circ$	Prism, orange
$V = 1930.6 (3) \text{ \AA}^3$	$0.16 \times 0.06 \times 0.04 \text{ mm}$
$Z = 2$	

Table S 27 Data collection of [8]CPP-C=O.

D8 VENTURE diffractometer	Bruker AXS	4364 independent reflections
Radiation source: Incoatec microfocus sealed tube		3361 reflections with $I > 2\sigma(I)$
Multilayer monochromator		$R_{\text{int}} = 0.086$
Detector resolution: 7.39 pixels mm^{-1}		$\theta_{\max} = 27.6^\circ, \theta_{\min} = 2.1^\circ$
rotation images scans		$h = -16 \rightarrow 16$
Absorption correction: multi-scan [Sheldrick, G.M. (2014). <i>SADABS</i> Bruker AXS Inc., Madison, Wisconsin, USA]		$k = -19 \rightarrow 19$
$T_{\min} = 0.995, T_{\max} = 0.997$		$l = -13 \rightarrow 11$
33915 measured reflections		

Table S 28 Refinement of [8]CPP-C=O.

Refinement on F^2	0 constraints
Least-squares matrix: full	Hydrogen site location: inferred from neighbouring sites
$R[F^2 > 2\sigma(F^2)] = 0.101$	H-atom parameters constrained
$wR(F^2) = 0.260$	$w = 1/[\sigma^2(F_o^2) + (0.0942P)^2 + 1.6887P]$ where $P = (F_o^2 + 2F_c^2)/3$
$S = 1.16$	$(\Delta/\sigma)_{\max} < 0.001$
4364 reflections	$\Delta\rho_{\max} = 0.35 \text{ e \AA}^{-3}$
271 parameters	$\Delta\rho_{\min} = -0.26 \text{ e \AA}^{-3}$
0 restraints	

Table S 29 Special details of [8]CPP-C=O.

Geometry. All esds (except the esd in the dihedral angle between two l.s. planes) are estimated using the full covariance matrix. The cell esds are taken into account individually in the estimation of esds in distances, angles and torsion angles; correlations between esds in cell parameters are only used when they are defined by crystal symmetry. An approximate (isotropic) treatment of cell esds is used for estimating esds involving l.s. planes.

Table S 30 Fractional atomic coordinates and isotropic or equivalent isotropic displacement parameters (\AA^2) for (shelx) of **[8]CPP-C=O**.

	<i>x</i>	<i>y</i>	<i>z</i>	$U_{\text{iso}}^*/U_{\text{eq}}$	Occ. (<1)
O1A	0.7743 (3)	0.4411 (3)	0.2868 (4)	0.0509 (10)	0.5
C1A	0.8034 (4)	0.5100 (4)	0.3439 (5)	0.0387 (11)	0.5
C2A	0.7816 (5)	0.6024 (4)	0.2938 (6)	0.0409 (12)	0.5
C3A	0.7002 (5)	0.6282 (4)	0.1836 (6)	0.0433 (13)	0.5
H3A	0.666086	0.584826	0.119418	0.052*	0.5
C4A	0.6670 (2)	0.7197 (2)	0.1653 (3)	0.0502 (7)	0.5
C5A	0.7301 (10)	0.7777 (10)	0.2609 (16)	0.049 (3)	0.5
H5A	0.715191	0.839745	0.24896	0.059*	0.5
C6A	0.8112 (7)	0.7530 (6)	0.3700 (10)	0.0429 (19)	0.5
H6A	0.849598	0.794478	0.434595	0.051*	0.5
C7A	0.8333 (2)	0.6562 (2)	0.3778 (3)	0.0542 (8)	0.5
C8A	0.8852 (2)	0.6016 (2)	0.4966 (4)	0.0630 (10)	0.5
C9A	0.9310 (3)	0.6313 (2)	0.6266 (4)	0.0662 (10)	0.5
H9A	0.95142	0.692135	0.64251	0.079*	0.5
C10A	0.9466 (2)	0.5722 (2)	0.7321 (4)	0.0576 (8)	0.5
H10A	0.977561	0.593566	0.82012	0.069*	0.5
C11A	0.9181 (2)	0.4820 (2)	0.7136 (3)	0.0498 (7)	0.5
C12A	0.8827 (2)	0.4520 (2)	0.5818 (3)	0.0500 (7)	0.5
H12A	0.869135	0.390267	0.564007	0.06*	0.5
C13A	0.8675 (2)	0.5111 (3)	0.4785 (3)	0.0607 (9)	0.5
C2B	0.8115 (5)	0.6174 (4)	0.2320 (7)	0.0485 (13)	0.5
H2B	0.854698	0.570629	0.212446	0.058*	0.5
C3B	0.7280 (6)	0.6533 (4)	0.1339 (7)	0.0522 (15)	0.5
H3B	0.713126	0.631799	0.044864	0.063*	0.5
C4B	0.6670 (2)	0.7197 (2)	0.1653 (3)	0.0502 (7)	0.5
C5B	0.7011 (10)	0.7650 (11)	0.2801 (16)	0.058 (3)	0.5
H5B	0.670762	0.821206	0.292241	0.069*	0.5
C6B	0.7841 (8)	0.7259 (7)	0.3830 (10)	0.051 (2)	0.5
H6B	0.803937	0.757282	0.465385	0.061*	0.5
C7B	0.8333 (2)	0.6562 (2)	0.3778 (3)	0.0542 (8)	0.5
C8B	0.8852 (2)	0.6016 (2)	0.4966 (4)	0.0630 (10)	0.5
C9B	0.9310 (3)	0.6313 (2)	0.6266 (4)	0.0662 (10)	0.5
H9B	0.95142	0.692135	0.64251	0.079*	0.5
C10B	0.9466 (2)	0.5722 (2)	0.7321 (4)	0.0576 (8)	0.5
H10B	0.977561	0.593566	0.82012	0.069*	0.5

C11B	0.9181 (2)	0.4820 (2)	0.7136 (3)	0.0498 (7)	0.5
C12B	0.8827 (2)	0.4520 (2)	0.5818 (3)	0.0500 (7)	0.5
H12B	0.869135	0.390267	0.564007	0.06*	0.5
C13B	0.8675 (2)	0.5111 (3)	0.4785 (3)	0.0607 (9)	0.5
H13B	0.843485	0.488833	0.38986	0.073*	0.5
C14	0.8983 (2)	0.4243 (2)	0.8208 (3)	0.0523 (7)	
C15	0.8620 (3)	0.4615 (3)	0.9233 (4)	0.0677 (9)	
H15	0.879293	0.521862	0.948537	0.081*	
C16	0.8012 (3)	0.4122 (3)	0.9891 (4)	0.0681 (9)	
H16	0.77745	0.43977	1.058479	0.082*	
C17	0.7742 (2)	0.3244 (2)	0.9571 (3)	0.0546 (8)	
C18	0.8276 (3)	0.2833 (2)	0.8720 (4)	0.0640 (9)	
H18	0.822177	0.220481	0.859483	0.077*	
C19	0.8881 (3)	0.3324 (2)	0.8058 (4)	0.0616 (9)	
H19	0.923391	0.302567	0.748849	0.074*	
C20	0.6726 (3)	0.2868 (2)	0.9780 (3)	0.0593 (9)	
C21	0.6097 (3)	0.3345 (4)	1.0437 (3)	0.0848 (14)	
H21	0.643643	0.375027	1.112423	0.102*	
C22	0.4998 (3)	0.3244 (4)	1.0118 (3)	0.0851 (13)	
H22	0.459231	0.359519	1.05697	0.102*	
C23	0.4466 (3)	0.2640 (2)	0.9146 (3)	0.0579 (8)	
C24	0.5118 (3)	0.2046 (2)	0.8707 (5)	0.0818 (12)	
H24	0.47985	0.154882	0.817889	0.098*	
C25	0.6227 (3)	0.2157 (2)	0.9018 (5)	0.0812 (13)	
H25	0.665072	0.173476	0.870112	0.097*	

Table S 31 Atomic displacement parameters (\AA^2) for [8]CPP-C=O.

	U^{11}	U^{22}	U^{33}	U^{12}	U^{13}	U^{23}
O1A	0.050 (2)	0.048 (2)	0.056 (2)	-0.0073 (18)	0.0169 (19)	-0.0157 (19)
C1A	0.031 (2)	0.045 (3)	0.044 (3)	-0.005 (2)	0.018 (2)	-0.005 (2)
C2A	0.045 (3)	0.046 (3)	0.040 (3)	-0.005 (2)	0.024 (3)	-0.003 (2)
C3A	0.047 (3)	0.053 (3)	0.036 (3)	-0.007 (3)	0.022 (3)	-0.001 (3)
C4A	0.0484 (16)	0.0581 (18)	0.0477 (16)	-0.0041 (13)	0.0190 (13)	0.0088 (13)
C5A	0.045 (6)	0.044 (4)	0.065 (6)	0.000 (4)	0.026 (4)	-0.001 (4)
C6A	0.042 (4)	0.036 (4)	0.053 (4)	-0.013 (3)	0.018 (3)	-0.003 (3)
C7A	0.0339 (14)	0.0555 (18)	0.075 (2)	-0.0086 (13)	0.0175 (14)	0.0150 (16)
C8A	0.0272 (13)	0.075 (2)	0.088 (2)	-0.0045 (14)	0.0176 (14)	0.0316 (19)
C9A	0.0371 (16)	0.064 (2)	0.098 (3)	-0.0032 (14)	0.0194 (17)	0.0181 (19)
C10A	0.0407 (15)	0.0619 (19)	0.068 (2)	-0.0040 (14)	0.0106 (14)	0.0004 (16)

C11A	0.0292 (13)	0.0564 (17)	0.0622 (18)	0.0035 (12)	0.0093 (12)	0.0072 (14)
C12A	0.0351 (14)	0.0564 (17)	0.0593 (18)	-0.0039 (12)	0.0139 (12)	0.0045 (14)
C13A	0.0316 (14)	0.088 (2)	0.0615 (19)	-0.0087 (15)	0.0107 (13)	0.0191 (17)
C2B	0.055 (4)	0.043 (3)	0.049 (3)	-0.003 (3)	0.016 (3)	-0.006 (3)
C3B	0.065 (4)	0.052 (4)	0.040 (3)	-0.012 (3)	0.015 (3)	0.000 (3)
C4B	0.0484 (16)	0.0581 (18)	0.0477 (16)	-0.0041 (13)	0.0190 (13)	0.0088 (13)
C5B	0.048 (7)	0.071 (8)	0.056 (6)	0.021 (5)	0.019 (5)	0.000 (5)
C6B	0.051 (5)	0.055 (6)	0.047 (4)	-0.002 (4)	0.014 (3)	-0.008 (4)
C7B	0.0339 (14)	0.0555 (18)	0.075 (2)	-0.0086 (13)	0.0175 (14)	0.0150 (16)
C8B	0.0272 (13)	0.075 (2)	0.088 (2)	-0.0045 (14)	0.0176 (14)	0.0316 (19)
C9B	0.0371 (16)	0.064 (2)	0.098 (3)	-0.0032 (14)	0.0194 (17)	0.0181 (19)
C10B	0.0407 (15)	0.0619 (19)	0.068 (2)	-0.0040 (14)	0.0106 (14)	0.0004 (16)
C11B	0.0292 (13)	0.0564 (17)	0.0622 (18)	0.0035 (12)	0.0093 (12)	0.0072 (14)
C12B	0.0351 (14)	0.0564 (17)	0.0593 (18)	-0.0039 (12)	0.0139 (12)	0.0045 (14)
C13B	0.0316 (14)	0.088 (2)	0.0615 (19)	-0.0087 (15)	0.0107 (13)	0.0191 (17)
C14	0.0324 (13)	0.0646 (19)	0.0551 (17)	0.0041 (13)	0.0034 (12)	0.0087 (15)
C15	0.070 (2)	0.071 (2)	0.060 (2)	-0.0161 (18)	0.0145 (17)	-0.0046 (17)
C16	0.072 (2)	0.078 (2)	0.0556 (19)	-0.0079 (19)	0.0194 (17)	0.0004 (17)
C17	0.0444 (15)	0.066 (2)	0.0471 (16)	0.0080 (14)	0.0021 (12)	0.0220 (15)
C18	0.069 (2)	0.0538 (19)	0.069 (2)	0.0170 (16)	0.0188 (17)	0.0208 (16)
C19	0.0566 (19)	0.060 (2)	0.071 (2)	0.0188 (15)	0.0216 (16)	0.0206 (16)
C20	0.0547 (18)	0.071 (2)	0.0459 (16)	0.0058 (16)	0.0028 (14)	0.0287 (15)
C21	0.056 (2)	0.156 (4)	0.0402 (17)	-0.011 (2)	0.0090 (15)	-0.012 (2)
C22	0.061 (2)	0.156 (4)	0.0416 (17)	-0.012 (2)	0.0196 (15)	-0.015 (2)
C23	0.0538 (17)	0.071 (2)	0.0485 (17)	-0.0041 (15)	0.0134 (14)	0.0232 (15)
C24	0.060 (2)	0.0481 (19)	0.130 (4)	0.0015 (17)	0.012 (2)	0.013 (2)
C25	0.055 (2)	0.051 (2)	0.135 (4)	0.0098 (16)	0.021 (2)	0.015 (2)

Table S 32 Geometric parameters (\AA , $^\circ$) for **[8]CPP-C=O**.

O1A—C1A	1.199 (6)	C6B—H6B	0.95
C1A—C13A	1.420 (6)	C7B—C8B	1.482 (5)
C1A—C2A	1.478 (8)	C8B—C13B	1.378 (5)
C2A—C7A	1.241 (6)	C8B—C9B	1.394 (5)
C2A—C3A	1.384 (9)	C9B—C10B	1.382 (5)
C3A—C4A	1.432 (7)	C9B—H9B	0.95
C3A—H3A	0.95	C10B—C11B	1.400 (5)
C4A—C5A	1.403 (16)	C10B—H10B	0.95
C4A—C23 ⁱ	1.495 (4)	C11B—C12B	1.397 (4)
C5A—C6A	1.37 (2)	C11B—C14	1.485 (4)

C5A—H5A	0.95	C12B—C13B	1.364 (4)
C6A—C7A	1.476 (10)	C12B—H12B	0.95
C6A—H6A	0.95	C13B—H13B	0.95
C7A—C8A	1.482 (5)	C14—C19	1.386 (5)
C8A—C13A	1.378 (5)	C14—C15	1.390 (5)
C8A—C9A	1.394 (5)	C15—C16	1.384 (5)
C9A—C10A	1.382 (5)	C15—H15	0.95
C9A—H9A	0.95	C16—C17	1.378 (5)
C10A—C11A	1.400 (5)	C16—H16	0.95
C10A—H10A	0.95	C17—C18	1.401 (5)
C11A—C12A	1.397 (4)	C17—C20	1.492 (5)
C11A—C14	1.485 (4)	C18—C19	1.380 (5)
C12A—C13A	1.364 (4)	C18—H18	0.95
C12A—H12A	0.95	C19—H19	0.95
C2B—C3B	1.377 (9)	C20—C25	1.379 (5)
C2B—C7B	1.576 (7)	C20—C21	1.388 (6)
C2B—H2B	0.95	C21—C22	1.372 (5)
C3B—C4B	1.360 (8)	C21—H21	0.95
C3B—H3B	0.95	C22—C23	1.391 (6)
C4B—C5B	1.341 (17)	C22—H22	0.95
C4B—C23 ⁱ	1.495 (4)	C23—C24	1.383 (6)
C5B—C6B	1.419 (18)	C24—C25	1.387 (6)
C5B—H5B	0.95	C24—H24	0.95
C6B—C7B	1.230 (11)	C25—H25	0.95
O1A—C1A—C13A	121.3 (5)	C13B—C8B—C9B	117.3 (3)
O1A—C1A—C2A	128.7 (5)	C13B—C8B—C7B	114.0 (3)
C13A—C1A—C2A	110.0 (4)	C9B—C8B—C7B	127.6 (3)
C7A—C2A—C3A	123.1 (5)	C10B—C9B—C8B	119.9 (3)
C7A—C2A—C1A	110.1 (5)	C10B—C9B—H9B	120
C3A—C2A—C1A	125.6 (5)	C8B—C9B—H9B	120
C2A—C3A—C4A	120.6 (5)	C9B—C10B—C11B	122.1 (3)
C2A—C3A—H3A	119.7	C9B—C10B—H10B	118.9
C4A—C3A—H3A	119.7	C11B—C10B—H10B	118.9
C5A—C4A—C3A	113.7 (7)	C12B—C11B—C10B	116.7 (3)
C5A—C4A—C23 ⁱ	125.9 (7)	C12B—C11B—C14	118.2 (3)
C3A—C4A—C23 ⁱ	116.3 (3)	C10B—C11B—C14	123.3 (3)
C6A—C5A—C4A	126.0 (12)	C13B—C12B—C11B	120.3 (3)
C6A—C5A—H5A	117	C13B—C12B—H12B	119.8
C4A—C5A—H5A	117	C11B—C12B—H12B	119.8

C5A—C6A—C7A	113.8 (9)	C12B—C13B—C8B	123.1 (3)
C5A—C6A—H6A	123.1	C12B—C13B—H13B	118.5
C7A—C6A—H6A	123.1	C8B—C13B—H13B	118.5
C2A—C7A—C6A	122.6 (5)	C19—C14—C15	116.2 (3)
C2A—C7A—C8A	105.4 (4)	C19—C14—C11A	121.5 (3)
C6A—C7A—C8A	128.7 (5)	C15—C14—C11A	120.2 (3)
C13A—C8A—C9A	117.3 (3)	C19—C14—C11B	121.5 (3)
C13A—C8A—C7A	114.0 (3)	C15—C14—C11B	120.2 (3)
C9A—C8A—C7A	127.6 (3)	C16—C15—C14	121.1 (4)
C10A—C9A—C8A	119.9 (3)	C16—C15—H15	119.4
C10A—C9A—H9A	120	C14—C15—H15	119.4
C8A—C9A—H9A	120	C17—C16—C15	122.0 (4)
C9A—C10A—C11A	122.1 (3)	C17—C16—H16	119
C9A—C10A—H10A	118.9	C15—C16—H16	119
C11A—C10A—H10A	118.9	C16—C17—C18	115.9 (3)
C12A—C11A—C10A	116.7 (3)	C16—C17—C20	119.9 (3)
C12A—C11A—C14	118.2 (3)	C18—C17—C20	121.7 (3)
C10A—C11A—C14	123.3 (3)	C19—C18—C17	121.3 (3)
C13A—C12A—C11A	120.3 (3)	C19—C18—H18	119.3
C13A—C12A—H12A	119.8	C17—C18—H18	119.3
C11A—C12A—H12A	119.8	C18—C19—C14	121.4 (3)
C12A—C13A—C8A	123.1 (3)	C18—C19—H19	119.3
C12A—C13A—C1A	133.7 (4)	C14—C19—H19	119.3
C8A—C13A—C1A	100.2 (3)	C25—C20—C21	115.8 (4)
C3B—C2B—C7B	118.1 (5)	C25—C20—C17	119.9 (3)
C3B—C2B—H2B	120.9	C21—C20—C17	121.9 (4)
C7B—C2B—H2B	120.9	C22—C21—C20	121.7 (4)
C4B—C3B—C2B	119.6 (6)	C22—C21—H21	119.2
C4B—C3B—H3B	120.2	C20—C21—H21	119.2
C2B—C3B—H3B	120.2	C21—C22—C23	121.5 (4)
C5B—C4B—C3B	120.8 (7)	C21—C22—H22	119.3
C5B—C4B—C23 ⁱ	116.7 (7)	C23—C22—H22	119.3
C3B—C4B—C23 ⁱ	121.9 (4)	C24—C23—C22	115.7 (4)
C4B—C5B—C6B	117.6 (12)	C24—C23—C4A ⁱ	120.8 (3)
C4B—C5B—H5B	121.2	C22—C23—C4A ⁱ	121.0 (4)
C6B—C5B—H5B	121.2	C23—C24—C25	121.6 (4)
C7B—C6B—C5B	127.6 (10)	C23—C24—H24	119.2
C7B—C6B—H6B	116.2	C25—C24—H24	119.2
C5B—C6B—H6B	116.2	C20—C25—C24	121.2 (4)
C6B—C7B—C8B	123.6 (6)	C20—C25—H25	119.4

C6B—C7B—C2B	113.2 (6)	C24—C25—H25	119.4
C8B—C7B—C2B	121.5 (4)		
O1A—C1A—C2A—C7A	-174.0 (5)	C6B—C7B—C8B—C13B	135.9 (6)
C13A—C1A—C2A—C7A	6.4 (6)	C2B—C7B—C8B—C13B	-28.2 (5)
O1A—C1A—C2A—C3A	18.3 (10)	C6B—C7B—C8B—C9B	-31.4 (7)
C13A—C1A—C2A—C3A	-161.3 (6)	C2B—C7B—C8B—C9B	164.4 (4)
C7A—C2A—C3A—C4A	-3.8 (9)	C13B—C8B—C9B—C10B	-6.5 (5)
C1A—C2A—C3A—C4A	162.4 (5)	C7B—C8B—C9B—C10B	160.5 (3)
C2A—C3A—C4A—C5A	5.2 (8)	C8B—C9B—C10B—C11B	0.3 (5)
C2A—C3A—C4A—C23 ⁱ	-153.4 (5)	C9B—C10B—C11B—C12B	6.0 (4)
C3A—C4A—C5A—C6A	-5.1 (12)	C9B—C10B—C11B—C14	-158.6 (3)
C23 ⁱ —C4A—C5A—C6A	151.1 (8)	C10B—C11B—C12B—C13B	-6.1 (4)
C4A—C5A—C6A—C7A	3.1 (13)	C14—C11B—C12B—C13B	159.3 (3)
C3A—C2A—C7A—C6A	1.5 (9)	C11B—C12B—C13B—C8B	-0.2 (5)
C1A—C2A—C7A—C6A	-166.5 (5)	C9B—C8B—C13B—C12B	6.5 (5)
C3A—C2A—C7A—C8A	162.5 (6)	C7B—C8B—C13B—C12B	-162.2 (3)
C1A—C2A—C7A—C8A	-5.6 (5)	C12A—C11A—C14—C19	26.5 (4)
C5A—C6A—C7A—C2A	-1.0 (10)	C10A—C11A—C14—C19	-169.1 (3)
C5A—C6A—C7A—C8A	-157.3 (6)	C12A—C11A—C14—C15	-136.7 (3)
C2A—C7A—C8A—C13A	3.4 (5)	C10A—C11A—C14—C15	27.6 (4)
C6A—C7A—C8A—C13A	162.8 (5)	C12B—C11B—C14—C19	26.5 (4)
C2A—C7A—C8A—C9A	-164.0 (4)	C10B—C11B—C14—C19	-169.1 (3)
C6A—C7A—C8A—C9A	-4.5 (6)	C12B—C11B—C14—C15	-136.7 (3)
C13A—C8A—C9A—C10A	-6.5 (5)	C10B—C11B—C14—C15	27.6 (4)

C7A—C8A—C9A—C10A	160.5 (3)	C19—C14—C15—C16	-11.7 (5)
C8A—C9A—C10A—C11A	0.3 (5)	C11A—C14—C15—C16	152.4 (3)
C9A—C10A—C11A—C12A	6.0 (4)	C11B—C14—C15—C16	152.4 (3)
C9A—C10A—C11A—C14	-158.6 (3)	C14—C15—C16—C17	0.3 (6)
C10A—C11A—C12A—C13A	-6.1 (4)	C15—C16—C17—C18	11.2 (5)
C14—C11A—C12A—C13A	159.3 (3)	C15—C16—C17—C20	-151.1 (3)
C11A—C12A—C13A—C8A	-0.2 (5)	C16—C17—C18—C19	-11.3 (5)
C11A—C12A—C13A—C1A	-156.3 (4)	C20—C17—C18—C19	150.6 (3)
C9A—C8A—C13A—C12A	6.5 (5)	C17—C18—C19—C14	-0.1 (5)
C7A—C8A—C13A—C12A	-162.2 (3)	C15—C14—C19—C18	11.6 (5)
C9A—C8A—C13A—C1A	169.3 (3)	C11A—C14—C19—C18	-152.3 (3)
C7A—C8A—C13A—C1A	0.5 (4)	C11B—C14—C19—C18	-152.3 (3)
O1A—C1A—C13A—C12A	-23.5 (8)	C16—C17—C20—C25	154.1 (3)
C2A—C1A—C13A—C12A	156.2 (4)	C18—C17—C20—C25	-7.2 (4)
O1A—C1A—C13A—C8A	176.7 (4)	C16—C17—C20—C21	-7.7 (4)
C2A—C1A—C13A—C8A	-3.7 (5)	C18—C17—C20—C21	-168.9 (3)
C7B—C2B—C3B—C4B	-0.6 (10)	C25—C20—C21—C22	-14.0 (6)
C2B—C3B—C4B—C5B	15.8 (11)	C17—C20—C21—C22	148.5 (4)
C2B—C3B—C4B—C23 ⁱ	-154.6 (5)	C20—C21—C22—C23	1.9 (7)
C3B—C4B—C5B—C6B	-18.1 (12)	C21—C22—C23—C24	11.2 (6)
C23 ⁱ —C4B—C5B—C6B	152.8 (7)	C21—C22—C23—C4A ⁱ	-150.9 (4)
C4B—C5B—C6B—C7B	3.8 (15)	C22—C23—C24—C25	-12.0 (6)
C5B—C6B—C7B—C8B	-154.8 (8)	C4A ⁱ —C23—C24—C25	150.1 (4)
C5B—C6B—C7B—C2B	10.5 (12)	C21—C20—C25—C24	13.1 (6)

C3B—C2B—C7B— C6B	-12.0 (9)	C17—C20—C25— C24	-149.8 (4)
C3B—C2B—C7B— C8B	153.6 (5)	C23—C24—C25— C20	-0.1 (7)

Symmetry code: (i) $-x+1, -y+1, -z+1$.

10 References

- [1] G. R. Fulmer, A. J. M. Miller, N. H. Sherden, H. E. Gottlieb, A. Nudelman, B. M. Stoltz, J. E. Bercaw, K. I. Goldberg, *Organometallics* **2010**, *29*, 2176-2179.
- [2] E. Lippert, *Zeitschrift für Naturforschung A* **1955**, *10*, 541-545.
- [3] N. Mataga, Y. Kaifu, M. Koizumi, *Bull. Chem. Soc. Jpn.* **1955**, *28*, 690-691.
- [4] P. H. a. W. Kohn, *Phys. Rev.*, **136**, B864.
- [5] J.-L. Calais, *Int. J. Quantum Chem.* **1993**, *47*, 101.
- [6] A. D. Becke, *J. Phys. Chem.* **1993**, *98*, 1372.
- [7] A. D. Becke, *J. Phys. Chem.* **1993**, *98*, 5648.
- [8] A. D. Becke, *Phys. Rev. A* **1988**, *38*, 3098.
- [9] C. Lee, W. Yang, R. G. Parr, *Phys Rev B Condens Matter* **1988**, *37*, 785-789.
- [10] G. W. T. M. J. Frisch, H. B. Schlegel, G. E. Scuseria, M. A. Robb, J. R. Cheeseman, G. Scalmani, V. Barone, B. Mennucci, G. A. Petersson, H. Nakatsuji, M. Caricato, X. Li, H. P. Hratchian, A. F. Izmaylov, J. Bloino, G. Zheng, J. L. Sonnenberg, M. Hada, M. Ehara, K. Toyota, R. Fukuda, J. Hasegawa, M. Ishida, T. Nakajima, Y. Honda, O. Kitao, H. Nakai, T. Vreven, J. A. J. Montgomery, J. E. Peralta, F. Ogliaro, M. Bearpark, J. J. Heyd, E. Brothers, K. N. Kudin, V. N. Staroverov, T. Keith, R. Kobayashi, J. Normand, K. Raghavachari, A. Rendell, J. C. Burant, S. S. Iyengar, J. Tomasi, M. Cossi, N. Rega, J. M. Millam, M. Klene, J. E. Knox, J. B. Cross, V. Bakken, C. Adamo, J. Jaramillo, R. Gomperts, R. E. Stratmann, O. Yazyev, A. J. Austin, R. Cammi, C. Pomelli, J. W. Ochterski, R. L. Martin, K. Morokuma, V. G. Zakrzewski, G. A. Voth, P. Salvador, J. J. Dannenberg, S. Dapprich, A. D. Daniels, O. Farkas, J. B. Foresman, J. V. Ortiz, J. Cioslowski, D. J. Fox, **2010**, Gaussian 09, Revision B.01, Gaussian, Inc., Wallingford CT, 2010.
- [11] J. P. Mora-Fuentes, M. D. Codesal, M. Reale, C. M. Cruz, V. G. Jimenez, A. Sciortino, M. Cannas, F. Messina, V. Blanco, A. G. Campana, *Angew Chem Int Ed Engl* **2023**, e202301356.
- [12] S. M. Bachrach, *J. Chem. Educ.* **1990**, *67*, 907.
- [13] F. Lucas, N. McIntosh, E. Jacques, C. Lebreton, B. Heinrich, B. Donnio, O. Jeannin, J. Rault-Berthelot, C. Quinton, J. Cornil, C. Poriel, *J. Am. Chem. Soc.* **2021**, *143*, 8804-8820.
- [14] W. Xiong, Y. Gong, Y. Che, J. Zhao, *Anal Chem* **2019**, *91*, 1711-1714.
- [15] T. J. Sisto, M. R. Golder, E. S. Hirst, R. Jasti, *J. Am. Chem. Soc.* **2011**, *133*, 15800-15802.
- [16] E. P. Jackson, T. J. Sisto, E. R. Darzi, R. Jasti, *Tetrahedron* **2016**, *72*, 3754-3758.
- [17] V. K. Patel, E. Kayahara, S. Yamago, *Chem. Eur. J.* **2015**, *21*, 5742-5749.
- [18] E. M. Espinoza, J. A. Clark, J. Soliman, J. B. Derr, M. Morales, V. I. Vullev, *Journal of The Electrochemical Society* **2019**, *166*, H3175.
- [19] A. P. Kulkarni, C. J. Tonzola, A. Babel, S. A. Jenekhe, *Chem. Mater.* **2004**, *16*, 4556-4573.
- [20] J. Xia, J. W. Bacon, R. Jasti, *Chem. Sci.* **2012**, *3*, 3018.